



UIT

THE ARCTIC
UNIVERSITY
OF NORWAY

Faculty of Science and Technology

Department of Geosciences

A sedimentological study of the Lower Cretaceous Glitrefjellet Member, Svalbard

Thea Marie Engen

*GEO-3900 Master Thesis in Geology
May 2018*





Abstract

Detailed facies analysis of the Early Cretaceous Helvetiafjellet Formation (Barremian-Aptian) indicates deposition during a long-term transgression. The formation has received a lot of attention in previous published papers, particularly the lowermost Festningen Member has been detailed in numerous papers. However, the uppermost Glitrefjellet Member is typically poorly exposed in outcrops, and consequently difficult to study. There are therefore few available studies that have investigated the Glitrefjellet Member in great detail. This study investigates stratigraphic cores (DH-1 and DH-1A) stored in Longyearbyen, aiming at describing sedimentary facies at a detail not achievable in outcrop. The detailed facies analysis presented in this thesis consequently contributes to the general understanding of the depositional evolution of the Helvetiafjellet Formation in general, and the Glitrefjellet Member in particular. Fourteen facies grouped into nine facies association have been defined. The underlying Rurikfjellet Formation consists of prodelta deposits (FA-1) and is overlain by the Helvetiafjellet Formation. The Festningen Member consists of fluvial braidplain deposits (FA-2). The overlying Glitrefjellet Member encompasses a wide range of facies associations. The lowermost part include floodplain deposits (FA-3), crevasse splay deposits (FA-4), fluvial distributary channel deposits (FA-5). The uppermost part of the Glitrefjellet Member includes delta plain deposits (FA-6), delta front deposits (FA-7) and wave-reworked delta deposits (FA-8). The overlying Carolinefjellet Formation consists of offshore transition deposits (FA-9). The results of the facies analysis are compared and correlated to published sections across Svalbard, which has observed an overall thickening towards the south. However, an overall thickening towards the northwest was observed in this thesis. The significant variations in thickness are possibly related to basin subsidence or major fault zones. The depositional model is further compared to some modern analogues to the (Mahakam delta and Pamlico Sound), which is considered to be a close planform. The modern analogues contributes with information with regards to the depositional process and paleogeographic evolution and reconstruction of the Helvetiafjellet Formation shoreline. Of particular interest is the lateral relationship between barrier deposits in Kvalvågen in the east, tidally-influenced estuarine deposits to the west and a transgressive lag documented in the uppermost part of the Glitrefjellet Member to the north in the Adventdalen area. This suggests a large backstepping barrier bar complex.

Acknowledgment

I would first like to thank my supervisor Assoc. Prof. Sten-Andreas Grundvåg (University of Tromsø) for guidance through this thesis. Your advice was always highly appreciated and pointed me towards the right direction when I needed help.

I would also like to thank my co-supervisor, Prof. Snorre Olausen (The University Center in Svalbard) for his advice while logging the cores in Svalbard.

I gratefully acknowledge ARCEX and the Research Council of Norway (grant number 228107) for funding this research and making this master thesis possible.

I would like to express my gratitude to my family for good support through my studies. Special thanks to my sister, Karen Emilie, for making my last years in Tromsø extra enjoyable.

Finally, I must thank my best friend Ingrid Tennvassås for five amazing years in Tromsø! Thank you for memorable hikes, movie nights and the courses we have taken together over the years. I would also like to thank my friends in Tromsø for great memories and for their support. I must also thank Hannah for taking the time to read through the thesis and give me valuable feedback.

Thea Marie Engen

Tromsø, May 2018

Contents

1	Preface.....	1
2	Introduction.....	3
2.1	Background and motivation	3
2.2	Objectives	5
3	Geological setting.....	6
3.1	Introduction to the Mesozoic.....	6
3.1.1	Triassic (252.17—201.3 Ma).....	8
3.1.2	Jurassic (201.3—145.0 Ma)	9
3.1.3	Cretaceous (145.5—66 Ma)	11
3.2	Tectonic framework.....	14
3.2.1	Structural evolution.....	14
3.2.2	HALIP (High Arctic Large Igneous Provinces)	15
3.3	Lithostratigraphy of the Adventdalen Group	15
3.3.1	The Agardhfjellet Formation (Middle Jurassic to earliest Cretaceous).....	15
3.3.2	The Rurikfjellet Formation (Valanginian to early Barremian).....	16
3.3.3	The Helvetiafjellet Formation (Barremian to early Aptian)	17
3.3.4	The Carolinefjellet Formation (Aptian to Albian).....	19
3.4	Depositional architecture of the Helvetiafjellet Formation	19
3.5	Age of the Helvetiafjellet Formation	23
3.6	Palaeo-climatic indicators in the Lower Cretaceous succession	24
3.7	Paleo-eustatic sea-level during the Cretaceous Era	25
4	Methods	27
4.1	Study area	27
4.2	Data collection and analysis	29
4.3	Post data collection work	29
4.4	Reference data.....	30
5	Results – facies analysis.....	31
5.1	Lithofacies.....	31
5.2	Facies associations.....	36
5.2.1	FA-1: Prodelta deposits	40
5.2.2	FA-2: Fluvial braidplain deposits	42
5.2.3	FA-3: Floodplain deposits	44
5.2.4	FA-4: Crevasse splay deposits	46
5.2.5	FA-5: Fluvial distributary channel deposits	48

5.2.6	FA-6: Delta plain deposits	51
5.2.7	FA-7: Delta front deposits	53
5.2.8	FA-8: Wave-reworked delta deposits.....	54
5.2.9	FA-9: Offshore transition deposits	56
5.3	Vertical stacking trends	57
5.3.1	Description	57
5.3.2	Interpretation.....	58
5.4	Sequence stratigraphic surfaces.....	61
5.4.1	Barremian subaerial unconformity	61
5.4.2	Intraformational flooding surface (IFS).....	62
5.4.3	Intraformational unconformities (IU)	63
5.4.4	Transgressive ravinement surface (TRS)	64
5.4.5	lower Aptian flooding surface	65
5.5	Depositional model of the Helvetiafjellet Formation.....	66
5.5.1	Transect 1 - Festningen to Agardhfjellet (W-E).....	66
5.5.2	Transect 2 - Festningen to Kvalvågen (NW-SE)	70
6	Discussion	74
6.1	Revised depositional model of the Helvetiafjellet Formation	74
6.2	Regional depositional trends and controls.....	76
6.2.1	Movements along regional faults, possibly governed by HALIP activity	79
6.2.2	A secondary source area	81
6.3	Modern analogues for the Glitrefjellet Member	83
6.3.1	The Mahakam delta	84
6.3.2	The Pamlico Sound	86
6.4	Depositional evolution and sequence stratigraphic development.....	89
6.4.1	Relative high-sea level: the Rurikfjellet Formation.....	91
6.4.2	Fall in relative sea-level: Barremian SU.....	91
6.4.3	Rise in relative sea-level and high sediment input: IFS.....	92
6.4.4	Continued rise in relative sea-level and high sediment input: IU.....	93
6.4.5	Increased rate in relative sea-level and low sediment input: TRS.....	93
6.4.6	Flooding of the Helvetiafjellet Formation: lower Aptian FS	101
6.4.7	High sea-level: The Carolinefjellet Formation.....	102
7	Conclusions.....	104
8	References.....	107
9	Appendix.....	I

9.1 Appendix A: DH-1 in scale 1:50 cm..... I
9.2 Appendix B: DH-1A in scale 1:50 cm..... VII

1 Preface

In relation to a CO₂ storage project (Braathen et al., 2012), seven fully cored wells were drilled in the Adventpynten and Adventdalen area (DH-1, DH-1A, DH-3, DH-4, DH-5R, DH-6 and DH-7; Fig. 9). The primary targets were the Triassic to Middle Jurassic successions, but Lower Cretaceous succession was also penetrated. The wells DH-5R, DH-6 and DH-7 were the initially targeted wells for this thesis, because they are known to contain well-developed palaeosols. These cores were stored in Endalen outside Longyearbyen. Unfortunately, parts of the road to the core storage facility collapsed prior to the data collection, effectively hindering access to these cores. Therefore the cores DH-1 and DH-1A, stored in a container at UNIS were examined and logged instead. The examination of these cores offers a unique opportunity in describing features within the Helvetiafjellet Formation at a level of detail not achievable in conventional outcrop studies.

Two students (Thea Engen and Ingrid Tennvassås) have been working together on the logging aspect of this project. Although the logging was done together, the two students have different aims for their theses. In thesis 1 (Thea Engen), cores DH-1 and DH-1A are used as a basis for a detailed facies analysis and sedimentological characterization of the Helvetiafjellet Formation in general and the Glitrefjellet Member in particular. In thesis 2 (Ingrid Tennvassås), the described cores are used as a basis for a petrographic characterization of palaeosols in the Glitrefjellet Member of the Helvetiafjellet Formation. This is done with the intention of evaluating the palaeosols potential as palaeo-climatic proxies.

Due to the similarities of the projects, the chapters 1 to 4 were largely written as a collaboration between the two students. From chapter 5 and onward, this thesis will focus on the project objectives of thesis 1.

2 Introduction

2.1 Background and motivation

The Lower Cretaceous succession in Svalbard have received considerable attention in literature. This largely relates to coal prospecting (e.g. Smith & Pickton, 1976; Nemeč, 1992) as well as hydrocarbon exploration efforts between 1960 and the early 1990s (e.g. Nøttvedt et al., 1992). The succession also offers insights into the tectonostratigraphic evolution of the northern Barents Shelf margin and adjacent Arctic terranes, including the opening of the Canada Basin (Maher, 2001) and timing and consequences of igneous activity related to the High Arctic Large Igneous Province (HALIP; Maher 2001; Maher et al., 2004). In addition, parts of the succession have received attention due to the ever-growing interest for the Cretaceous greenhouse climate.

The Lower Cretaceous in Svalbard belongs to the Adventdalen Group and is subdivided into the Rurikfjellet, Helvetiafjellet and Carolinefjellet formations (Mørk et al, 1999). The Rurikfjellet Formation (Valanginian to early Barremian) is mainly dominated by shale, sandstone and siltstone of offshore to shallow marine origin (Midtkandal et al., 2008; Grundvåg & Olausson, 2017). The Helvetiafjellet Formation is divided into the lower Festningen Member and the upper Glitrefjellet Member (Parker, 1967; Nemeč, 1992). The Festningen Member consists of fluvial braidplain deposits (Nemeč, 1992; Midtkandal et al., 2007; Mørk, et al., 1999; Steel, 1977). The overlying Glitrefjellet Member consists of floodplain and isolated fluvial channel deposits and their associated overbank deposits (Edwards, 1976; Steel et al., 1978 ; Midtkandal et al., 2008). The uppermost part of the Helvetiafjellet Formation consists of deltas prograding eastwards into the basin (Edwards, 1979). The Carolinefjellet Formation (Aptian to Albian) represents deposits from inner and outer shelf environments, respectively (Parker, 1967; Nagy, 1970; Midtkandal & Nystuen, 2009; Hurum et al., 2016; Mutrux et al., 2008).

A Barremian subaerial unconformity is present at the base of the Helvetiafjellet Formation and incises down into the underlying Rurikfjellet Formation (Parker, 1967; Midtkandal & Nystuen, 2009). The boundary between the Helvetiafjellet and the Carolinefjellet Formation

is defined by a lower Aptian flooding surface, and makes a conformable transition into the Carolinefjellet Formation (Midtkandal et al., 2016; Grundvåg et al., 2017).

In general, facies analysis has been given a lot of attention over the past decades in order to define a particular sedimentary environment. During the last decades, numerous work has investigated the Helvetiafjellet Formation (Parker, 1967; Birkenmajer, 1984; Edwards, 1976; Nemec et al., 1988; Nemec, 1992; Nøttvedt et al., 1992; Gjelberg & Steel, 1995; Midtkandal et al., 2007; Grundvåg & Olausson, 2017). Overbank deposits are often very fine-grained and thereby difficult to distinguish in the sedimentary record due to weathering and scree cover. Detailed facies analysis of fine-grained overbank deposits remains rare or limited.

The depositional architecture (Fig. 6) of the unit have been debated; the original model for the Helvetiafjellet Formation was the layer-cake model (Parker, 1967; Nagy, 1970). However, a transgressive and diachronous model (Gjelberg & Steel, 2012) evolved from previous studies (Steel & Worsley, 1984; Nemec, 1992; Gjelberg & Steel, 1995). All models however, point to an overall transgressive setting.

The examination of these cores (DH-1 and DH-1A), therefore offers a unique opportunity in describing sedimentary features within the Helvetiafjellet Formation at a level of detail not achievable in outcrop, and may contribute to the understanding of the depositional environment. Correlation panels will be used to observe regional trends, thus providing observations to make a depositional model and detailed paleogeographic maps.

2.2 Objectives

This study uses core data in order to make a detailed facies analysis of the Helvetiafjellet Formation in general, and the Glitrefjellet Member in particular. The detailed facies analysis and interpreted depositional model aims to give a better understanding of the vertical stratigraphic setting and helps to expand the current understanding of the Helvetiafjellet Formation in general. The boundary to the underlying Rurikfjellet Formation and the overlying Carolinefjellet Formation has also been given attention for the purpose of stratigraphic context. Furthermore, the logged cores are compared and correlated to other published sections from different localities in Svalbard (Festningen, Grundvåg, 2017, unpublished; Helvetiafjellet, Gjelberg & Steel, 1995; Glitrefjellet, Midtkandal et al., 2008, Dypvik et al, 1991; Innerknausen, Nemeč, 1992; Myklegardfjellet, Birkenmajer, 1984; Agardhfjellet, Midtkandal & Nystuen, 2009; Ullaberget, Grundvåg, 2017, unpublished; Kvalvågen, Onderdonk & Midtkandal, 2010) in order to better understand the regional stratigraphic context of the Helvetiafjellet Formation.

Based on sedimentological investigations of DH-1 and DH-1A, the specific aims of this thesis are to:

- Provide a detailed facies analysis of the Helvetiafjellet Formation, focusing particularly on the Glitrefjellet Member.
- Interpret observed facies and facies associations in terms of depositional processes and depositional environments, respectively.
- Develop, if possible, criteria that can aid in distinguishing between depositional sub-environments in a predominantly fine-grained paralic succession.
- Compare and correlate the logged cores with previously published sections in order to delineate the regional architecture of the unit and lateral changes in facies
- Discuss the regional sequence stratigraphic development of the Helvetiafjellet Formation and alternative depositional models.

3 Geological setting

The Svalbard archipelago (Fig. 1) represents the uplifted and exposed northwestern corner of the Barents Shelf (Worsley, 2008; Dörr et al., 2013; Grundvåg et al., 2017). The archipelago consists of several islands, with Spitsbergen being the largest (Fig. 1). In the west, the area is bounded by a sheared margin while in the north, it is bounded by a passive continental margin (Faleide et al., 1984; Grogran et al., 1999). In the south and east the area is bounded by the Baltic Shield and Novaya Zemlya, respectively (Steel & Worsley, 1984; Dallmann, 2015; Grundvåg et al., 2017). The timing and causes of uplift of Svalbard and the Barents Shelf is debated, but it has been suggested to be the result of tectonic and magmatic activity in the Mesozoic and the Cenozoic times (e.g. Worsley, 2008; Dörr et al., 2013). Today, the different islands are situated between 74 to 81° N, and 10 to 35° E (Steel & Worsley, 1984; Senger et al., 2014; Fig. 1). The sedimentary record in Svalbard contains sediments ranging in age from Devonian to Eocene (Harland et al., 1976; Grogran et al., 1999; Grundvåg & Olausen, 2017; Fig. 1).

3.1 Introduction to the Mesozoic

The Mesozoic Era can be divided into the Triassic (Fig. 2), Jurassic (Fig. 3) and Cretaceous (Fig. 4) periods, and extends from 252.17 Ma–66 Ma (Mørk, et al., 1999; Cohen et al., 2013; Fig. 5). This was an era dominated globally by climatic and tectonic changes. During the Mesozoic Era, Svalbard was a part of an intracratonic sagbasin which was covered by an epicontinental sea (Midtkandal et al., 2007; Faleide et al., 2008; Midtkandal & Nystuen, 2009; Henriksen et al., 2011; Hurum et al., 2016; Grundvåg & Olausen, 2017).

Epicontinental seas are often recognized as being relatively shallow, generally with a depth of less than 200 m (Midtkandal & Nystuen, 2009). Another characteristic feature is a gently dipping ramp shelf morphology, typically lacking a pronounced shelf-break. The dip of these shelves can be as little as 0.001–1°, often steepening slightly towards the central part of the basin. The gentle gradient of the ramp shelf makes epicontinental seas very sensitive to sea-level change (Midtkandal et al., 2008; Midtkandal & Nystuen, 2009). The exposure of Mesozoic deposits throughout Svalbard is illustrated in Fig. 1. These deposits are generally well preserved.

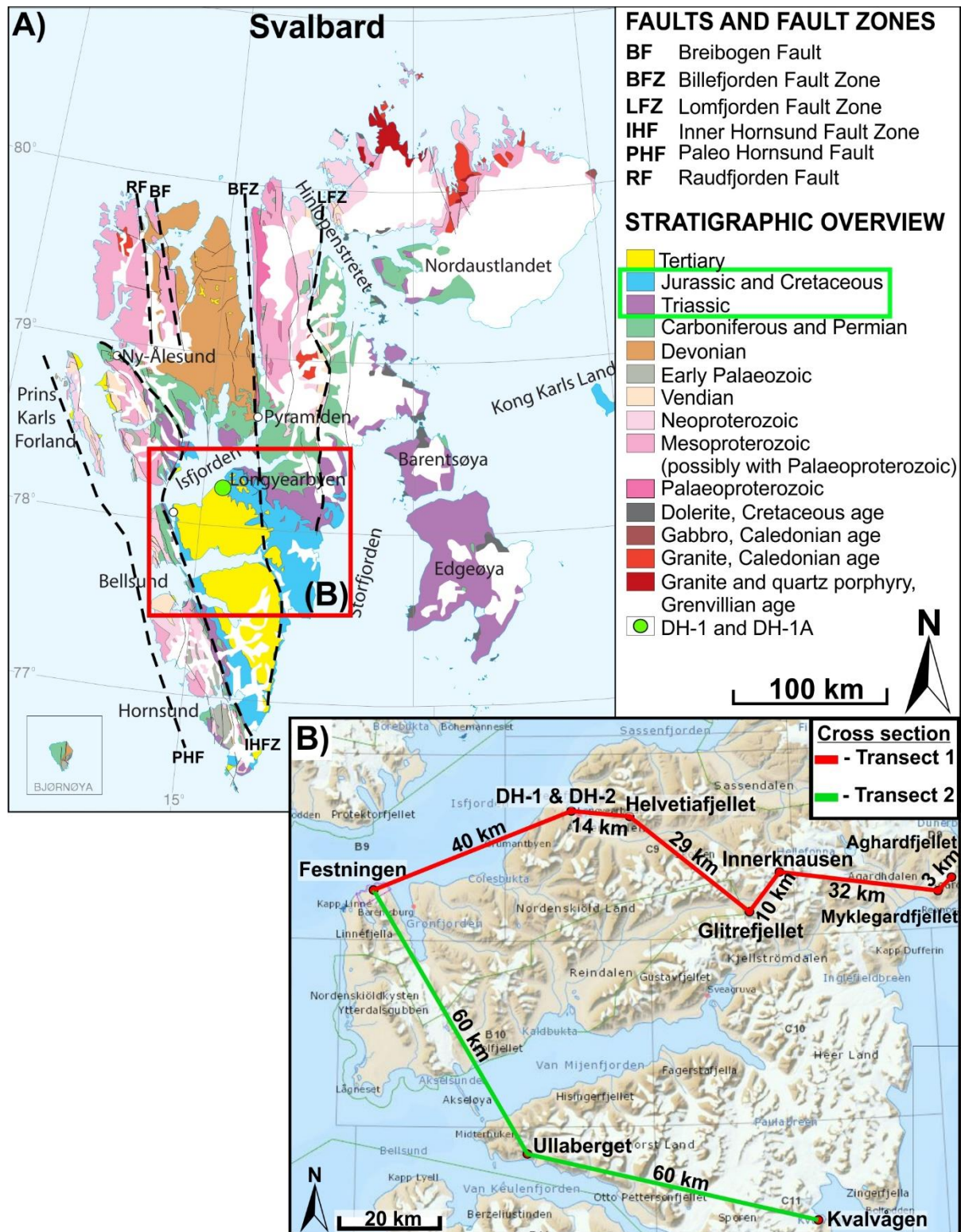


Figure 1: A) Geological map of Svalbard showing the the distribution of sediments deposited at different periods in Svalbard. The green rectangle indicates the important periods in the Mesozoic Era (252.17-66 Ma) for this thesis. The Jurassic and Cretaceous periods (marked by a green square) are represented by a light blue colour, while the Triassic period is displayed in a purple colour. The red square indicates the study area, including the Billefjorden Fault Zone and Lomfjorden Fault Zone, which will be discussed in this study. The green circle indicates where the cores DH-1 and DH-1A are located in Svalbard. B) Study area of the depositional model. Transect 1 is represented by the red line, which goes from west (the Festningen locality) to east (the Agardhfjellet locality). The transect is approximately 128 km from west to east. Transect 2 is represented by the green line, which goes from northwest (the Festningen locality) to southeast (the Kvalvågen locality). The transect is approximately 120 km from northwest to southeast. Map A is modified from Elvevold et al. (2007) and map B is retrieved from <http://toposvalbard.npolar.no>.

3.1.1 Triassic (252.17–201.3 Ma)

Triassic is the first period of the Mesozoic Era (Mørk et al, 1999). It extends from 252.17–201.3 Ma (Cohen et al., 2013; Fig. 5). The period can be further subdivided into the Early, Middle and Late Triassic Epochs (Fig. 2). In Svalbard, stable shelf conditions and fluctuating sea-level are characteristic for the Triassic Period (Buchan et al., 1965; Mørk et al, 1982; Faleide et al., 1984; Mørk et al, 1999; Fig. 2). As a result, the Triassic succession largely consists of both marine and non-marine shales, siltstones and sandstones (Buchan et al., 1965; Nakrem et al., 2008). The sedimentary deposits display a varying thickness, changing from a maximum thickness of as little as 200 m to approximately 1000 m at its thickest (Buchan et al, 1965). In Svalbard, the Lower to Middle Triassic deposits are represented within the Sassendalen Group, while the Upper Triassic succession belongs to the Kapp Toscana Group (Buchan et al., 1965; Mørk et al., 1999).

Triassic

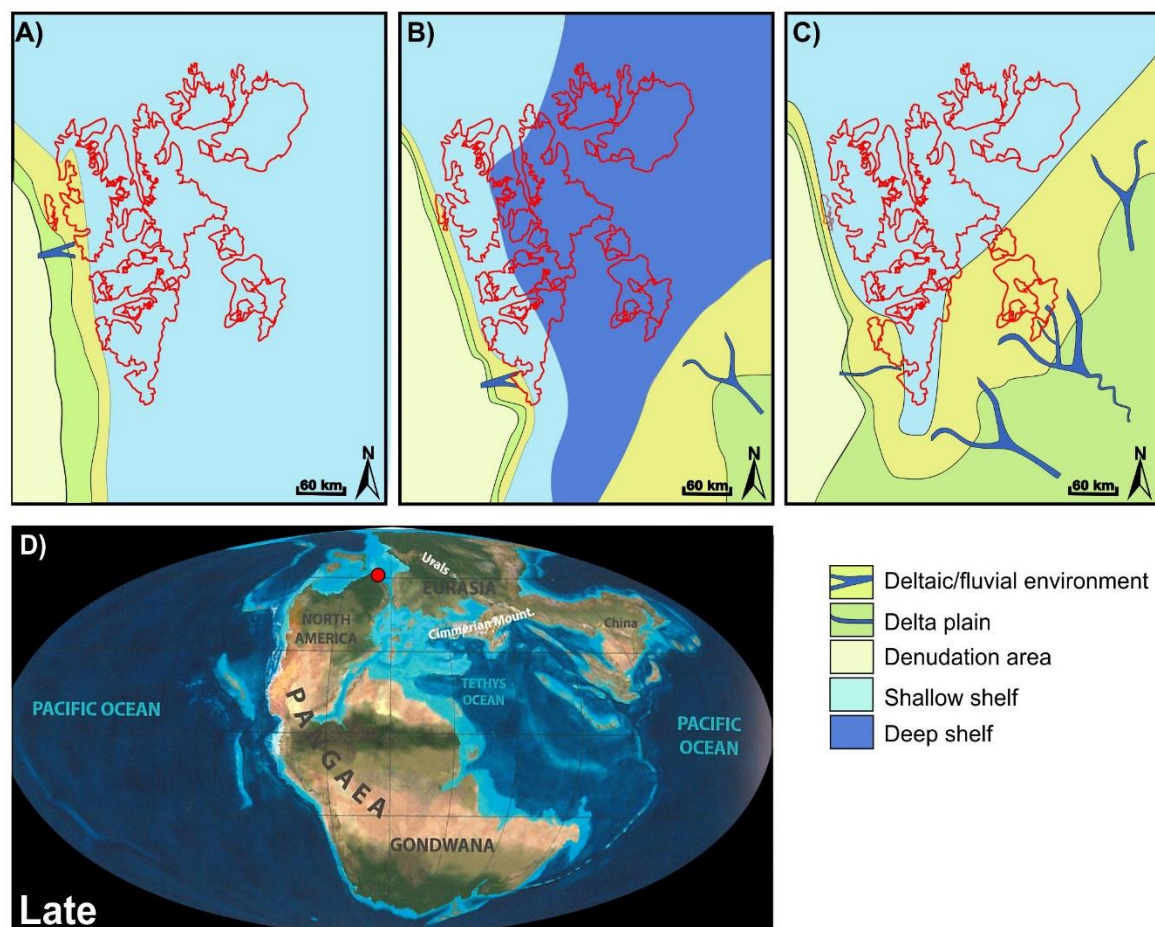


Figure 2: Illustration of the fluctuating sea level conditions throughout Early (A), Middle (B) and Late (C) Triassic. The variation in depositional conditions during Triassic has resulted in a variety of deposits, such as shales, siltstone and sandstone. Palaeogeography during Late Triassic is illustrated in image D) The approximate position of Svalbard is indicated with a red circle. The figure is not to scale and is modified from Dallmann (2015).

3.1.2 Jurassic (201.3—145.0 Ma)

Jurassic is the middle period of the Mesozoic Era. The period extends from 201.3—145.0 Ma, and can be further subdivided into the Early and Late Jurassic Epochs (Cohen et al., 2013; Fig. 5). The dissolution of the supercontinent Pangea began during Early Jurassic. By the end of Late Jurassic, two continents were fully formed; Laurasia in the north, and Gondwana in the south (Dallmann, 2015; Fig. 3).

The Jurassic period as a whole was dominated by several cycles of eustatic sea-level fluctuations (Fig. 8). In Late Jurassic, the sea-level rose once more. This led to the formation of an epicontinental sea in the Svalbard region (Fig. 3 B). The seafloor topography of an epicontinental sea is not ideal for ocean currents, and in combination with high CO₂ levels, large amounts of organic matter were produced and stored. The shales deposited in the Late Jurassic, suggest anoxic shelf environments. Today, the Upper Jurassic succession has been proven as a valuable source rock of the Barents Shelf (Steel & Worsley, 1984; Nøttvedt & Johannessen, 2013; Dallmann, 2015; Fig. 7).

The Lower Jurassic succession is represented within the Kapp Toscana Group, while the Upper Jurassic deposits can be seen within the Adventdalen Group. For further discussion of the Adventdalen Group, and the formations it includes, please see chapter 3.3.

Jurassic

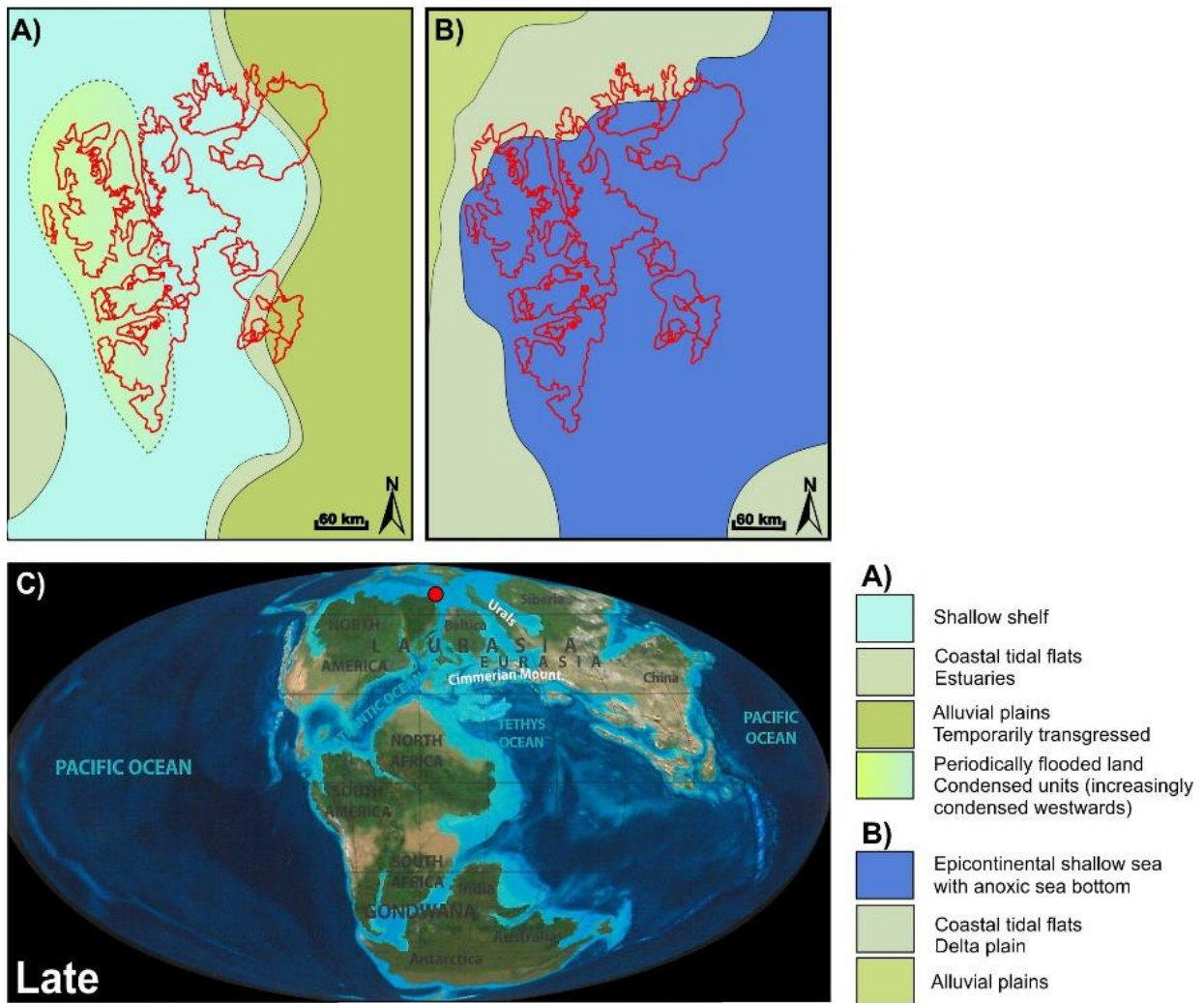


Figure 3: Illustration of the development of Svalbard during the Jurassic period. Several periods of eustatic sea-level rise and subsequent fall have been documented throughout both Early (A) and Late (B) Jurassic. The Jurassic period culminated in a relative sea level fall, where large shale successions were deposited. Global palaeogeography during Late Jurassic is illustrated in image C) The approximate position of Svalbard is indicated with a red circle. The figure is not to scale and is modified from Dallmann (2015).

3.1.3 Cretaceous (145.5—66 Ma)

The Cretaceous is the final period of the Mesozoic Era (Fig. 5). Sediments found in the rock recorded with an age ranging from 145.5 Ma to 66 Ma are considered to have been deposited in the Cretaceous period. The period is subdivided into the Early Cretaceous (145 Ma- 100.5 Ma) and the Late Cretaceous Epochs (100.5 Ma–66 Ma) (Cohen et al., 2013; Fig. 4).

In Svalbard, regional uplift took place in the Late Cretaceous, thus effectively removing Upper Cretaceous strata (Harland, 1969; Faleide et al., 1984; Steel & Worsley, 1984). As a result, only the Lower Cretaceous succession is preserved in Svalbard. Therefore, only the sediments deposited during the Early Cretaceous will be discussed further.

During the Cretaceous period, the opening of the Canada Basin, as well as the later parts of the Amerasian Basin, took place (Grantz et al., 2011). This led to volcanic activity and the following emplacement of the High Arctic Large Igneous Province (HALIP) (Maher, 2001; Maher et al., 2004; Brekke & Olausen, 2013; Senger et al., 2014). The HALIP activity caused most severe uplift in the northwestern part of the Svalbard archipelago (Dörr et al., 2011; Fig. 4). As a result, the sedimentary package of the Lower Cretaceous decreases in thickness towards the northwest (Parker, 1967; Nagy, 1970). A change from a more than 1000 m thick sedimentary package in the south to an approximate package thickness of 300 m in the north can be observed.

In Svalbard, the Lower Cretaceous succession is accompanied by the Upper Jurassic deposits within the Adventdalen Group. For the lithostratigraphic features of the Adventdalen Group, please see chapter 3.3.

Cretaceous

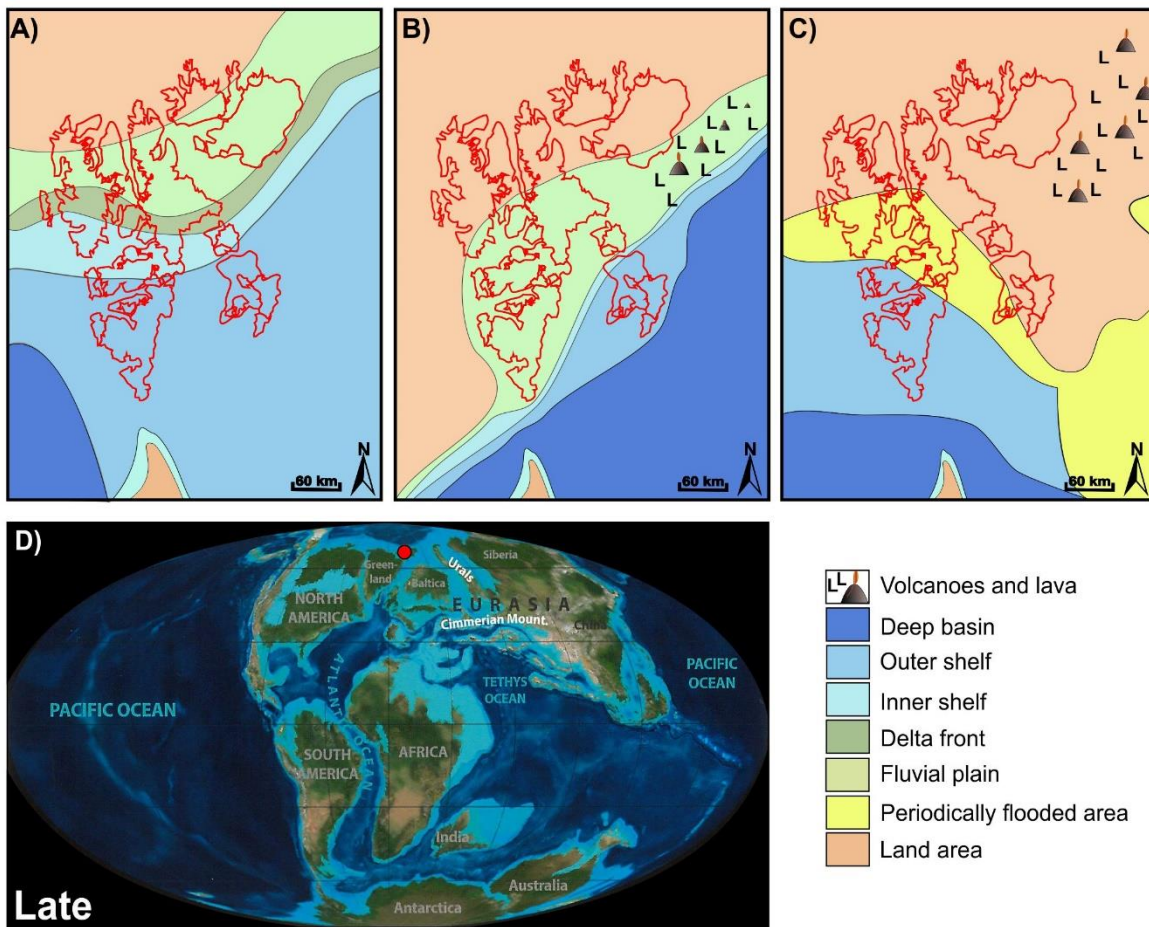


Figure 4: Geological illustration of the dominating depositional environment of the Cretaceous period. Illustration A-C represents a paleogeographic reconstruction of the Rurikfjellet Formation (A), the Helvetiafjellet Formation (B) and the Carolinefjellet Formation (C). A regional uplift occurred throughout the period (A-C), caused by crustal doming and HALIP activity. This is interpreted to have caused the removal of the Upper Cretaceous succession. Global palaeogeography during Late Cretaceous is illustrated in image D) The approximate position of Svalbard is indicated by a red circle. The figure is not to scale and is modified from Dallmann (2015).

3.2 Tectonic framework

3.2.1 Structural evolution

The collapse of the early Paleozoic orogen in the Early Devonian marks the beginning of the structural evolution that would later lead to the uplift and exposure of the Svalbard archipelago (Mørk et al., 1999). After the collapse, several basins were formed due to extensional rifting (Steel & Worsley, 1984; Grogran et al., 1999). With the onset of the Svalbardian orogen in the Late Devonian, rift basins that formed during the Early Devonian were compressed. Although the area has been documented as more stable from here on out, the Middle Carboniferous period (and some intervals throughout Permian) was dominated by discrete regional extensional events (Nøttvedt et al., 1992; Grogran et al., 1999).

Regional uplift in the Late Cretaceous and Tertiary also led to the reactivation of older fault systems. These were primarily the Lomfjorden/Agardhbukta and Billefjorden Fault Zones during the Cretaceous (Onderdonk & Midtkandal, 2010; Fig. 1), and the Inner Hornsund and Palaeo-Hornsund Fault Zones during Tertiary (Steel & Worsley, 1984; Grogran et al., 1999; Fig. 1). The uplift of Svalbard, caused by the reactivation of fault systems, led to erosion during the Late Cretaceous (Dörr et al., 2011).

The most recent major tectonic event in the structural evolution in Svalbard is the Paleogene development of the West Spitsbergen Fold Belt (WSFB) (Harland, 1969; Steel & Worsley, 1984; Steel et al., 1985; Fig. 8). The WSFB is north-north west to south-southeast trending, and extends along the western coast of Svalbard for approximately 300 km. The belt is approximately 50 km wide (Steel & Worsley, 1984). The onset of the WSFB is related to the opening of the Norwegian-Greenland Sea, which is seen as a major continental transform fault (Harland, 1969; Steel & Worsley, 1984; Dörr et al., 2011). An associated foreland basin, the Central Tertiary Basin, consists of a relatively broad north-northwest to south-southeast trending syncline, formed as a foreland basin of the WSFB (Müller & Spielhagen, 1990; Dörr et al., 2011). As a result, the Lower Cretaceous succession can be observed as relatively steeply dipping to the east along the western coast of Spitsbergen. Whereas to the east of Spitsbergen (and the rest of Svalbard), the strata is observed as relatively horizontal.

3.2.2 HALIP (High Arctic Large Igneous Provinces)

In association with fast-moving sea-floor spreading and the opening of the Canada Basin, the magmatic activity rose. As a result, the basaltic Alpha Ridge formed during Early Cretaceous (Lane, 1997; Grogran et al., 1999; Maher, 2001). Also emplaced during the Early Cretaceous was the High Arctic Large Igneous Province (HALIP) (Maher, 2001; Corfu et al., 2013; Senger et al., 2014). Such large igneous provinces are generally characterized as very large, predominantly mafic magmatic bodies (Coffin & Eldholm, 1994; Corfu et al., 2013). They can be observed as both extrusive and intrusive units. In Svalbard, the HALIP emplacement can today be observed as predominantly sills, but also occasionally as dykes, and as basalt flows in the east (Maher, 2001; Senger et al., 2014; Polteau et al., 2016; Fig. 4).

The extensive intrusion caused by the HALIP led to crustal updoming. Tectonic activity was therefore not the only cause for the uplift of Svalbard and the northern margin of the Barents Shelf in the Early Cretaceous. The crustal updoming is interpreted as the cause for the tectonically forced regression which led to the formation of the Barremian subaerial unconformity at the boundary between the Rurikfjellet and the Helvetiafjellet formations (Gjelberg & Steel, 1995; Maher, 2001).

3.3 Lithostratigraphy of the Adventdalen Group

The Adventdalen Group (Parker, 1967; Fig. 7) consists of four formations: the Agardhfjellet, the Rurikfjellet, the Helvetiafjellet, and the Carolinefjellet, respectively (Parker, 1967; Birkenmajer, 1975; Fig. 7). In this section, the characteristics of these four formations will be highlighted. Special attention will be given to the Helvetiafjellet Formation and its members, as they are the focal point of this study.

3.3.1 The Agardhfjellet Formation (Middle Jurassic to earliest Cretaceous)

The Agardhfjellet Formation (Fig. 7) is the oldest unit within the Adventdalen Group. The formation is Middle to Late Jurassic in age, and is commonly subdivided into four members. The lowermost member is the Oppdalen Member, which is dominated by silty sediments. The overlying member is mainly organic-rich sediments, known as the Lardyfjellet Member (Dypvik et al., 1991; Koevoets et al., 2018). The next member is the Oppdalssåta Member, which primarily consists of sandstone and siltstone. Similar to the Lardyfjellet Member, the

top member within the formation is also dominated by organic-rich mudstone. This member is known as the Slottsmøya Member, which is dated to be of Tithonian age (Harland & Kelly, 1997; Olausen, 2015; Koevoets et al., 2016).

The formation varies in thickness throughout the Svalbard archipelago. This can be seen as a decrease in thickness when moving in a west-to-east direction. The formation is approximately 250 m thick in the central part of Spitsbergen in the west, whereas it is reduced to a unit that is less than 50 m thick on Kong Karls Land in the east. This change in thickness is believed to be caused by erosion prior to the deposition of the Early Cretaceous Helvetiafjellet Formation (Collignon & Hammer, 2002; Olausen, 2015).

Because the Agardhfjellet Formation contains large quantities of organic material, it has proven to be an important source rock for hydrocarbon formation. An example here is in the time and lateral equivalent Hekkingen Formation, which is found in several basins on the southwest Barents Shelf (Mørk et al., 1999).

The boundary between the Agardhfjellet Formation and the overlying Rurikfjellet Formation is generally recognized as a light-coloured claystone bed, known as the Myklegardfjellet Bed (Dypvik et al., 1991; Collignon & Hammer, 2002; Smelror & Dypvik, 2006; Fig. 7). However, this bed may be poorly developed, thus making it difficult to distinguish the Agardhfjellet Formation from the Rurikfjellet Formation. Where this is the case, both the Agardhfjellet Formation and the Rurikfjellet Formation are combined and referred to as the Janusfjellet Subgroup (Parker, 1967; Dypvik et al., 1991; Grundvåg, et al., 2017).

3.3.2 The Rurikfjellet Formation (Valanginian to early Barremian)

The Rurikfjellet Formation (Fig. 7) is the second unit in the Adventdalen Group, and the lowermost unit of the Lower Cretaceous succession. The formation is Valanginian to Barremian in age (Grøsfjeld, 1992), and has a recorded maximum thickness of up to 400 m (Midtkandal & Nystuen, 2009). The formation can also be referred to as a part of the Janusfjellet Subgroup in areas where the Myklegardsfjellet Bed is not present and separation from the Agardhfjellet Formation is problematic (Fig. 7).

The Rurikfjellet Formation has two recognized members. The lower member is the shaley Wimanfjellet Member (Dypvik et al., 1991). This is overlain by the Kikutodden Member, which is more dominated by sandstone and siltstone (Midtkandal et al., 2008).

3.3.3 The Helvetiafjellet Formation (Barremian to early Aptian)

The Helvetiafjellet Formation (Parker, 1967; Fig. 7) contains mainly coarse-grained braidplain deposits in its lower part, changing upwards into coastal plain and shallow marine facies in its uppermost member (Steel & Worsley, 1984; Nemeč, 1992; Gjelberg & Steel, 1995). There is an abrupt erosional contact between the Rurikfjellet Formation and the overlying the Helvetiafjellet Formation, which can be seen as a change in lithologies from a marine to a fluvial environment (Birkenmajer, 1984; Grundvåg et al., 2017). This boundary is recognized as a Barremian subaerial unconformity (Parker, 1967; Nemeč, 1992; Midtkandal & Nystuen, 2009; Midtkandal et al., 2016; Fig. 7). This unconformity represents a sudden drop in relative sea-level due to tectonic uplift related to HALIP activity (Gjelberg & Steel, 1995; Maher, 2001; Maher et al., 2004; Figs. 7, 10 & 11). The unconformity is regionally extensive and can be observed throughout Svalbard (Nemeč et al., 1988; Gjelberg & Steel, 1995; Maher, 2001; Midtkandal & Nystuen, 2009; Grundvåg & Olausen, 2017). The architecture and facies stacking of the formation reflect a long-term transgression subsequent to the forced regression that formed the subaerial unconformity (Nemeč, 1992; Gjelberg & Steel, 1995; Grundvåg & Olausen, 2017).

The Helvetiafjellet Formation has a varying thickness, from up to 150 m in south-southeast of Spitsbergen to approximately 40 m in the northeast (Gjelberg & Steel, 1995; Brekke & Olausen, 2013). The formation is diachronous and is observed as progressively younger northwards (Steel & Worsley, 1984; Gjelberg & Steel, 1995; Midtkandal & Nystuen, 2009). The Helvetiafjellet Formation has two recognized members. These are the Festningen Member at the base and the overlying Glitrefjellet Member (Parker, 1967; Midtkandal, Nystuen & Nagy, 2007; Fig. 7).

3.3.3.1 *The Festningen Member*

The lowermost unit of the Helvetiafjellet Formation is the Festningen Member (Parker, 1967; Figs. 10 & 11). The base of the member is defined by a Barremian subaerial unconformity, which is dated to be 127 Ma (Parker, 1967; Edwards, 1976; Midtkandal & Nystuen, 2009). It is commonly agreed upon that the deposits of the Festningen Member are primarily fluvial in origin (Steel, 1977; Nemeč, 1992; Mørk et al., 1999). The deposition of the Festningen Member is interpreted to have commenced as a result of relative sea-level rise during Early

Cretaceous, subsequent to the Barremian uplift and the creation of continental accommodation space that followed (Midtkandal & Nystuen, 2009). Despite the clastic input being relatively high, the deposition took place in a backstepping manner (Nemec, 1992; Gjeldberg & Steel, 1995; Midtkandal & Nystuen, 2009). The large-scale cross bedding that is seen in the sandstone units in the member are interpreted to owe their geometry to migration of composite sand and gravel bars in a fluvial braidplain setting (Birkenmajer, 1984; Nemec, 1992). The fluvial facies may locally alternate or interfinger with floodplain, crevasse splay, bay head delta deposits or fluvial mouth bars (Gjelberg & Steel, 1995; Midtkandal et al, 2008; Fig. 20). The Festningen Member consist of medium to very-coarse grained sandstone and conglomerates. These deposits are interpreted to be deposited in a low-gradient braidplain setting (Nemec, 1992; Midtkandal et al., 2007; Midtkandal & Nystuen, 2009; Grundvåg et al., 2017). The lower parts of the Festningen Member display lateral thickness variations, indicating that sediment accumulations were controlled by an incised valley topography (Midtkandal & Nystuen, 2009; Grundvåg et al., 2017). The upper part of the member is characterized by a coal layer at some locations, possibly reflecting a semi-regional flooding (Grundvåg et al., 2017; Figs. 18, 19 & 20).

3.3.3.2 The Glitrefjellet Member

In general, the Glitrefjellet Member is mainly dominated by mudstone. However, sandstone is most prominent in the cores (Figs. 10 & 11). The Glitrefjellet Member consists of coarse-grained sandstones with cross-bedding, ripple cross-lamination, an abundance of plant debris, interbedded silty shales with thin coal seams, and subordinate conglomerate (Parker, 1967; Birkenmajer, 1984). The sedimentary units of the Glitrefjellet Member are, due to basinal subsidence and a relative rise in sea-level, interpreted to have been deposited as a part of a delta plain. The deposition occurred under overall transgressive conditions (Gjelberg & Steel, 1995; Midtkandal et al., 2008; Chp. 3.4). Therefore the marine influence generally increases upwards towards the boundary to the overlying Carolinefjellet Formation, where there is an abrupt deepening across a regional marine flooding surface of early Aptian age (Midtkandal et al., 2016; Grundvåg et al., 2017).

3.3.4 The Carolinefjellet Formation (Aptian to Albian)

The Carolinefjellet Formation (Fig. 7) is the youngest formation of the Adventdalen Group. The formation is Aptian to Albian in age, and has a maximum recorded thickness of 850 m (Nagy, 1970; Steel & Worsley, 1984; Dypvik et al., 2002). The formation consists of five units: the Dalkjegla, the Innkjegla, the Langstakken, the Zillberget and the Schönrockfjellet members (Fig. 7). These members alternate between being dominated by sandstone and mudstone, respectively. The formation is interpreted to have been deposited in a more marine-influenced environment than the underlying Helvetiafjellet Formation (Nagy, 1970; Gjelberg & Steel, 1995; Maher et al., 2004; Grundvåg, 2015; Hurum et al., 2016). Traditionally, the boundary between the Helvetiafjellet Formation and the base of the overlying Carolinefjellet Formation have been described as gradational (e.g. Gjelberg & Steel, 1995; 2012). However, in more recent studies, a relatively thick (approx. 10–30 m) black shale unit of early Aptian age has been suggested as the transition between the two formations (Midtkandal et al., 2016; Grundvåg et al., 2017). This unit has been recognized across most of the outcrop window in Spitsbergen. The upper part of the Carolinefjellet Formation is truncated by the Palaeocene unconformity. This is interpreted as a consequence of uplift and erosion. The truncation corresponds to a major hiatus in sedimentation, equivalent to the Late Cretaceous to earliest Tertiary time interval. Therefore, no Upper Cretaceous strata is present in Svalbard (Grundvåg, 2015; Hurum et al., 2016; Smelror & Larssen, 2016).

3.4 Depositional architecture of the Helvetiafjellet Formation

The Helvetiafjellet Formation was first named by Parker (1967) with its subdivision into the Festningen Member and overlying Glitrefjellet Member. Gjelberg and Steel (1995) found it difficult to use this subdivision of the formation in many of the locations on Spitsbergen because the boundary between the two members was observed as repeated, interfingering and difficult to define. The Helvetiafjellet Formation records a gradual facies change upwards, reflecting a transgressive setting (Gjelberg & Steel, 1995; Fig. 6). Midtkandal et al (2008) re-established the Festningen Member in the lower part and the Glitrefjellet Member in the upper part of the Helvetiafjellet Formation.

Several contributions have discussed the regional depositional system of the Helvetiafjellet Formation. These are summarized in Fig. 6. The first depositional model was presented by Parker (1967) and later modified by Nagy (1970), and is known as the layer-cake model. This model suggests that the basal Helvetiafjellet Formation depositional system was deposited with a sheet-like geometry at a very low angle shelf or platform. As the figure illustrates, the units covered large areas of Spitsbergen (Midtkandal & Nystuen, 2009). However, it did not take into account how the system developed outside of the outcrop window. Several attempts have been made in order to illustrate this development. However, many stratigraphic correlation problems were encountered which led to the abandonment of this model.

A regressive-transgressive model (Steel & Worsley, 1984; Nemec, 1992) explains how the Rurikfjellet and Helvetiafjellet formations are stratigraphically linked by the transition between braided stream and mouth bar deposition. This leads to an overall transgressive development. Based on this, a more complex transgressive diachronous model was suggested by Gjelberg & Steel (1995). This model is similar to the regressive-transgressive model, but gives a better understanding of the backstepping trend with inferred delta lobes pinching out within the outcrop window. This model contains a shoreline, possibly a shelf-break and a maximum regression point just south of the present-day coastline in Svalbard. The self-break model also suggests thick, sandy basin-floor fans offshore (Steel et al., 2000). Midtkandal & Nystuen (2009) argued for a model similar to the layer-cake model. This model shows aggrading facies belts in large scale with a regression-transgression point which can be found somewhere out on the Barents Shelf.

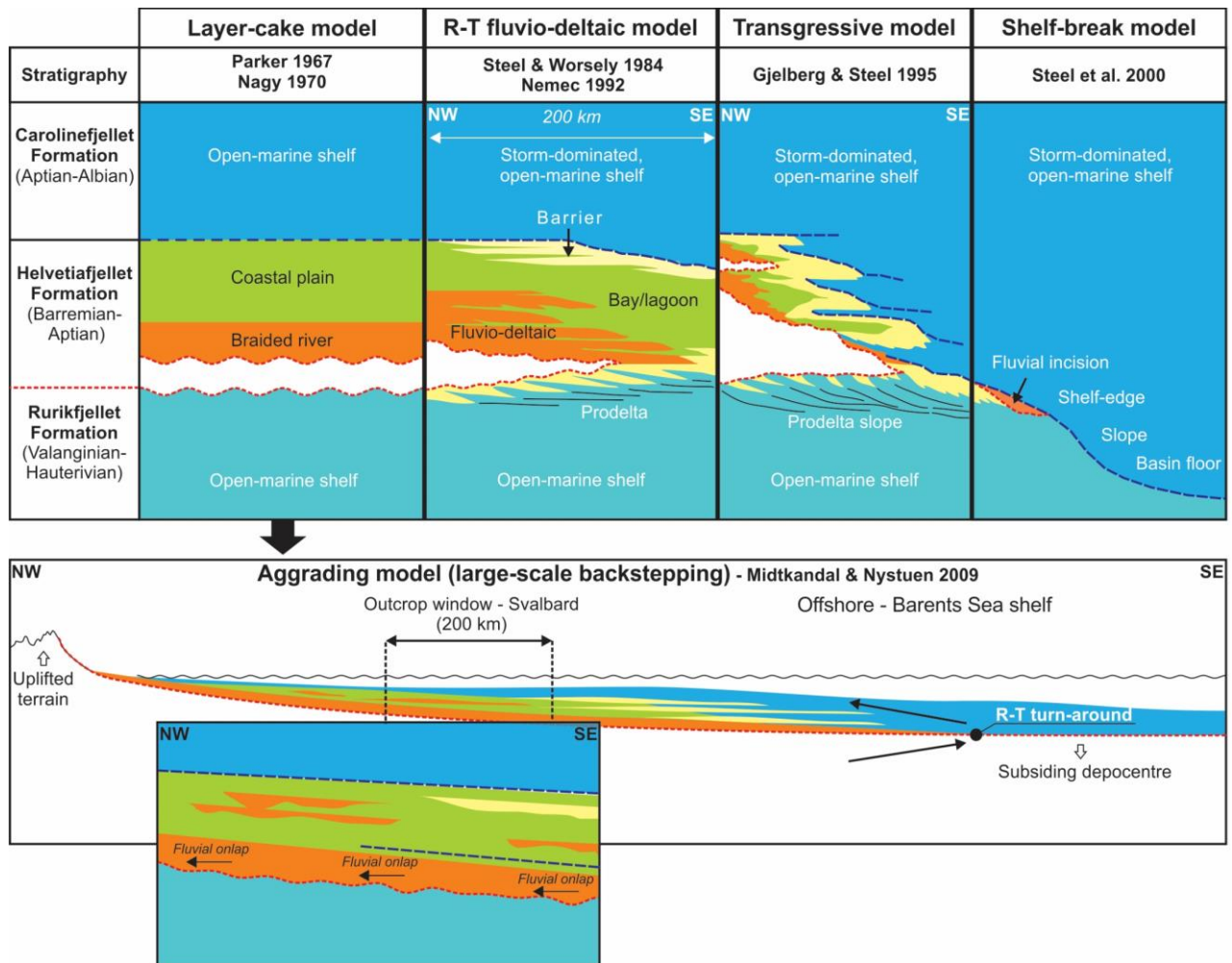


Figure 6: Simplified summary of previous depositional models showing the development of the Helvetiafjellet Formation. Modified from Nemec et al. (1988), Nemec (1992), Gjeldeberg & Steel (1995), Steel et al. (2000), Midtkandal & Nystuen (2009), and Grundvåg & Olaussen (2017). See chapter 3.4 for further details.

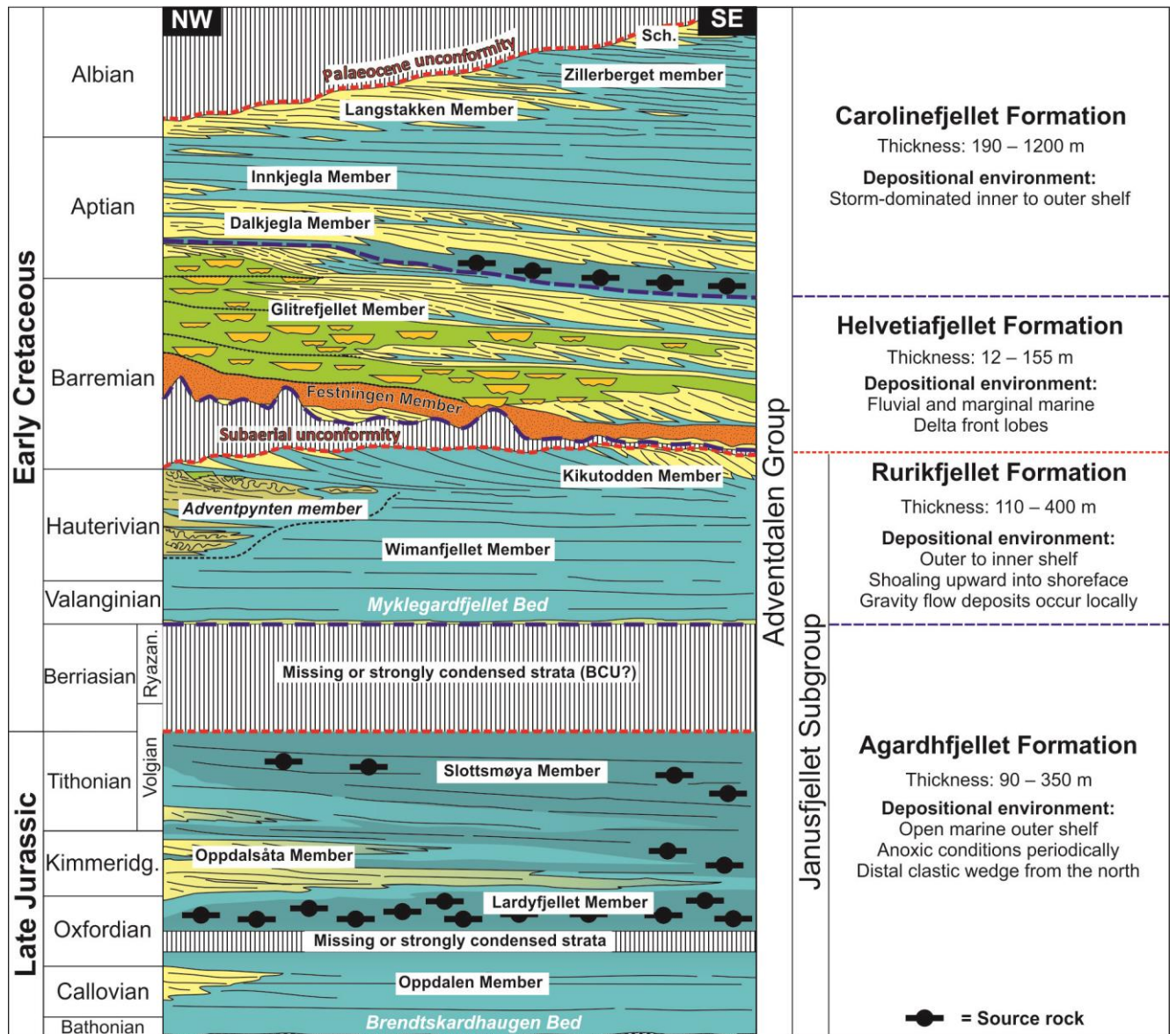


Figure 7: Cross-section from north-west to south-east illustrating the current lithostratigraphic understanding of the Rurikfjellet, Helvetiafjellet and Carolinefjellet formations. Retrieved from Grundvåg & Olaussen (2017).

3.5 Age of the Helvetiafjellet Formation

The age of the Lower Cretaceous succession in Svalbard has been a long-standing problem with regards to geological age (Parker, 1967; Grøsfjeld, 1992; Midtkandal et al., 2008; Vickers et al., 2017). Biostratigraphy is regarded as the traditional way to date a sedimentary succession. In the Helvetiafjellet Formation, however, macrofossils are scarce, making the dating of the succession problematic. Therefore, it was until recently common practice to use lithostratigraphy and relative ages as the primary tool for defining the age of the Helvetiafjellet Formation. Plant- and microfossils and dinoflagellate were also used when possible (Århus, 1992; Grøsfjeld, 1992; Hurum et al., 2016).

The discovery of bentonites within the Helvetiafjellet Formation offered a more precise way to determine the age of the formation (Corfu et al., 2013; Midtkandal et al., 2016; Polteau et al., 2016; Vickers et al., 2017). In this section, the age of the Helvetiafjellet Formation will be discussed with references to both biostratigraphy and bentonite dates.

Parker (1967) was the first to mention the age of the Helvetiafjellet Formation. The formation was assigned a Barremian age, based on ammonites and bivalves in the over and underlying formations.

Lower Cretaceous dinoflagellate assemblages were detected in both the underlying Rurikfjellet Formation and the Helvetiafjellet Formation (Grøsfjeld, 1992). Though the dinoflagellate assemblage could not be used to date the Helvetiafjellet Formation directly, the assemblage contributed to defining the age of the underlying formation, the Rurikfjellet Formation. This formation was defined as being Valanginian and Valanginian to Hauterivian in age, and early Barremian in its uppermost part (Grøsfjeld, 1992; Midtkandal et al., 2008; Grundvåg et al., 2017). Knowing that the overlying Carolinefjellet Formation was Aptian in age, a Barremian age was suggested for the Helvetiafjellet Formation (Grøsfjeld, 1992).

Based on biostratigraphic data, the subaerial unconformity that defines the transition from the Rurikfjellet Formation to the Helvetiafjellet Formation is believed to be earliest Barremian in age (Grøsfjeld, 1992; Grundvåg et al., 2017). It is therefore commonly referred to as the Barremian subaerial unconformity.

The discovery of bentonite layers in several of the onshore CO₂ wells in Svalbard (e.g. wells DH-3 and DH-5R; Fig. 9) within the upper part of the Helvetiafjellet Formation, and in close proximity to the lithostratigraphical boundary between the Helvetiafjellet Formation and the Carolinefjellet Formation (Fig. 7) provided a more reliable method of dating the formation. The bentonites found within the Helvetiafjellet Formation were dated to an age of 123.3±0.2 Ma, indicating a Barremian age for the formation (Corfu et al., 2013; Midtkandal et al., 2016; Polteau et al., 2016; Vickers et al., 2017). The transition from the Helvetiafjellet to the Carolinefjellet Formation was not as easily dated, and has a broader age of Barremian-Aptian transition. This corresponds to approximately 121-122 Ma in age (Midtkandal et al., 2016).

3.6 Palaeo-climatic indicators in the Lower Cretaceous succession

The Cretaceous period is known as one of the warmest periods recorded in Earth's history (Nemec, 1992; Harland & Kelly, 1997). This is interpreted to be related to overall greenhouse conditions on Earth, which prevented permanent ice caps from forming in polar areas (Hallam, 1985; Nemec, 1992; Grundvåg & Olausson, 2017). Consequently, the eustatic sea-level rose (Fig. 8). In the Early Cretaceous period, the Svalbard archipelago was located at 63 to 66 °N (Torsvik et al., 2012; Hurum et al., 2016). The area was dominated by a relatively warm climate when considering its latitude at the time, with a mean temperature of 7-10°C (Hurum et al., 2016 A; Grundvåg & Olausson, 2017).

During the Barremian, the temperature gradients were low, and the overall climate was relatively humid. This is supported by findings of coal seams, seatearths and transported tree remains, which also suggests abundant vegetation (Nemec, 1992; Harland et al., 2007). Traces from several different dinosaur species have also been observed within the Lower Cretaceous succession (Heintz, 1962; Hurum et al., 2016). Examples here are Ornithopod and Iguanodon traces, observed within the Festningen Member of the Helvetiafjellet Formation. This furthermore supports the theory that the Early Cretaceous in Svalbard was dominated by abundant vegetation, which was luxuriant enough to support a herbivore dinosaur population (Heintz, 1962; Nemec, 1992; Hurum et al., 2016).

However, there has been some debate with regards to the climate in the Early Cretaceous in Svalbard. Despite the abovementioned indicators of an at least seasonally warm climate, observations that contradict this have also been made. Belemnites have been reported within the Lower Cretaceous succession in Svalbard, and were identified as Arctic belemnites

(Harland & Kelly, 1997; Price & Nunn, 2010). Glendonites ($\text{CaCO}_3 \cdot 6\text{H}_2\text{O}$), which are calcite pseudomorphs of the mineral ikaite (Suess et al., 1982), alongside observations of potential ice rafted debris, are both indicative of cold, polar oceanic conditions (Harland & Kelly, 1997; Price & Nunn, 2010; Hurum et al., 2016 A). This suggests that the shelf area of Svalbard was at least periodically influenced by polar water during the Early Cretaceous, rather than solely being dominated by warm climatic conditions (Price & Nunn, 2010; Grundvåg & Olausen, 2017).

3.7 Paleo-eustatic sea-level during the Cretaceous Era

A change in global sea-level can in general influence the formation and preservation of deposits, as it can change by several meters. It may, therefore, be used as evidence to local relative sea-level rise or fall. Facies analysis can therefore be used in order to locate relative sea-level changes. The main factors causing the variations are volume of land ice and changes in oceanic ridge systems (Donovan & Jones, 1979).

The relative sea-level cycle (Fig. 8) was first published by Vail et al (1977). It has later been revised by e.g. Haq et al (1987; 1988). Significantly variations in the eustatic sea-level has been recorded since Precambrian (Fig. 8).

During Early Cretaceous the sea-level was generally rising (Ramkumar, 2016; Fig. 8). Haq (2014) argues that the sea-level during the Cretaceous was much higher than the present day mean sea-level. The greenhouse climate was one of the warmest periods in Earth's history (Nemec, 1992; Harland & Kelly, 1997), which gave rise to very high eustatic sea-level (Markwick & Rowley, 1998), by preventing formation of major permanent ice caps at the Earth (Hallam, 1985). However, there has been some debate with regards to the relative sea-level in Svalbard. A general agreement is an overall transgressive trend (Nemec et al., 1988; Gjelberg & Steel, 1995; Grundvåg & Olausen, 2017), with is in accordance with the eustatic sea-level curve (Fig. 8).

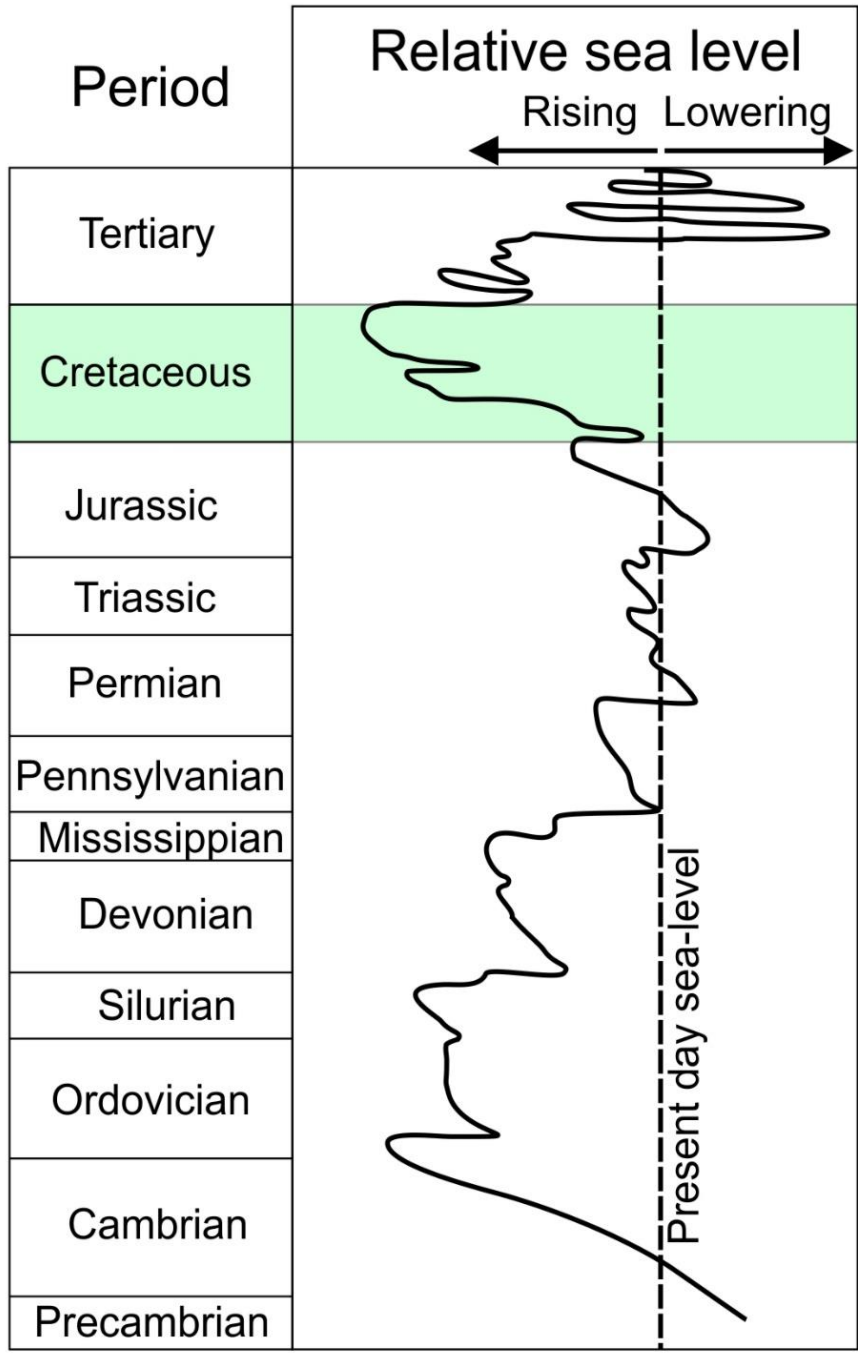


Figure 8: Eustatic sea-level curve showing the rising and lowering of relative sea-level compared to the present day sea-level. Note the high eustatic sea-level during the Cretaceous Era. Based on Vail et al. (1977) and Ramkumar (2016).

4 Methods

4.1 Study area

Seven wells were drilled in Adventdalen in proximity to Longyearbyen (Fig. 9). The wells were drilled in relation to the CO₂ sequestration and capture project (Braathen et al., 2012). The main target of the wells was an inferred reservoir consisting of Jurassic and Upper Triassic deposits. The Lower Cretaceous succession, including the Helvetiafjellet Formation, was cored as well. The location of the different drill holes is indicated in Fig. 9 C.

Lower Cretaceous strata is generally well preserved, and is primarily exposed in the south and west of Svalbard (Fig. 1). As a result of the West Spitsbergen Fold Belt (WSFB), the exposed strata is observed dipping steeply on the western coast of Spitsbergen (Parker, 1967; Figs. 1 & 9B). Despite the fact that the drill sites for DH-1 and DH-1A are located near the West Spitsbergen Fold Belt, the Lower Cretaceous succession is still approximately horizontal. A semi-regional detachment zone can be recognized at the bottom of the Lower Cretaceous strata in the study area (Braathen et al., 2012). Based on previous palaeogeographic reconstructions of the deposition the Helvetiafjellet Formation, the clastic source area has been interpreted to have been located in the northwest (Steel & Worsley, 1984; Worsley, 1986; Gjelberg & Steel, 1995; 2012). The sediments within cores DH-1 and DH-1A are therefore interpreted to represent the proximal areas of the Helvetiafjellet Formation.

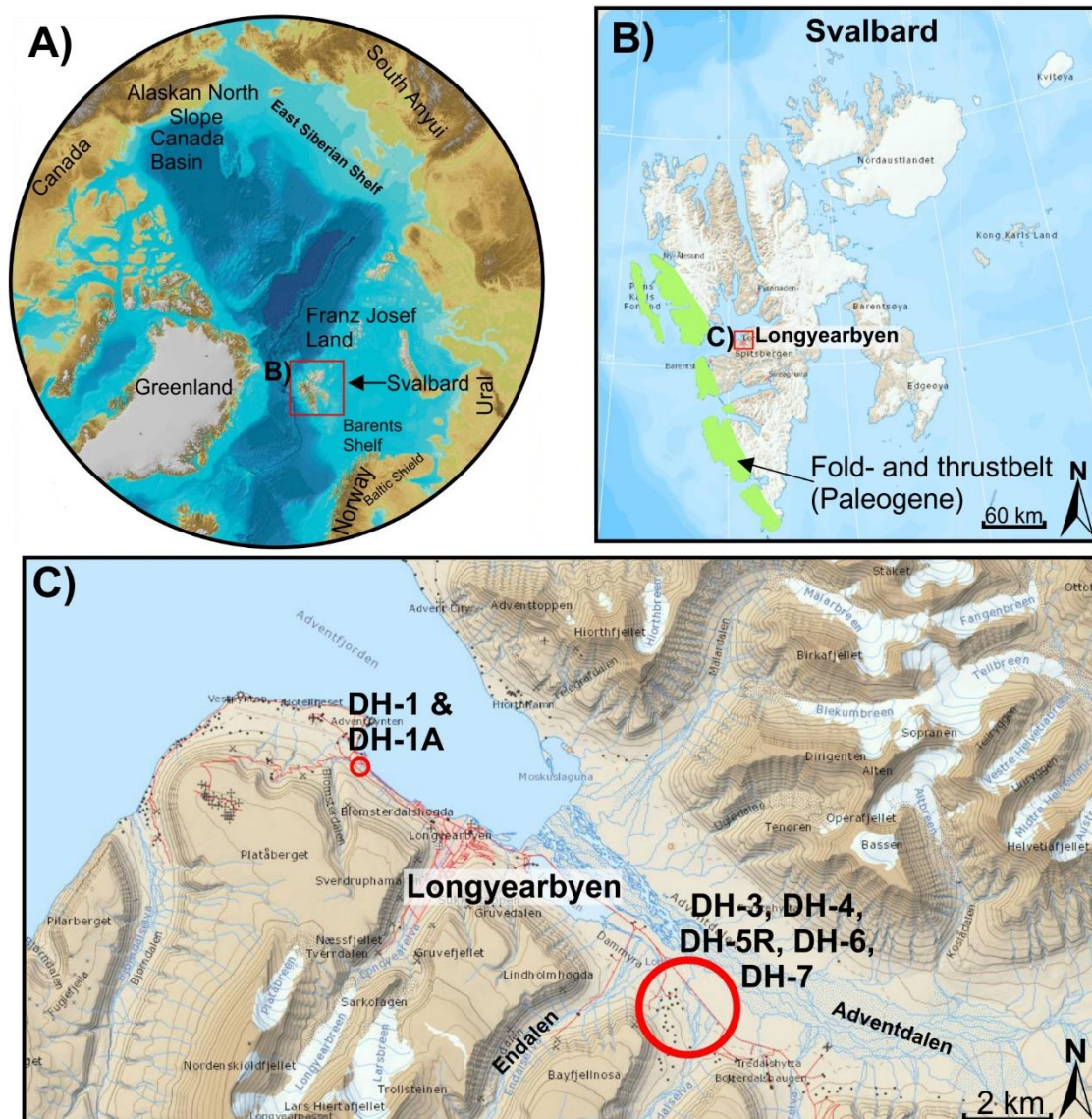


Figure 9: A) Bathymetry map showing the location of the study area. The map is retrieved from IBCAO (https://www.ngdc.noaa.gov/mgg/bathymetry/arctic/maps/version3_0/) B) Map of Svalbard and the location of the investigated cores marked in a red square. C) Topographic map, showing the location of the drill holes drilled in Spitsbergen. In this thesis, DH-1 and DH-1A were used, both located in Adventdalen. They are located 20 m apart. Image is retrieved from <http://toposvalbard.npolar.no/>.

4.2 Data collection and analysis

In this thesis, core DH-1 and DH-1A were logged from 216–144 meters and 214–142 meters below the present day surface, respectively. One sedimentary log (1:50 cm) was made for each of the cores, and they are displayed in their entirety in the thesis Appendix A and Appendix B. These logs illustrate the observed lithology, thickness and boundaries related to facies variations occurring within the Helvetiafjellet Formation.

The cores were stored in a container at UNIS, Longyearbyen, Spitsbergen (Fig. 9). The logging took place between September 24th and October 2nd, with guidance from supervisor Assoc. Prof. Sten-Andreas Grundvåg (UiT) and co-supervisor Prof. Snorre Olausen (UNIS). The equipment that was used in the logging process was a tool for grain size measurement, a folding rule, graph paper, a geological hammer, a hand lens and a camera.

The cores were logged in 1:50 cm scale. Grain size, primary- and secondary sedimentary structures, thickness of layers, colours, boundaries, and degree of bioturbation were thoroughly noted, thus forming the basis for the detailed facies analysis presented here in thesis 1 (Thea Engen). In relation to thesis 2 (Ingrid Tennvassås), special attention was also given to finding coal seams and associated root structures and potential palaeosols.

4.3 Post data collection work

A presentation log (1:200 cm) for each of the cores was made based on the observations noted in the original raw logs (Figs. 10 and 11). Detailed logs of DH-1 and DH-1A (1:50 cm) are presented in Appendix A and B.

Some interesting intervals marking change in depositional environments from the logged section are presented in 1:10 cm and 1:20 cm scale with pictures representing the interesting features (Figs. 12-17).

Corel Draw X8 has been used in all figures in order to produce the best visualization of the pictures and the logged sections, as well as for making depositional models.

4.4 Reference data

To be able to discuss the lateral distribution of the study area of this thesis (Figs. 1 & 9), data from previous published works on the same formation was used as a reference and was re-evaluated. The logs are gathered from previous published and unpublished works (Birkenmajer, 1984; Nemeč et al., 1988; Dypvik et al., 1991; Nemeč, 1992; Midtkandal et al., 2008; Midtkandal & Nystuen, 2009; Onderdonk & Midtkandal, 2010; Grundvåg, 2017) and were re-drawn in Corel Draw X8. The logs are used as a reference in the interpretation of the depositional model for the Helvetiafjellet Formation.

5 Results – facies analysis

5.1 Lithofacies

Fourteen lithofacies have been recognized based on observations of DH-1 and DH-1A (Table 1; Figs. 10 & 11). The recognized facies are described and grouped based on the lithology, sediment texture, sediment structures, colour, bioturbation and geometry of the sediments. The 14 lithofacies are arranged according to energy-level during deposition, where F-1 represent the higher energy and F-14 lowest energy. A brief description followed by an interpretation of the depositional process is given in Table 1. Vertical successions provide beneficial insights into vertical stacking patterns by revealing minor changes, allowing an understanding of depositional evolution to be gained. The Helvetiafjellet Formation consists mainly of sandstone, mudstone and thin coals (table 1).

Table 1: Summary of the facies in the Helvetiafjellet Formation

Grain size: cl-clay, slt-silt, vf-very fine, f- fine, m-medium, c-coarse, vc- very coarse, pbl- pebble, grvl- gravel

Facies	Name	Grain size	Description	Interpretation
F-1	Fine to medium-grained conglomerate	f-m (grvl)	F-1 consists mainly of chaotic and poorly sorted sub-angular to sub-rounded clasts. The polymictic conglomerate consists of clasts of a light grey to darker grey colour. The set is < 20 cm thick. Matrix supported (fine to medium sand matrix) to weakly clast supported. The conglomerate occurs as non-stratified, but normal grading occurs in some units. Internal structures are not observed within the unit. Erosive contacts to the underlying units (F-3 and/or F-5). The overlying unit has a gradational to sharp base to F-3 or F-12. Mudstone layer is present within one of the conglomerates.	Deposition by high-energy unidirectional currents, upper flow regime.
F-2	Massive sandstone	vf-m	Mainly medium grey structureless very fine to medium-grained sandstone. The deposits are poorly to	High sediment influx and rapid deposition

			well sorted. Coal clasts and bioturbation are present in some of the units. The average thickness of the units are 20 to 60 cm. The base and top of the unit is often gradational. The underlying units are F-1, F-4, F-6, or F-13, whereas the overlying units are F-5, F-6, F-3 or F-8.	
F-3	High angle tabular cross bedded sandstone	vf-c	<p>Well sorted fine to very coarse high angle tabular cross-bedded sandstone. The colour is very light grey to medium grey, while some of the thin layers are darker. Sharp base to the underlying unit (F-1, F-2, F-4, F-8, F-9 or F-10). Sharp to gradational contact to the overlying unit (F-1, F-2, F-3, F-4, F-8, F-9, F-10, F-11, F-14), where F-8 and F-11 are the most commonly observed.</p> <p>A fining upward trend is commonly seen within the unit. The unit is <9 m thick. The bedsets are <5 cm thick and can be seen due to change in grain size or thin (<1 cm) darker layers. Internal structures are current ripples cross-lamination. Root structures, coal clasts and bioturbation is common within the strata. F-3 is one of the most common lithofacies of the logged section of the Helvetiafjellet Formation (Figs. 10 & 11).</p>	Cross bedding produced by the migration of 2D dunes.
F-4	Trough cross bedding	f- c sand	<p>Trough-cross stratified sandstone of fine to coarse grain size. The colour is light grey to dark grey. The trough-cross bedded layers can be seen due to the presence of darker colour showing the cross cutting feature. The units are less than 240 cm thick. The dipping layers are on average 2 cm thick. Absence of fauna and root structures. F-5 has only been seen in DH-1A and within the Glitrefjellet Member.</p>	Cross bedding produced by the migration of 3D dunes in the lower flow regime.

F-5	Low angle tabular cross bedded sandstone	f- m	Low angle tabular cross bedded sandstone of fine to medium grain size. Characterized by well sorted sediments and normal grading. The base is typically erosive to the underlying unit (F-1, F-2, F-3, F-8 and F-10). Sharp boundary to the overlying unit (F-1, F-8, F-9, F-10, F-13). One of the most common lithofacies within the Helvetiafjellet Formation (Figs. 1 & 2).	Cross bedding produced by the migration of 2D dunes.
F-6	Interbedded sandstone and mudstone	vf-f	Light grey sandstone interbedded by dark grey to light black mudstone. The grain size tends to fine upwards. The sediments are sorted well. The unit is < 80 cm and the thickness of the bedsets varies from 2- 4 cm. Affected by soft sediment deformation and bioturbation. Sharp contact to underlying (F-2) and gradational contact to the overlying unit (F-8). The facies is only observed within the Glitrefjellet Member.	Radpid deposition of intervals of sand-and mud.
F-7	Lenticular/wavy/flaser bedded heterolithic sandstone	Slt- f	Heterolithic bedding is present at the upper part of the logged section (Fig. 10 & 11). The lithofacies is consisting of siltstone and the lenses are sandstone prominent. Some of the sandstone lenses are disturbed by bioturbation and filled with sand. Some loading are present, but rare. Set thickness of the sandstone lenses are less than 2.5 cm. The mudstone beds are approximately 1 cm thick.	Flaser, lenticular and wavy bedding is not common, but occurs within Glitrefjellet Member. This sedimentary structure may occur where mud is deposited out of suspension over ripples of sand or silt. In some studies, it has been used as an indication on tidal influence, but it is debated whether this is true.
F-8	Inter-laminated sandstone and mudstone	slt- c	Intervals of laminated sand- and mudstone ranging from silt to coarse-grained sandstone. The laminae are very thin (approximately 0.8 cm thick). The sandstone laminations are	Tidal influenced deposits formed at the tidal flat or subtidal coastline settings.

			typically 0.5 cm and the mudstone lamination are <0.3 cm. The boundary to the underlying unit (F-3, F-7 and F-9) is gradational. The contact to the overlying unit (F-3, F-7, F-9 and F-11) is gradational to sharp. F-8 is less frequent within the Helvetiafjellet Formation.	Result of rapid deposition of intervals of sand- and mud sediments.
F-9	Ripple cross-laminated sandstone	f	F-9 consists of well sorted fine-grained sandstone beds, typically with a grey to brown colour. The F-9 is associated with F-11 and F-5. Internal sedimentary structures are mud drapes. The unit is < 10 cm. The set is <2 cm. Internal structures are ripples.	Migration of 2D and 3D ripples. The ripples are asymmetrical, suggesting that they were formed by current ripples.
F-10	Heterolithic lamination	vf-f	Typically light grey to dark grey sandstone. Gradational boundaries to overlying and underlying unit. Small, thin seams of black mudstone are present in sandstone. Most prominent structure is flaser bedding, where the sand dominates and is interrupted by thin mud lamina. Set thickness is < 5 cm, but occasionally 10 cm.	Occurs in association with ripple-cross laminated sand in 2D or 3D ripples, where the structure is broken by lamination or lenses of silt or mud.
F-11	Siltstone/mudstone	slt	Siltstone/mudstone occurs as units ranging from 2 to 50 cm in thickness. The beds, light brown to dark brown in colour, show homogeneous to weakly laminated layers. Colour varies from light brown to dark brown/green. F-11 is present at all parts of the logged section. The contact between F-11 and the underlying unit (F-3, F-5, F-7, F-8, F-10 and F-13) appears to be sharp, where F-8 and F-13 are the most common units. The overlying unit is gradational to F-13 and/or F-14 or show loading	Deposits of mud-grade sediments in a tranquil setting.

			structures if sandstone is present above.	
F-12	Black shale	cl- silt	F-12 is a very dark-coloured shale containing organic matter and very fine sediments in clay - silt size. The sequence is approximately 1 m thick. The beds are hard to distinguish due to the fine-grained sediments and the dark colour. However weak lamination may be present in the lower part of the sequence. Fauna and bioturbation is absent.	Suspension fallout of mud-grade sediments in a tranquil setting/ low energy setting.
F-13	Coaly shale	cl-silt	High organic content shales that form thin layers where the thickness is ranging from 2-10 cm. F-13 is homogenous and internal structures are hard to see due to the very fine-grained sediments and black, shiny colour. Weak lamination to bedding may be present in some intervals. Has a semi-shiny surface. Ranging from 2 to 10 cm of thickness. Coaly shales are typically very fissile and break apart easily. They commonly occur between F-11 and F-14 with a gradational to sharp boundary between both the underlying and overlying unit.	Occurs in environments with abundant vegetation.
F-14	Coal	cl-silt	Coal occurs as beds thinner than 10 cm (occasionally 25 cm) and has a very dark black to shiny black colour. Mostly found in the upper part of the logged section (Glitrefjellet Member, Figs. 10 & 11). Often a sharp contact to the overlying (F-11 and F-13) and underlying unit (F-11 and F-13).	Accumulation of plant material in a protected, low energy setting.

5.2 Facies associations

Based on the analysis of the facies (summarized in Table 1), nine facies associations (FA; Table 2), are recognized within DH-1 and DH-1A. The two cores are located only 20 meters apart, which makes the FAs representative for both. In the following sub-chapters in 5.2, the different FAs will be presented and interpreted individually in turns of depositional environment, from distal to more proximal parts. Detailed logs with photos of the cores illustrate the different facies within the facies associations (Figs. 12-17).

FA-1 and FA-9 will only be described and interpreted briefly as they represent the Rurikfjellet and Carolinefjellet formations, respectively. The facies associations have been numbered based on the vertical stacking pattern, thus indicating their first occurrence within the included formations (the Rurikfjellet, the Helvetiafjellet and the Carolinefjellet formations).

The interpretation of the lithology will be supported by the gamma ray log (Figs. 10 & 11). The gamma ray log can be used to record the radioactivity of a formation and is based on the three radioactive groups of thorium, uranium and potassium. Of the three elements, potassium is the most abundant. As a first indicator, high gamma rays suggest a high percentage of shales. However, some lithologies other than shale may also show high values resulting in misinterpretations. Locating major sequence boundaries may be difficult in stratigraphic cores, thus gamma ray logs may help to find these. These surfaces are important as they represent long periods of time (Rider & Kennedy, 2011).

Table 2: Summary of the facies associations

Facies Associations	Depositional environment	Lithofacies included
FA-1	Prodelta	F-2, F-3, F-8, F-9, F-11
FA-2	Fluvial braidplain	F-1, F-3, F-6, F-8, F-9, F-11
FA-3	Floodplain	F-11, F-13, F-14
FA-4	Crevasse splay	F-6, F-8, F-9, F-11, F-13
FA-5	Fluvial distributary channel	F-1, F-3, F-4, F-5, F-6, F-9, F-10, F-11, F-13, F-14
FA-6	Delta plain	F-3, F-5, F-7, F-8, F-11, F-13
FA-7	Delta front	F-8, F-11, F-13
FA-8	Wave-reworked delta	F-1
FA-9	Offshore transition	F-12

DH-1 Scale 1:200 cm

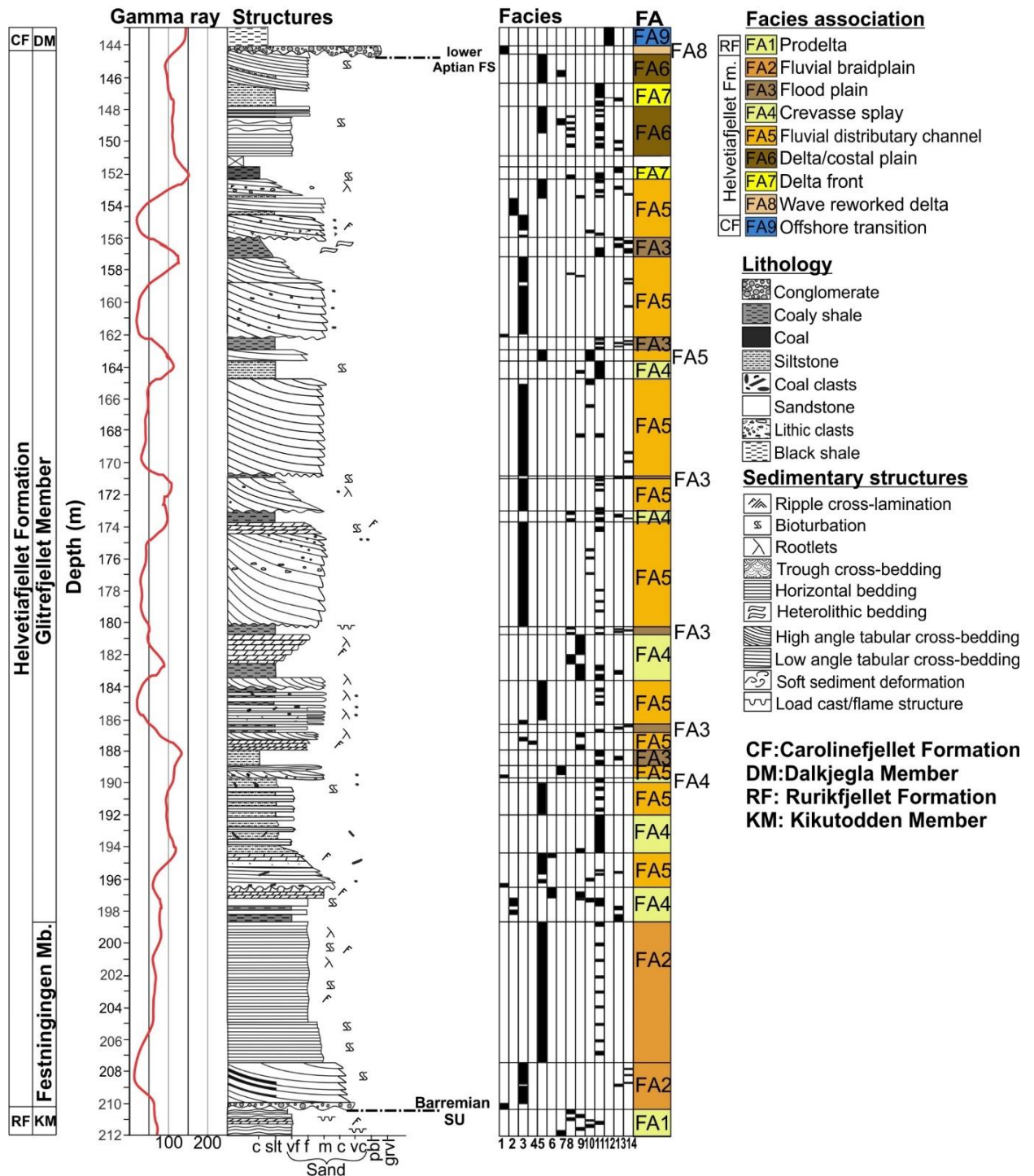


Figure 10: Sedimentary log (1:200 cm) from the logged section of the DH-1 core (Fig. 9). The facies associations (FA) are based on the pattern that the facies display. In total 14 lithofacies are recognized and have been grouped into 9 facies associations. The boundary to the underlying Rurikfjellet Formation is marked by the Barremian Subaerial Unconformity. The upper boundary to the Carolinefjellet Formation is marked by the lower Aptian Flooding Surface. The gamma ray is displayed as a red line. Low gamma ray suggests sediments with low radioactive content, respectively sandstone, while high gamma ray suggests high radioactive content, such as shale/mudstone. Note that coal has a very low gamma ray. See Appendix A for a more detailed log (1:50 cm).

DH-1A Scale 1:200 cm

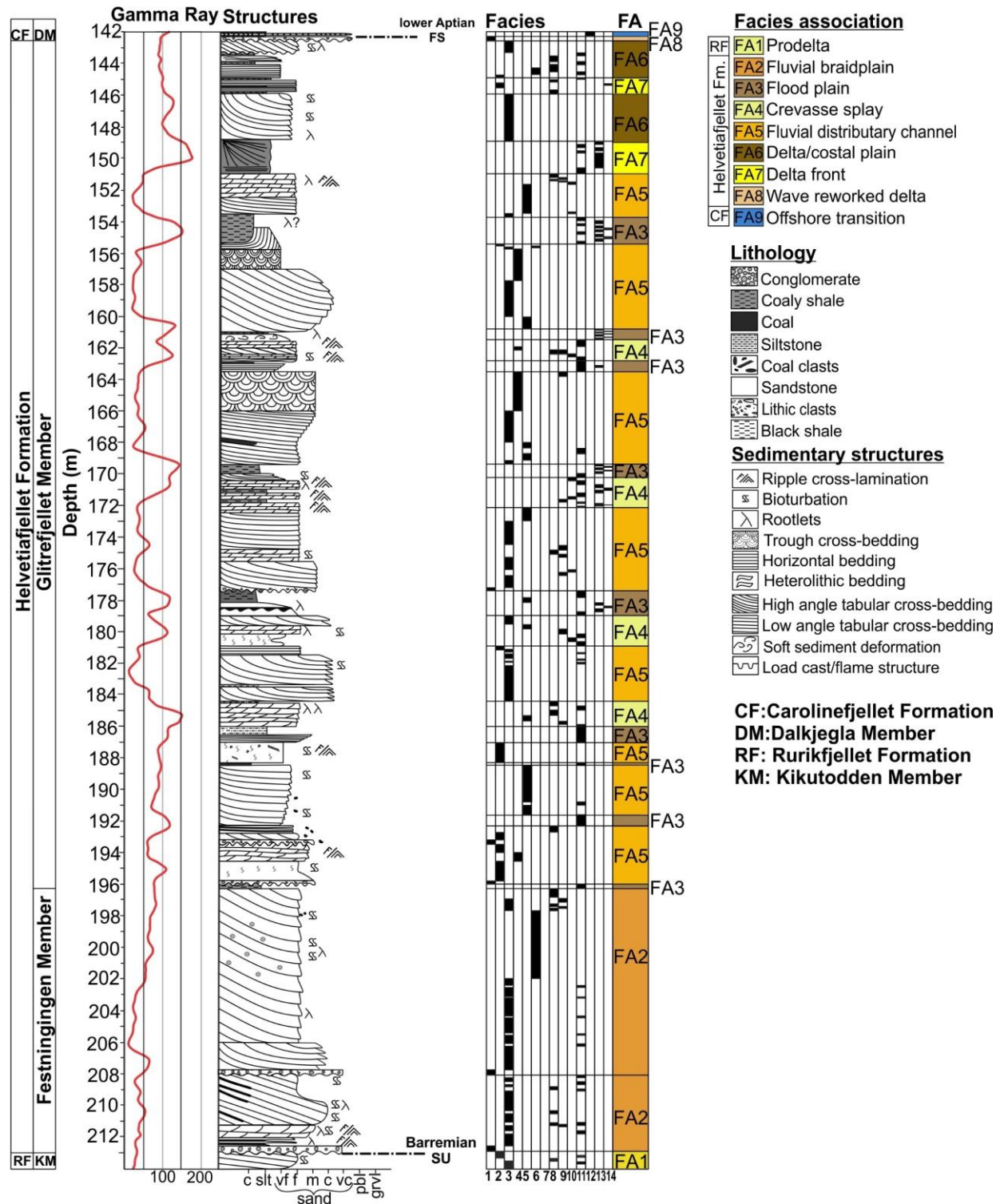


Figure 11: Logged section (1:200 cm) of DH-1A (Fig. 9) giving a graphical indication of the facies and facies associations. The gamma ray is displayed as a red line. Low gamma ray suggests sediments with low radioactive content, respectively sandstone, while high gamma ray suggests high radioactive content, such as shale/mudstone. Barremian Subaerial Unconformity marks the boundary between Rurikfjellet Formation and Helvetiafjellet Formation. The lower Aptian Flooding Surface marks the upper boundary between Carolinefjellet Formation and Helvetiafjellet Formation. A detailed log (1:50 cm) can be seen in Appendix B.

5.2.1 FA-1: Prodelta deposits

5.2.1.1 Description

This facies association is only recognized in the lowermost part of the logged section, and is stratigraphically belonging to the Rurikfjellet Formation and Kikutodden Member (Figs. 10, 11 & 12). The succession is approximately 1.5- 1.75 m thick and the units are typically <50 cm. FA-1 consists mainly of light to dark grey massive sandstone (F-2), high angle tabular cross-bedded sandstone (F-3), interlaminated sandstone and mudstone (F-8), ripple cross-laminated sandstone (F-9) and siltstone/mudstone (F-11). FA-1 shows a gradational, coarsening upward sequence grading from mudstone to very-fine sandstone. This facies association has an erosive boundary to the overlying unit and there is a drastic change from the mudstone to very coarse conglomerate. Sedimentary structures such as ripple cross-lamination (F-9), soft sediment deformation and minor bioturbation are present within the FA-1. As the gamma ray indicates, FA-1 consists of low gamma values, with a slight increase towards the top of the unit.

5.2.1.2 Interpretation

Based on the coarsening upwards grain-size trends, the presence of ripple cross-lamination and alternations between siltstone/mudstone and sandstone deposits, this FA shows similar characteristics of prodelta deposits (Fig. 12), as they are presented by Nichols (2009). This evidence, together with the low gamma ray values, is indicative of prodelta environment. The alterations between siltstone and sandstone deposits suggests fluctuating energy, whereas the siltstone is settled from suspension in a tranquil setting and the sandstone is introduced by storm events. In general, the prodelta represents the most distal part of the delta and the sediments are very fine-grained and deposited under the storm wave base (Allen, 1998; Allaby, 2013). Similar ancient prodelta deposits have been described from the Upper Cretaceous (Turonian) Ferron Sandstone in Utah, U.S.A (Fielding, 2010). The interpretation is also in line with previous studies of the Rurikfjellet Formation (Steel & Worsley, 1984; Nemeč et al., 1988; Dypvik et al., 1991; Midtkandal et al., 2008; Gjelberg & Steel, 2012). The lack of delta front deposits and the observations of an unconformity has previously been linked to the High Arctic Large Igneous Province (HALIP), which occurred in Early Cretaceous. The arrival of a mantle plume lead to crustal uplift in the northern part of

DH-1

Scale 1:10

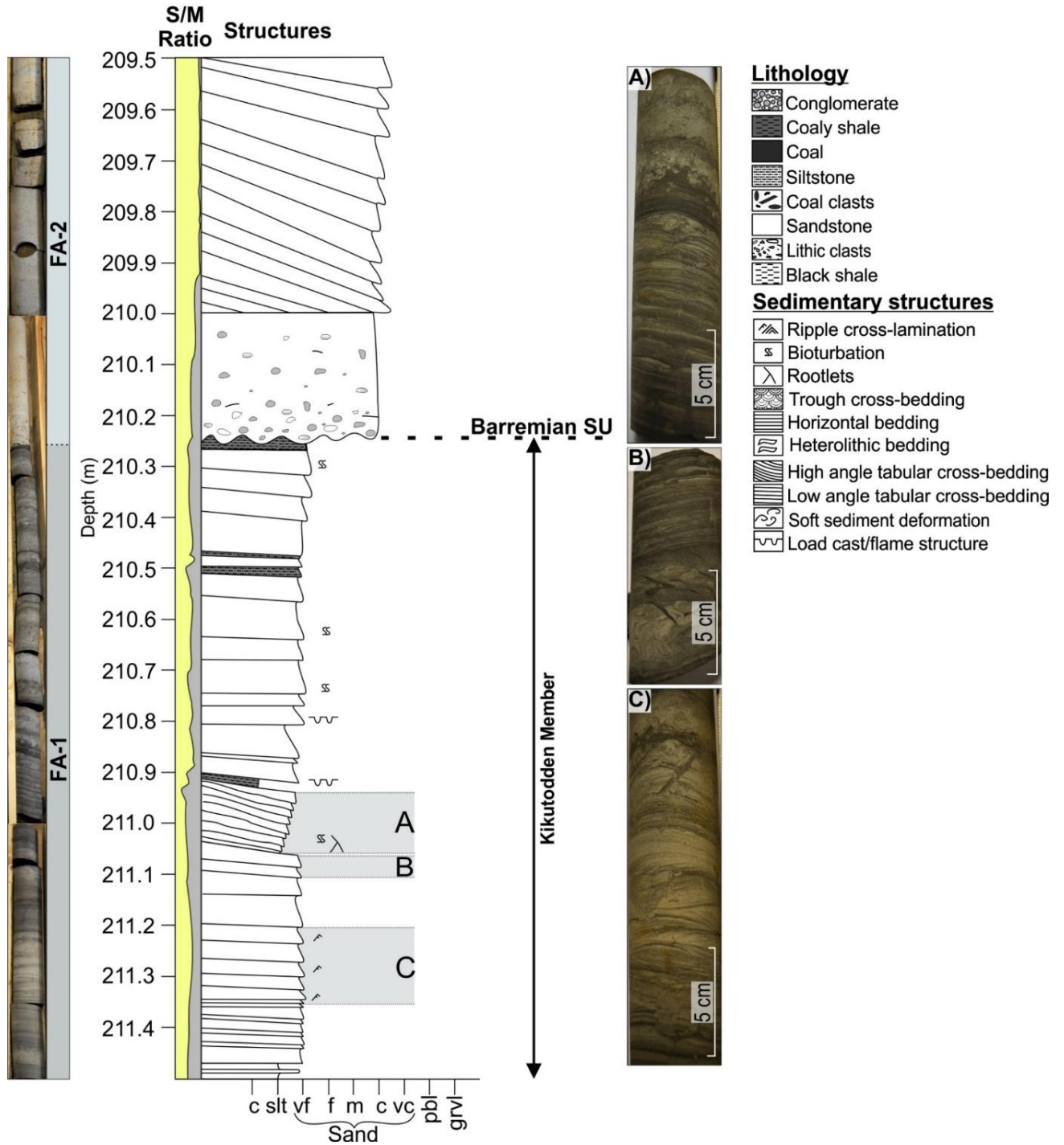


Figure 12: Detailed log (1:10 cm) of FA-1 from interval 209.5-211.5 m. S/M ratio stands for sand to mud ratio and is based on subjective visual observations of the cores. FA-1 is only observed at the uppermost part of the Rurikfjellet Formation and Kikutodden Member. It consists of siltstone to very fine-grained sandstones. The layers are mainly sub-horizontal to low angle tabular cross bedded. The sets are thickening upwards. Internal structures such as ripple cross-lamination and sediment loading are present. Rootlets and bioturbation are present mainly in the upper part of the sequence. The overlying facies association fluvial braidplain deposits (FA-2) are restricted to the Helvetiafjellet Formation and Festningen Member. It consists of conglomerate and coarse-grained sandstone. The boundary between the Rurikfjellet Formation and the Helvetiafjellet Formation is easily recognized due to the change in grain size and abrupt change in colour. The conglomerate represents the Barremian Subaerial Unconformity (SU). **A)** Area of interlaminated mud- and sandstone. **B)** Interlaminated mud- and sandstone on top. Root structures present. **C)** Current ripple cross-laminated sandstone.

Svalbard (Corfu et al., 2013). This extensive regional uplift resulted in stronger erosion in the northern parts towards the shallow epicontinental sea in the south (Nagy, 1970). The presence of ripple cross-lamination (Fig. 12C) suggests that the sands were wave-reworked during, or quickly after, deposition. The soft sediment deformation (Fig. 12A) may be due to difference in density, caused by sandy sediments being deposited above mudstone deposits.

5.2.2 FA-2: Fluvial braidplain deposits

5.2.2.1 Description

FA-2 is only recognized within the Festningen Member (Fig. 12) and consist of fining upward succession ranging from fine to coarse-grained sandstone. The total thickness varies from 11.5-17 m (Figs. 10 & 11). The beds are <80 cm, but more frequently <20 cm. Facies included in this FA is conglomerate (F-1), high angular tabular cross bedded sandstone (F-3), interbedded sandstone and mudstone (F-6), interlaminated sandstone and mudstone (F-8), ripple cross laminated sandstone (F-9), siltstone/mudstone (F-11). An erosive base cuts down into the underlying Rurikfjellet Formation marked by a conglomerate (F-1; Fig. 12). This boundary marks a change in lithology from mudstone to conglomerate to high angle tabular cross-bedded sandstone (Figs. 10 & 11). The light grey conglomerate consist of clasts of different lithology. The conglomerate shows normal grading, where most of the clasts are concentrated in the lowermost part of the conglomerate. The clasts are mainly sub-angular to sub-rounded. Some thin clasts of coal are observed within the conglomerate. The unit is characterized by relatively high angle dipping beds (<4 cm) in a coarse sandstone unit. The sandstone appears to be well sorted. Thin coal layers are present within the unit and are < 1 cm thick. Beds in the uppermost part are low angle dipping consisting of fine- to medium-grained sandstone. The unit shows an overall fining upwards trend. The overlying unit (FA-3) is a coaly shale/ mudstone and the boundary is sharp. Root structures are present within the unit. The gamma values are slowly increasing towards the top of the unit from very low to medium values.

5.2.2.2 Interpretation

Because of the fining upward grain-size trend, the presence of an erosive lower boundary marked by a conglomerate, the occurrence of low-angle to high-angle cross-bedded sandstone and general coarse grained sediments, this FA has been interpreted as fluvial braidplain deposits (FA-2; Fig. 12). Similar ancient fluvial braidplain deposits have been described from Upper Devonian to Lower Carboniferous in Gupton Formation in Dyfed, Wales (Marshall, 2000). Similar modern braidplains tend to have a higher gradient, but show some of the same characteristics. Examples of possible modern braidplains are the Scott fan and the Yana fan described by Gjelberg & Steel (2012). The interpretation is also in line with previous studies of the Helvetiafjellet Formation, and the Festningen Member in particular (Mørk, 1978; Nemeč, 1992; Gjelberg & Steel, 1995; Midtkandal et al., 2007; Midtkandal & Nystuen, 2009; Onderdonk & Midtkandal, 2010).

The fining upward trend implies deposition of sandbars within the braidplain. As a channel system is abandoned due to avulsion, the channel is filled and vegetation develops at the top. This is in accordance with the observed gamma ray value trends (Figs. 10 & 11). This assumption is further emphasized by the presence of coal clasts and ripple cross-lamination, which is typical for coastal plain deposits (Midtkandal et al., 2007).

One of the most common minerals in coarse-grained detrital rocks is quartz (Nichols, 2009). Quartz shows no radioactivity, thus sandstones usually tend to have low gamma values. However, some clay minerals (e.g. feldspar & micas) cause moderate to high gamma ray values (Rider & Kennedy, 2011). The gamma ray log for FA-2 shows increasing gamma ray values going from low to moderate, thus supporting the interpretation of fluvial sandstones with a higher content of clay minerals towards the top (Figs. 10 & 11).

5.2.3 FA-3: Floodplain deposits

5.2.3.1 Description

FA-3 (Fig. 13) is dominated by stacked beds of mudstone (F-11), coaly shale (F-13) and thin coal seams (F-14). The mudstone is mostly laminated, but appears as massive in some intervals. The unit shows an overall fine-grained character consisting of siltstone to very fine-grained sandstone. There is no clear evidence of coarsening or fining upwards trends. The thickness of the units are not thicker than 40 cm. FA-3 is stratigraphically overlying FA-2 and marks the boundary between the Festningen Member and The Glitrefjellet Member. The facies association is mainly present in the lower to middle part of the Glitrefjellet Member (Figs. 10 & 11). There is in general a sharp to gradational contact between the crevasse splay deposits (FA-4) and the fluvial distributary channels (FA-5), which bounds FA-3. For the most part, the very dark brown colour and the very fine-grained character of the deposits makes the primary structures hard to recognize. An abundance of plant fragments and rootlets within the facies association are observed. The gamma ray log (Figs. 10 & 11) indicates relative high values in some units and rather low values in others.

5.2.3.2 Interpretation

Based on the presence of mudstone, coaly shale and coal (Fig. 13), this FA is interpreted as floodplain deposits (Fig. 13). In addition to the very fine grained character of the deposits, this facies association is seen in relation to crevasse splay deposits (FA-4) and fluvial distributary channels (FA-5). Similar ancient floodplain deposits have been described from the Eocene Willwood Formation located in Wyoming (Bown & Kraus, 1981). The interpretation is also in line with previous studies of the Helvetiafjellet Formation (Nemec, 1992; Midtkandal et al., 2007; Onderdonk & Midtkandal, 2010). The gamma ray values in coaly shale depends on the amount of shale within the rock. Uranium is absorbed in the reduced conditions shales, thus causing high gamma values in organic rich shales. It is not absorbed by organic matter in swamps due to the lack of clay minerals present (Rider & Kennedy, 2011). Altogether, this explains why variations in gamma ray values within FA-3 are observed.

In general, flooding of the coastal plain was caused by a relative rise in sea-level and decrease in sediment input (Midtkandal et al, 2007). However, it also resulted in a high

ground water table (Nemec, 1992). Normally, water from the floodplain runs of into the river channels, but during a flood the water level rises above the ground water table and runs over the floodplain. After the flood, the water table stabilizes and drops (Jung et al., 2004). For this reason, it may be argued that the very dark black colour may be the result off an old ground water stand during a flood (Nemec, 1992).

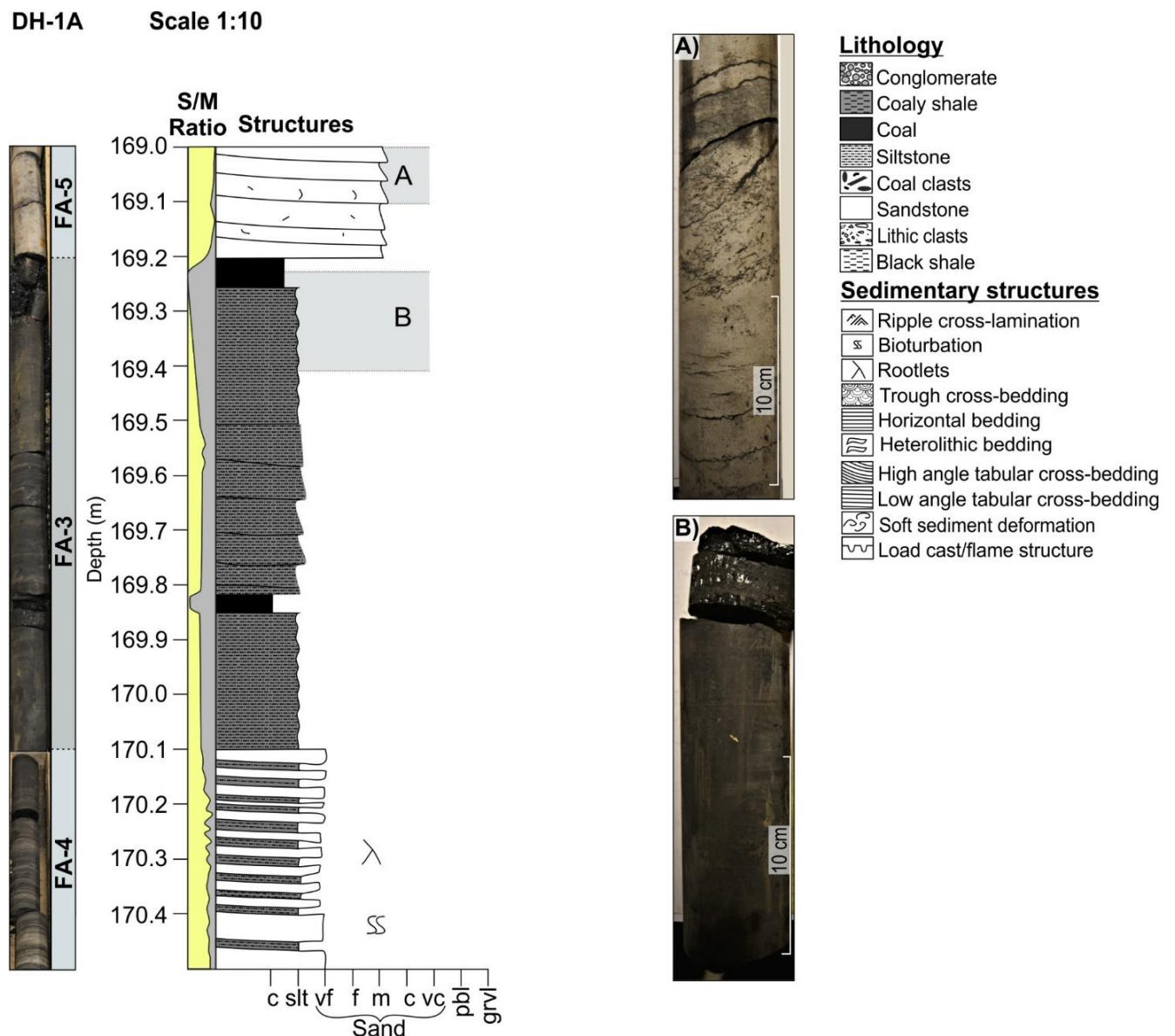


Figure 13: Detailed logged section (1:10 cm) from FA-3 and logged core DH-1A. The logged interval is 169- 170.5 m. This section consists of a gradational boundary to the underlying unit (FA-4) and a sharp boundary to the overlying unit (FA-5). This sequence is characterized by thin coal layers (<5 cm) and mudstone (<40 cm) deposits. Due to the dark colour and fine-grained sediments, internal structures are hard to recognize. **A)** High-angle tabular cross-bedded sandstone **B)** Coaly shale and coal.

5.2.4 FA-4: Crevasse splay deposits

5.2.4.1 Description

FA-4 (Fig. 14) is the most prominent facies association within the Glitrefjellet Member. Facies included in this FA is interbedded sand- and mudstone lamination (F-3), ripple cross-laminated sandstone (F-9), siltstone/mudstone (F-11) and coaly shale (F-13). A general thickness of the deposits varies from 25-150 cm, but locally up to 3 m. The beds vary in thickness from thinly bedded (1 cm) to medium bedded (30 cm) with a sharp base between the beds. The grain size of the sandstone beds range from very fine to fine-grained sandstone and show a coarsening upwards trend. The facies association is mainly present in the lowermost part of Glitrefjellet Member (Figs. 10 & 11). The facies association is partly bioturbated by roots, thus destroying some of the internal laminae and bedding (Figs. 14 A & B). The deposits typically occurs above floodplain deposits (FA-3) or fluvial distributary channel deposits (FA-5) with a sharp contact. The colour of the sediments ranges from light grey sandstones to dark fine-grained mudstones and coaly shale. The gamma ray log (Figs. 10 & 11) shows high to very high values at the intervals of FA-4.

5.2.4.2 Interpretation

Although these deposits share several characteristics with a floodplain (FA-3), there are some distinct differences. They are typically finer and consist of thinner bedsets than those associated with channel deposits (FA-5), but coarser and consists of a higher content of sandstone than those associated with floodplain deposits (FA-3). Based on the presence of interfingering of mudstone and fine-grained sandstone, this FA is interpreted as crevasse splay deposits (Fig. 14). This interpretation is supported by the funnel shaped gamma ray log, representing the upward coarsening trend seen in the succession (Rider & Kennedy, 2011; Figs. 10 & 11). Similar ancient crevasse splay deposits have been described from the Cretaceous the Castlegate Sandstone and Neslen Formation, located in eastern Utah, USA (Burns et al., 2017). The interpretation is also in line with previous studies of the Helvetiafjellet Formation (Steel et al., 1978; Nemec, 1992; Gjelberg & Steel, 1995; Midtkandal et al., 2007).

DH-1A

Scale 1:10

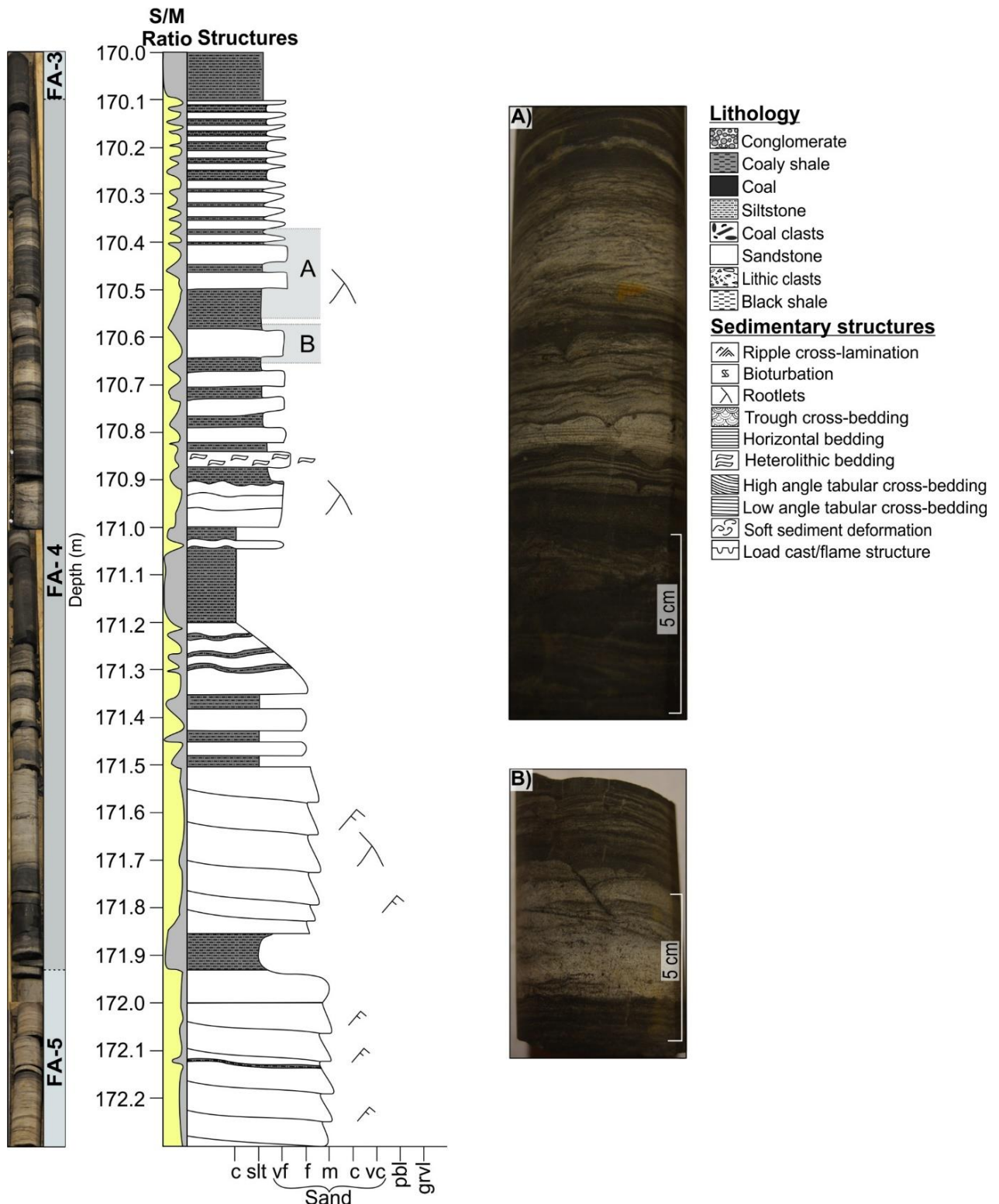


Figure 14: Detailed section of DH-1A in the interval 170.0 m -173.3 m. The section consists of very fine to medium-grained sandstone, often interbedded by thin mudstone layers (<10 cm) making an overall fining upwards succession. The beds starts as more sand rich and grades into more mud-rich towards the top. Ripple cross-lamination, roots and heterolithic lamination is present in this section. **A)** Root structures, thin layers to laminated layers of sand- and mudstone. **B)** Potential rootlets.

The beds are slightly inclining as the interfingering into mudstone and sandstone deposits develops. These beds indicate cyclic flooding events. During flooding, the river brings coarser material through the levée and over the low relief floodplain area. The presence of current ripple cross-lamination indicates a flow in one direction, from the confined river to the unconfined floodplain. In periods of lower water discharge, vegetation grows on the thin layers of sediments. This is supported by the root traces interpreted to be developed during subaerial exposure. During the next flooding event, new coarser material is deposited over the vegetated area. They may be hard to distinguish from levées, but crevasse splays are typically consist of a coarser grain size and are thicker successions than levée deposits (Brierly et al., 1997). Climbing current ripples indicate rapid deposition (Nichols, 2009), which is typical for crevasse splay deposits (van Gelder et al., 1994)

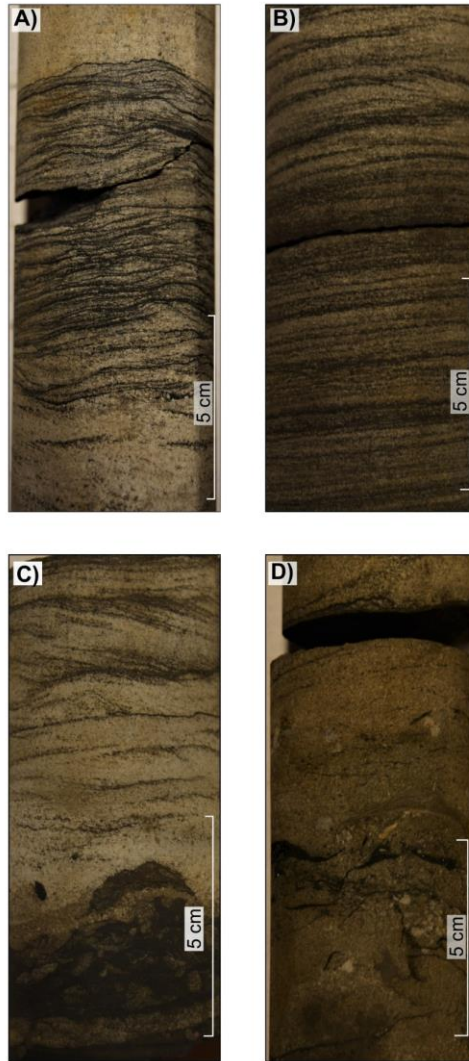
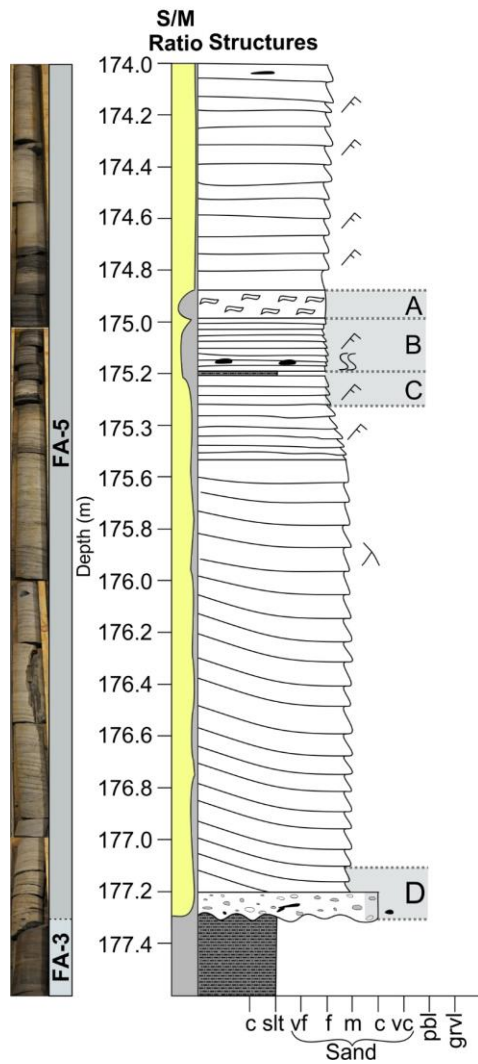
5.2.5 FA-5: Fluvial distributary channel deposits

5.2.5.1 Description

FA-5 is largely composed of fine- to coarse-grained sandstones, typically high angle tabular cross-bedded sandstone (F-3; Fig. 15 D), trough cross-bedded sandstone (F-4), and low angle tabular cross-bedded sandstone (F-5; Fig. 15 B). Other facies such as conglomerate (F-1; Fig. 15 D), heterolithic bedding (F-7), ripple cross-laminated sandstone (F-9; Fig. 15 B), lenticular/wavy/flaser bedded heterolithics (F-10; Fig. 15 A), siltstone/mudstone (F-11) and coaly shale (F-13) are also observed. This facies association is easily recognized due to the very light colour in contrast to the surrounding facies, and the sandstone units vary from 2 to 5 m thick. The FA shows a fining upward trend and occur at several different levels within the Glitrefjellet Member. The lower boundary is commonly incising down into floodplain deposits (FA-3) or crevasse splay deposits (FA-4; Fig.15). Rootlets and plant fragments are observed as well as coal clasts. Sedimentary structures such as current ripple cross lamination (Figs.15 B & C) and flaser bedding (Fig. 15 A) are present towards the top. An increase from low to high gamma values are observed within the facies association (Figs. 10 & 11).

DH-1A

Scale 1:20



Lithology

- Conglomerate
- Coaly shale
- Coal
- Siltstone
- Coal clasts
- Sandstone
- Lithic clasts
- Black shale

Sedimentary structures

- Ripple cross-lamination
- Bioturbation
- Rootlets
- Trough cross-bedding
- Horizontal bedding
- Heterolithic bedding
- High angle tabular cross-bedding
- Low angle tabular cross-bedding
- Soft sediment deformation
- Load cast/flame structure

Figure 15: Detailed log (1:20 cm) of the interval 174.0 -177.5 m showing FA-5. An erosive base to the underlying unit (FA-3) is made by a 5 cm thick conglomerate of coarse-grained sandstone. Steeply dipping sandstone beds of <3 cm thickness is overlying the conglomerate. Towards the top, the layers become more sub-horizontal to horizontal. Sedimentary structures such as ripple cross-lamination are present. Roots and bioturbation can also be seen. **A)** Flaser bedding (Heterolithic bedding) **B)** Horizontal lamination with ripple cross-lamination towards the top **C)** Rippled cross-stratified sandstone and coal clasts **D)** Conglomerate and high angle tabular cross-stratification. Coal clasts are present within the conglomerate.

5.2.5.2 Interpretation

Based on the presence of isolated coarse-grained sandstone with erosional base, in addition to facies of high energy such as conglomerate (F-1), high angle tabular cross-bedding (F-3), trough cross-bedding (F-4), and low angle tabular cross-bedding (F-5), this FA is interpreted as fluvial distributary channel deposits (Fig. 15). The evidence is further supported by the fining upwards trend that can be seen as an increase in gamma ray values (Figs. 10 & 11), indicating a higher content of clay minerals towards the top. Similar ancient fluvial distributary channel deposits have been described from the Panter Tongue of the Star Point Formation (Santonian) in Utah, U.S.A (Hwang & Heller, 2002) and in the Cretaceous Dakota Formation (Cenomanian) in southern Utah, U.S.A. (Ulicny, 1999). These observations are in agreement with previous studies of the Helvetiafjellet Formation (Nemec, 1992; Gjelberg & Steel, 1995; Midtkandal et al., 2007).

FA-5 is interpreted to represent channels transporting sediments from a proximal source area towards the ocean. The tabular cross-bedding deposited from migrating 2D dunes (Table 1) and trough cross-bedding deposited from migrating 3D dunes (Table 1) are interpreted to be migrating bars within the channel. As there is a high number of crevasse splay deposits (FA-4) within the unit, the channel is showing evidences of being meandering.

5.2.6 FA-6: Delta plain deposits

5.2.6.1 Description

This FA is generally observed as an upwards-coarsening succession consisting of mudstone and very fine to medium-grained sandstone. Facies included in this facies association is high angle tabular cross-bedding (F-4), low-angle tabular cross-bedding (F-6) and massive sandstone (F-2). FA-6 is restricted to the upper part of the Glitrefjellet Member (Figs. 10, 11 & 16) as two isolated units with a sharp boundary to delta front deposits (FA-7; Fig. 16 D). The facies association is capped by an erosive conglomerate as the overlying unit (FA-8; Fig. 16 B). The bed thickness varies from <5 cm to <1.5 cm. Internal structures include lenticular bedding (Fig. 16 E), which display cross lamination. The lenses seem to be disturbed by bioturbation in some areas. Plant remains can be seen occasionally within the unit. The bioturbation within the unit is strong to very strong (Fig. 16 C). The colour is mainly medium to dark grey. The gamma ray log shows high to very values (Figs. 10 & 11).

5.2.6.2 Interpretation

Based on the coarsening upwards grain-size trend, the presence of cross bedding and lenticular bedding, this FA is interpreted as delta plain deposits (Fig. 16). The unit shows similar characteristics as ancient delta plain deposits that have been described from the Holocene Yellow River delta in northern China (Xue, 1993). This is in accordance with previous published work from Svalbard, which has interpreted the similar deposits to represent prograding delta deposits (Mørk, 1977; Nemeč, 1992; Steel et al., 2000; Gjelberg & Steel, 1995).

The basinwards shift in facies associations indicates progradation, further supported by the coarsening and shallowing upwards trend. Together, these observations show similarities to those observed within a prograding delta. A delta is formed at the mouth of a river when it meets a standing body of water, in this case the shallow epicontinental sea. The velocity of the water decreases and the coarsest material is deposited first. The progradation is controlled by allogenic and autogenic factors. The allogenic factors include sediment supply and relative sea level, while the autogenic factors include bar migration and avulsion of channels (Nichols, 2009). If a delta is prograding, the sediment supply has to be greater than the sediment removal by waves and tides.

Internal structures, such as lenticular bedding (Fig. 16 E) are commonly observed in tidal flats and delta-front sediments. The conglomerate capping the FA-6 is interpreted to be wave-reworked delta (FA-8) deposits indicating a later delta retreat. However, the upwards coarsening trend interpreted to be caused by progradation may also be a result of other mechanisms. For example can an increase or decrease of coarsening upwards trends be a function of topography.

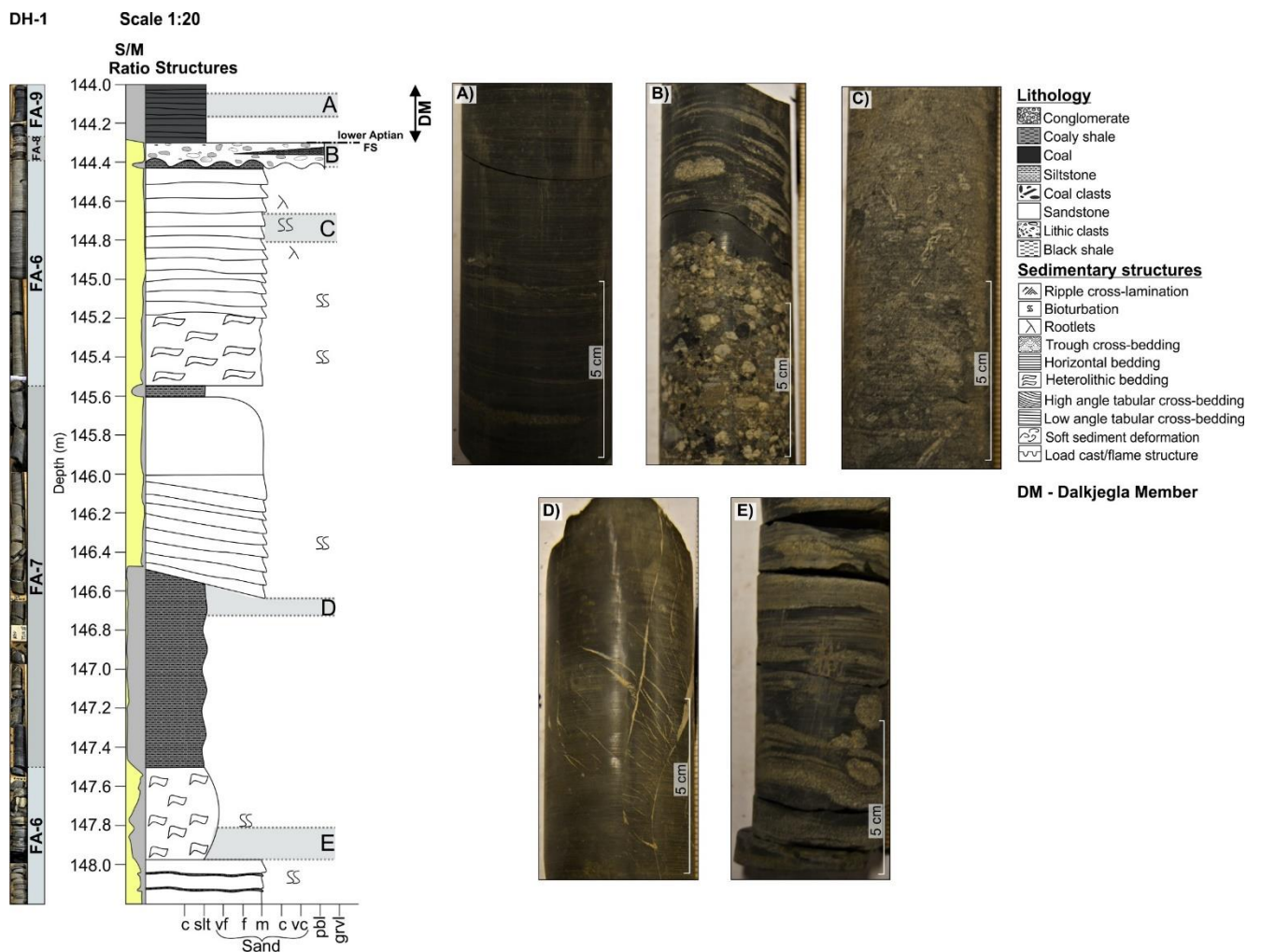


Figure 16: Detailed section (1:20) from interval 144-148 m. The section displays FA-6, FA-7 and FA-8. FA-7 is commonly found underlying FA-6. There is an abrupt change in grain size and lithology. FA-7 is mostly mudstone. FA-8 consists of high angle tabular cross bedded sandstone of medium grain size. Commonly lenticular heterolithic bedding is seen. **A)** Black shale (F-12) stratigraphically belonging to the Dalkjegla Member of the Aptian-Albian Carolinefjellet Formation. **B)** Matrix based conglomerate of pebble size. The clasts are sub-rounded to rounded. The clast does not show a preferred orientation. **C)** Root marks or bioturbation filled with sand. Note the circular and elongated marks. **D)** Mudstone **E)** Lenticular heterolithic bedding with an average set thickness of <2 cm. The lenses seems to be exposed to bioturbation. Loading structures are also present.

5.2.7 FA-7: Delta front deposits

5.2.7.1 Description

FA-7 (Fig. 16) is limited to the upper part of the Helvetiafjellet Formation (Figs. 10 & 11) and is recognized within two inclined separated units. The succession is < 270 cm thick and divided into different units consisting of less than 40 cm in thickness, but most frequently less than 5 cm in thickness. The main facies included in FA-7 consists of inter-laminated sandstone and mudstone (F-8), siltstone/mudstone (F-11) and coaly shale (F-13). FA-7 consists of grey fine to medium-grained sandstone and dark brown laminated clay/mudstone. Due to the dark colour and fine-grained characteristics, sedimentary structures are hard to define. Fauna is abundant in this FA. A gradational coarsening upward succession from mudstone (FA-7) to the overlying coarse sandstone (FA-6) is observed within the unit. The boundary to the underlying unit (fluvial distributary channel; FA-5) is gradational. The gamma values are decreasing upwards within the FA-7. However, the unit contains generally high values.

5.2.7.2 Interpretation

The presence of fine-grained sandstone and mudstone deposits together with upwards coarsening have been interpreted to represent delta front deposits (FA-7; Fig. 16). This is supported by the upwards decreasing in gamma ray values, suggesting a decrease in clay minerals towards the top of the facies association. Similar ancient delta front deposits have been described from Upper Cretaceous (Cenomanian) Frontier Formation in the Northeast Bighorn Basin from Wyoming, U.S.A (Hutsky et al., 2012). The interpretation is also in line with previous studies of the Helvetiafjellet Formation (Nemec et al., 1988; Midtkandal et al., 2007). The fine-grained sandstone and mudstone deposited above the delta plain deposits (FA-6) suggests an increase in water depth and deposition in a shallow marine environment. This is further supported by the rise in eustatic sea-level observed through the Early Cretaceous (Haq et al., 1987; Haq, 2014; Ramkumar, 2016; Fig 8). However, delta plain deposits (FA-6) are overlying the delta front deposits (FA-7) at the top, thus sediment influx must have been greater than the relative sea-level rise in order to prograde.

The uppermost part of the facies association is showing similar characteristics as an interdistributary bay (Fig.16). This is observed other places in Svalbard (e.g. the Kvalvågen locality described by Nemeč et al., 1988). In this setting, sheltered areas between the prograding delta lobes are protected from wave and tidal forces and represent low-energy environments. Further support for this interpretation is provided by similar findings within the upper part of the Glitrefjellet Member (Midtkandal et al., 2007), where anoxic bottom conditions have been recorded. The clay content and possible presence of organic matter in the deposits are represented by very high values of the gamma ray response (Figs. 10 & 11). This supports the evidence of possible anoxic bottom conditions.

5.2.8 FA-8: Wave-reworked delta deposits

5.2.8.1 Description

FA-8 (Fig. 17) stratigraphically belongs to the uppermost part of the Helvetiafjellet Formation, represented by a 15 cm thick conglomerate (F-1). The polymictic conglomerate is matrix supported. A thin layer of brown mudstone is present within the conglomerate (Fig. 17 B). It has an erosive boundary to the underlying delta plain deposits (FA-6; Figs. 10 & 11). The change in facies association is easily detected due to the change in colour and grain size from mainly fine grained sandstone to gravel conglomerate, abruptly overlain by black shale. The gamma ray (Figs. 10 & 11) varies from high to very-high values.

5.2.8.2 Interpretation

Despite the thin thickness of FA-8, the unit has been grouped into a separate unit due to its rare sedimentary characteristics. This facies association has been interpreted to represent wave-reworked delta deposits (FA-8; Fig. 16) based on the thin layer, coarse grained character, underlying delta front deposits (FA-7) and overlaying offshore transition deposits (FA-8). Similar ancient deposits have been reported from Upper Pennsylvanian (Virgilian) Oread cyclothem in Kansas and Oklahoma, U.S.A (Yang , 2007). Similar deposits have recently been interpreted to represent transgressive lag caused by wave ravinement during transgression in the Helvetiafjellet Formation (Grundvåg & Olausen, 2017). The overall basinwards jump in facies suggests a relative rise in sea level. This is supported by the eustatic sea-level curve, showing a general rise in sea-level during Cretaceous (Fig. 8). As the

delta plain was flooded, waves reworked the delta plain and left behind a transgressive lag.

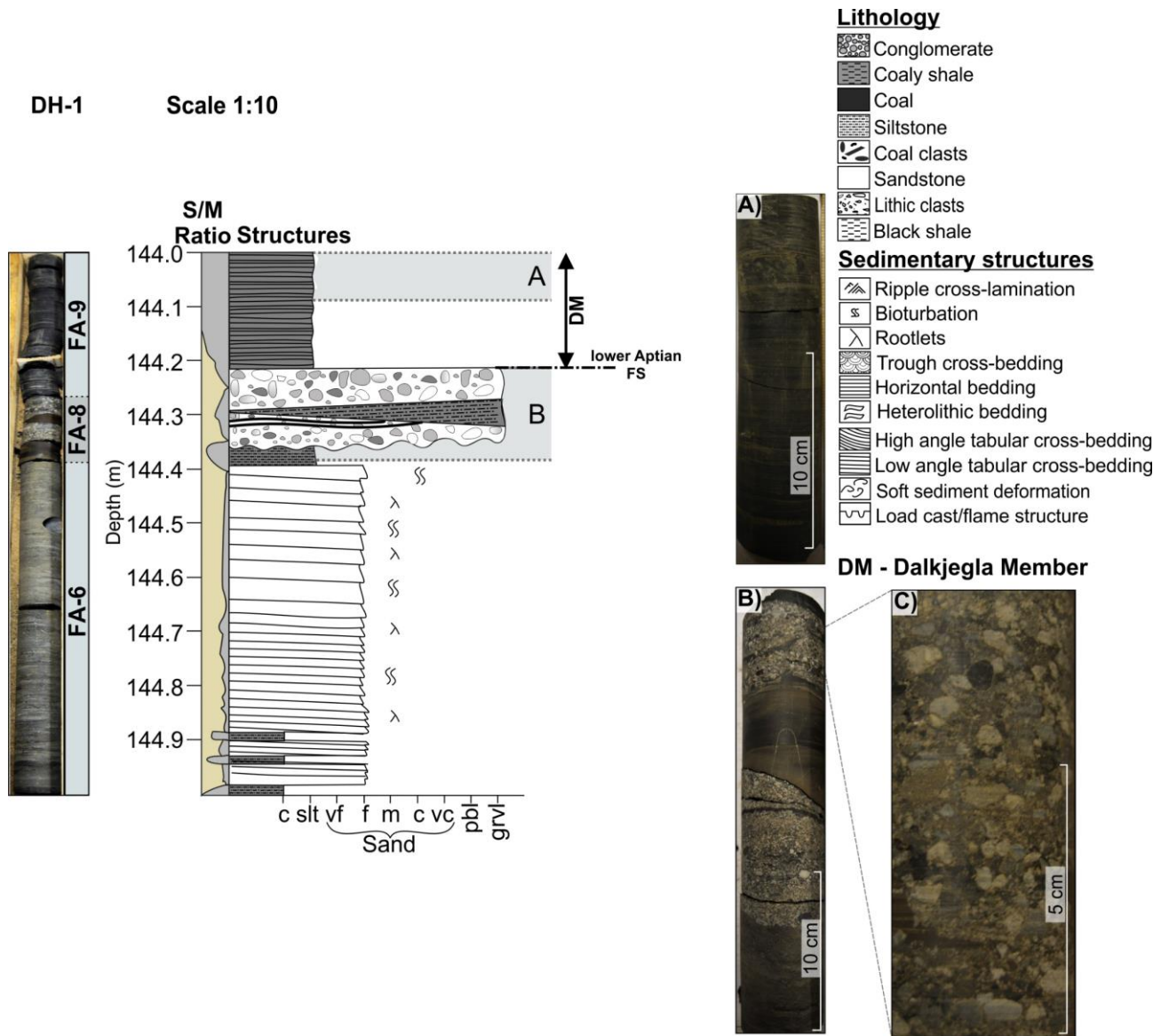


Figure 17: Detailed log (1:10 cm) of interval 144-145 m displaying the transition from the Helvetiafjellet Formation to the overlying Carolinefjellet Formation (Dalkjegla Member) in DH-1. FA-9 is mainly consisting of black shale (F-12) and is weakly laminated. The sand to mud ratio is based on visual observations of the core. **A)** Black shale (F-12) stratigraphically belonging to the Dalkjegla Member of the Aptian-Albian Carolinefjellet Formation and interpreted to represent offshore transition deposits (F-9). **B)** Matrix supported conglomerate belonging to the uppermost part of Glitrefjellet Member, interpreted to be wave-reworked delta deposits (FA-8) **C)** Closer picture of the polymictic conglomerate displaying the sub-rounded to sub-angular clasts.

5.2.9 FA-9: Offshore transition deposits

5.2.9.1 Description

FA-9 (Fig. 17) is only observed at the top of the logged section and is stratigraphically belonging to the Carolinefjellet Formation and Dalkjegla Member (Figs. 10 & 11). Facies included in this FA is predominantly of black shale (F-12), but locally isolated fine-grained sandstone is observed. These thin lenses and layers are less than 2 cm thick. The unit overlies a conglomerate (FA-8; F-1) and represents a major jump in facies association, with regards to depositional process. The unit is represented by a very high response in gamma ray values (Figs. 10 & 11).

5.2.9.2 Interpretation

Based on its stratigraphic position, the presence of black shale (F-12) and the sporadic occurrence of thin beds or lenses of sandstone, this facies association is interpreted as offshore transition deposits (Fig. 17). The presence of sandstone lenses and beds indicates strong wave activity and occasional storms. This indicates that the sediments are deposited between the mean fairwater wave base and storm wave base (Nichols, 2009). Similar ancient offshore transition deposits have been described from the Wasp Head Formation in the Lower Permian between Durras and Myrtle Beach in Australia (Rygel et al., 2008). The above interpretations are in accordance with several other works that seem to agree about the offshore deposits of the Carolinefjellet Formation (Mutrux et al., 2008; Midtkandal & Nystuen, 2009), and that the sediments stratigraphically belonging to the Dalkjegla Member are deposited between normal wave base and storm wave base. Additionally, the black shales have been correlated to the Oceanic Anoxic Event (OAEs), thus indicating anoxic conditions (Midtkandal et al., 2016). Organic matter has a very high preservation potential in anoxic water. This is supported by the very high response in gamma ray values (Fig. 10 & 11), indicating a high content of clay minerals.

5.3 Vertical stacking trends

5.3.1 Description

Based on the vertical stacking, the FAs, and recognized unconformities (i.e. abrupt facies change), seven different depositional units were recognized within DH-1 (Fig. 18). These provide the framework for local and regional correlative surfaces. A general trend shows that the facies are going from proximal to more distal environments based on the interpretation in this thesis (Fig. 18). Similar facies associations have been reported from numerous works from other locations in Svalbard (e.g. Nemeč, 1992; Gjelberg & Steel, 1995; Midtkandal & Nystuen, 2009). However, variations in the stacking trends have been observed.

Depositional unit 1 is restricted to the Rurikfjellet Formation and consists solely of prodelta deposits (FA-1) which form a slightly coarsening upwards unit (Fig. 18). The abrupt boundary between depositional unit 1 and 2 is marked by the Barremian subaerial unconformity (Fig. 18), which also represent the stratigraphic boundary between the Rurikfjellet Formation and the Helvetiafjellet Formation. Depositional unit 2 abruptly and erosively overlies depositional unit 1, and consists of fluvial braidplain deposits (FA-2) stratigraphically belonging to the Festningen Member (Fig. 18). These sediments form a distinct fining upward trend. There is a landward jump in facies associations from depositional unit 2 to depositional unit 3. Depositional unit 3 consists of alternating floodplain (FA-3), crevasse splay (FA-4) and fluvial channel (FA-5) deposits and is restricted to the Glitrefjellet Member. The facies associations within this unit are interfingering. Depositional unit 4 is restricted to the upper part of Glitrefjellet Member and consists mainly of fluvial channel deposits (FA-5). It has several intraformational unconformities (IU) (Fig. 18), typically confined to the base of fluvial channel bodies (FA-5; Fig. 19). The boundary between depositional unit 4 and 5 is marked by an intraformational flooding surface. Depositional unit 5 consists of delta plain deposits (FA-6) and delta front deposits (FA-7). The boundary between depositional unit 5 and 6 is represented by a transgressive ravinement surface (TRS) overlain by depositional unit 6, which consists of wave-reworked delta deposits (FA-8). The boundary between depositional unit 6 and 7 and is marked by a lower Aptian flooding surface (Fig. 18). Depositional unit 7 consists of offshore transition deposits (FA-9) and stratigraphically belongs to the Dalkjegla Member and the Carolinefjellet Formation.

5.3.2 Interpretation

Previous published work has documented changes in the vertical succession within Helvetiafjellet Formation, indicating an overall transgressive trend (Torsvik et al., 2002). In general, transgression is created when the accommodation is created more rapidly than it is consumed by sedimentation (Catuneanu, 2006). This suggests a long term rise in relative sea-level. This is further supported by a Cretaceous cycle chart displaying the eustatic sea-level (Haq et al., 1988; Ramkumar, 2016; Fig. 8).

The depositional system is considered to be progradational in the lower part of Glitrefjellet Member, thus coastal plain and delta deposits have formed (e.g. Midtkandal & Nystuen, 2009). In the upper part of the Glitrefjellet Member, transgressive deposits have been observed as estuaries, lagoons and barrier bar complexes (e.g. Nemeč et al., 1988; Nemeč, 1992; Gjelberg & Steel, 1995). There is an abrupt change from distal to proximal facies association in the lower part of the succession, suggesting prograding facies (depositional unit 1). The uppermost part of Rurikfjellet Formation is interpreted to consist of prodelta deposits (FA-1) and shows distal facies associations (Midtkandal & Nystuen, 2009). This has been interpreted to be due to uplift and relative sea-level fall (Gjelberg & Steel, 2012). As a consequence, sediments got exposed to subaerial exposure and eroded towards the basin in the south. This is marked by the Barremian Subaerial Unconformity (Fig.18).

The sandstone dominated Festningen Member shows a proximal jump in facies associations and marks depositional unit 2, interpreted to be due to uplift and high sediment influx. An abrupt basinwards jump in facies associations marks the transition to depositional unit 3, which marks the boundary between Festningen Member and Glitrefjellet Member. This intraformational flooding surface is represented by a package of coaly shale unit. This unit has previously been observed in Svalbard by Grundvåg & Olausen (2017).

The lower part of the Glitrefjellet Member is dominated by fluvial channels consisting of erosional bases, referred to as intraformational unconformities (IU; Fig. 18). As the channels migrate over the coastal plain towards the sea, crevasse splays occur during flooding of the river (Midtkandal & Nystuen, 2009). A minor flooding surface is observed when the fluvial distributary channel is overlaid by delta front deposits, belonging to depositional unit 4. This change in facies association represents a basinward migration of the shoreline where marine

facies are overlying non-marine facies. A transgressive ravinement surface (TRS) marks the base of the wave-reworked delta deposits represented by a conglomerate (FA-8; depositional unit 5).

The last section is marked by a bigger jump basinwards and is marked by a flooding surface. The wave-reworked delta deposits (FA-8) are abruptly overlain by offshore transition deposits (FA-9), suggesting a change in sediment influx or stronger wave influence. The flooding surface has been recognized with a regional extent. The lower part of the Carolinefjellet Formation belongs to Dalkjegla Member and is interpreted to be deposited under transgression (depositional unit 7).

Given the above, the vertical stacking trends show a distal-proximal-distal trend interpreted to be due to a relative fall in sea-level during deposition of the uppermost Rurikfjellet Formation, and long term relative rise in sea-level during deposition of the Helvetiafjellet Formation. The uppermost Carolinefjellet Formation also indicates a continuance of the relative sea-level rise.

DH-1 Scale 1:200 cm

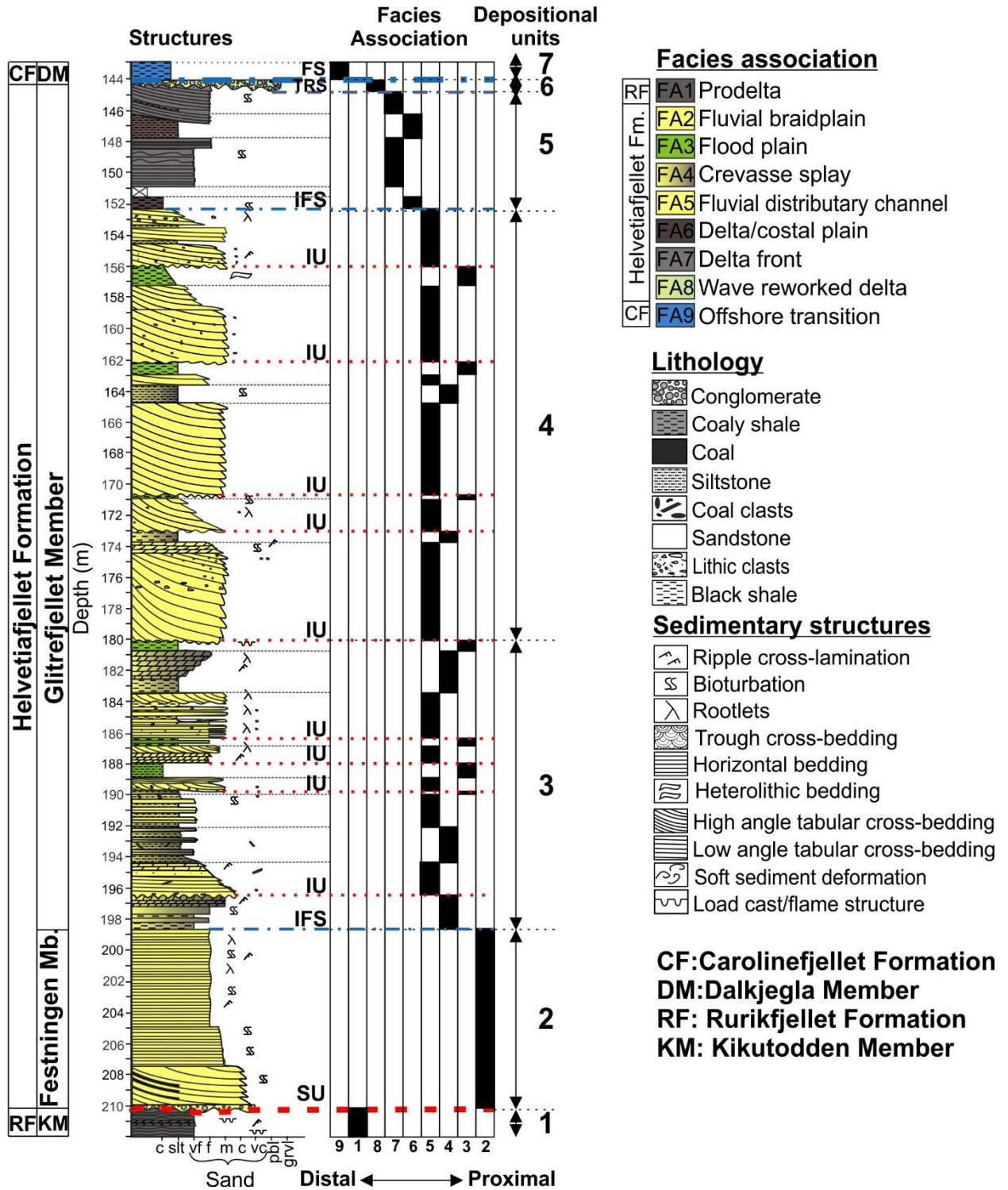


Figure 18: Vertical facies stacking pattern of the Helvetiafjellet Formation showing an overall increase in distal facies towards the top of the formation. The vertical stacking trends in DH-1 can be subdivided into 7 depositional units. Rurikfjellet Formation (depositional unit 1) and Carolinefjellet Formation (depositional unit 7) show a regressive trend and are interpreted to represent more distal facies associations. Helvetiafjellet Formation (unit 2, 3, 4, 5 and 6) shows an overall shift towards more basinwards and distal facies associations due to a long-term relative rise in sea level. Sequence stratigraphic surfaces, include: SU: Barremian subaerial unconformity, IFS: Intraformational flooding surface, IU: Intraformational unconformities, TRS: transgressive ravinement surface, FS: lower Aptian flooding surface.

5.4 Sequence stratigraphic surfaces

Sequence stratigraphic surfaces mark shifts through time in depositional regimes caused by change in depositional environments, sediment load or environmental energy flux (Catuneanu, 2006). The sequence stratigraphic boundaries in this thesis are defined by the depositional units presented in the previous section, mainly reflecting flooding surfaces and unconformities. The key sequence stratigraphic surfaces are observed as major landward/basinward shifts in facies associations and include Barremian Subaerial Unconformity and lower Aptian Flooding Surface (Fig. 18). They are usually a response to external influences on sedimentation and may reflect sea-level changes, tectonic subsidence or sediment supply (Nichols, 2009). Several smaller erosional surfaces have been recognized within the core (IU; Fig. 18). Flooding surfaces with semi-regional to regional extent have also been observed (IFS & TRS; Fig. 18). The five surfaces discussed in the following subchapters are representative of major and abrupt change in facies associations. However, the regional extent of the respective surfaces is observed to vary throughout the Helvetiafjellet Formation.

5.4.1 Barremian subaerial unconformity

5.4.1.1 Description

Unconformity 1 (Figs. 10, 11, 12 & 18) is confined to the lower part of the logged succession. The boundary is marked by an abrupt change in FAs, with depositional unit 2 (fluvial braidplain deposits; FA-2) sharply overlying depositional unit 1 (prodelta deposits; FA-1) (Fig. 18). A 25 cm thick polymictic sand-matrix conglomerate (Fig. 12) is present at the boundary of fluvial braidplain deposits (FA-2), immediately overlying the unconformity. The gamma ray values shows some indications of a decrease in values, but no clear trend.

5.4.1.2 Interpretation

In the cores, this erosive surface marks the dramatic change from mudstones to coarse-grained sandstones, simultaneously corresponding to a shift in Gamma Ray response from medium to low values. Given the above, this landwards jump in facies associations has been interpreted as the Barremian subaerial unconformity. Similar regional unconformities have been suggested to be present within the Triassic succession in the Barents Sea (Riis et al.,

2008; Glørstad-Clark et al., 2010). The interpretation is also in compliance with previous studies of the Helvetiafjellet Formation (Nemec, 1992; Gjelberg & Steel, 1995; Midtkandal et al., 2008; Grundvåg & Olausson, 2017).

In general, a subaerial unconformity is marked by the abrupt change from any type of depositional system (e.g. fluvial, coastal or marine) to the overlying non-marine deposits (Catuneanu, 2006). The drastic change is a consequence of a major fall in relative sea-level, often causing basinward extension of major river systems (Ahokas et al., 2014). With regards to the Helvetiafjellet Formation, it is interpreted to be caused by uplift related to HALIP and tilting during the Barremian accompanied by a fall in relative sea-level (Nemec et al, 1988; Nemec, 1992; Maher, 2001; Midtkandal et al., 2007; Dörr et al., 2011). This resulted in erosion of the shelf deposits and deposition of fluvial braidplains (FA-2) above the unconformity during relative sea-level rise. The unconformity extends regionally and marks the stratigraphic boundary between Rurikfjellet Formation (Valanginian to early Barremian) and Helvetiafjellet Formation (Barremian –early Aptian) (Midtkandal et al, 2008; Figs. 8, 18, 19 &20).

5.4.2 Intraformational flooding surface (IFS)

5.4.2.1 *Description*

This surface is observed at the boundary between depositional unit 2 and 3 and between depositional unit 4 and 5 (Fig. 18).

A distal change in facies observations marks the first surface from fluvial braidplain deposits (FA-2) to crevasse splay deposits (FA-4). The second surface is more distinct and marks the first significant sign of the overall transgressive trend in this proximal location. There is an abrupt upward deepening of FAs, with deltaic deposits on top of fluvial deposits (Fig. 18). Delta front deposits (FA-7) directly overly fluvial distributary channel deposits (FA-5) in the uppermost part of the Helvetiafjellet Formation (Fig. 18). The extent of the surface is unknown, but may be of semi-regional significance.

5.4.2.2 *Interpretation*

The intraformational flooding surface between depositional unit 2 and 3 acts as the stratigraphic boundary between the Festningen Member and the Glitrefjellet Member. There is a drastic jump from very coarse grained sandstone deposits from the proximal part, to very fine-grained mudstone deposits deposited in a more distal setting. The surface is observed as a coaly shale and mudstone bed (Figs. 10 & 11). Based on the abrupt change from fluvial distributary channel deposits (FA-5) to delta front deposits (FA-7), the second surface has also been interpreted as an intraformational flooding surface (Fig. 18). The change from proximal to distal facies association indicates flooding of the area. The interpretation is in line with previous studies of the Helvetiafjellet Formation. Midtkandal & Nystuen (2009) observed this surface across their transect as the boundary between the Festningen Member and the Glitrefjellet Member from the Festningen locality to the Kikutodden locality. The surface has also recently been interpreted as a coaly shale unit that represents an expansion surface from a lower to higher-accommodation system (Grundvåg & Olausen, 2017). The intraformational flooding surface is also in accordance with the eustatic sea-level during Early Cretaceous, which indicates high sea-levels in the given period (Haq et al, 1988; Fig. 8).

5.4.3 Intraformational unconformities (IU)

5.4.3.1 *Description*

Intraformational unconformities are located at the base of thick fining upwards packages composed of sandstone (FA-5; Fig. 15) overlying floodplain deposits (FA-3) or crevasse splay deposits (FA-4). They are restricted to the Glitrefjellet Member (Fig. 18). These surfaces do not attribute to regional extensive events, but represent local autogenic incisions created by isolated channels on the coastal plain and delta plain. As can be seen in the presentation logs (Figs. 10 & 11), no major facies changes occur in relation to these unconformities.

5.4.3.2 *Interpretation*

Based on the erosional boundary to the underlying units (FA-3 or FA-4) and the overlying isolated fining upwards sandstone, in addition to occasional presence of conglomerate at the base of the channels, the unconformity is interpreted to represent an intraformational

unconformity (Fig. 18). The interpretation is in line with previous studies from the Glitrefjellet Member, which has suggested that the basal erosive boundaries reflects channelized transport of sand across the coastal plain (Midtkandal et al., 2007).

5.4.4 Transgressive ravinement surface (TRS)

5.4.4.1 Description

The boundary is marked by an abrupt change in FAs, with depositional unit 6, consisting of wave-reworked delta deposits (FA-8), sharply overlying depositional unit 5, consisting of delta front deposits (FA-7; Fig. 18).

5.4.4.2 Interpretation

Based on the observation of the sharp-based conglomerate capping a deltaic succession, this surface has been interpreted to represent a transgressive lag formed by wave-erosion on the shoreface during transgression (Bache et al., 2014) and is referred to as a transgressive ravinement surface (Fig. 18). This is supported by the overall high eustatic sea level during Lower Cretaceous (Haq et al., 1987; Haq et al., 1988; Ramkumar, 2016; Fig. 8). They form therefore over a relative short range of water depths where erosion by waves can occur. The occurrence of a transgression is a consequence of nearshore subsidence or sea-level rise not being balanced by incoming sediment supply. As the coastal plain is flooded, a transgressive ravinement surface forms by erosion of the surface (Bache et al., 2014). The finer sediments will be brought out on the shelf in suspension, while the coarser material will be deposited as a transgressive lag. In general, the strata below a transgressive ravinement surface is variable (e.g. fluvial, coastal, shallow marine), whereas the facies above are always shallow-marine (Catuneanu, 2006). This supports the interpretation due to the wave-reworked delta deposits (FA-8) overlying the delta front deposits (FA-7). Similar ancient transgressive ravinement surfaces have been recorded in the Upper Pennsylvanian sandstone unit in Oklahoma, U.S.A. (Yang, 2007). Similar deposits have recently been observed in Svalbard (Grundvåg & Olausson, 2017), thus supporting the interpretation.

5.4.5 lower Aptian flooding surface

5.4.5.1 *Description*

The boundary is marked by an abrupt change in FAs, with depositional unit 7 overlying depositional unit 6 (Fig. 18). The drastic change basinwards in facies associations can be seen at the top of Helvetiafjellet Formation as a change from sandstone deposits to black shale deposits (Figs. 17 & 19). The gamma ray log shows very high values in the given interval (Figs. 10 & 11).

5.4.5.2 *Interpretation*

The change from wave-reworked delta deposits (FA-8) to offshore transition deposits (FA-9) indicates deposition in a more open marine environment and suggests an increase in water depth. Based on the observations above, this boundary is interpreted to represent a lower Aptian Flooding Surface (Fig. 18). These observations are in accordance with previous published work also recognizing a flooding surface at the boundary of both the Helvetiafjellet Formation and the Carolinefjellet Formation (Midtkandal et al., 2007; Midtkandal et al 2016; Grundvåg & Olausen, 2017). A mud blanket capping the underlying sediments was deposited during the flooding of the coastal plain. As the deposits were subjected to burial, they became shales. As the black shales have been interpreted to be associated with Oceanic Anoxic Events, they can be dated on the initial negative δ^{13} isotope (Midtkandal et al., 2016). The age of the Aptian-Barreman boundary is approximately 121-122 Ma (Midtkandal et al., 2016).

5.5 Depositional model of the Helvetiafjellet Formation

The depositional model presented herein is based on the results from this thesis in combination with previous published work (Birkenmajer, 1984; Nemec et al., 1988; Dypvik et al., 1991; Nemec, 1992; Midtkandal et al., 2008; Midtkandal & Nystuen, 2009; Onderdonk & Midtkandal, 2010; Grundvåg, 2017, unpublished). As the Helvetiafjellet Formation is represented over the whole Lower Cretaceous outcrop window in Svalbard (Parker, 1967), two transects (Figs. 18 & 19) have been made in order to show local variations, which are more or less parallel to sub-parallel to the inferred depositional dip direction. All previous studies show migration towards the south-east (Edwards, 1978; Nemec, 1992; Gjelberg & Steel, 1995; Midtkandal et al., 2007; Midtkandal & Nystuen, 2009). Therefore, a west-east oriented transect (Festningen to Agardhfjellet localities) and a northwest-southeast transect (Festningen to Kvalvågen localities) has been constructed in order to address vertical and lateral changes in facies associations. The logged sections are simplified and adjusted to scale 1:200 cm. The vertical scale aims to indicate the distance between the locations, but are not to scale. The lower Aptian flooding surface has been used as a correlation surface (Figs. 18 & 19) as it is a low angle surface compared to fluvial erosion surfaces (e.g. the Barremian subaerial unconformity; Figs. 12 & 18). The choice of reference surface will play a major role in how the correlations are made, thus affecting the interpretation of the stacking patterns and lateral developments (Bhattacharya, 2011). As previously mentioned, the facies development within Helvetiafjellet Formation is highly debated. This has resulted in the suggestion of several different depositional models, such as the layer-cake model and the diachronous model (Nemec, 1992; Gjelberg & Steel, 1995; Midtkandal & Nystuen, 2009; Fig. 7).

5.5.1 Transect 1 - Festningen to Agardhfjellet (W-E)

5.5.1.1 Description

Transect 1 is 128 km in total and includes eight locations going from west to east on Svalbard (Fig. 20). In general, very similar characteristics in the facies associations can be observed within the lower parts of the transect (Fig. 21) and will therefore be described together. The variations are greater in the middle and upper part of the logged intervals. Similar developments in facies associations are seen between the Festningen and Innerhausen

localities, whereas the Myklegardhfjellet and the Agardhfjellet localities show indications of stronger marine influenced deposits (Birkenmajer, 1984; Midtkandal & Nystuen, 2009). The most proximal part of the study area includes the localities of Festningen, DH-1, DH-1A, Helvetiafjellet, Glitrefjellet and Innerknausen. They show similar vertical stacking patterns and will therefore be described together. Offshore deposits and prodelta deposits (FA-1) are present at all locations. The erosive boundary is marked by an abrupt change in FAs, with fluvial braidplain deposits (FA-2) overlying the depositional unit. The boundary has a regional extent across the transect (Fig. 19). An abrupt change to more distal facies associations is marked by the boundary between the Rurikfjellet Formation and the Helvetiafjellet Formation. The Festningen Member is represented by fluvial braidplain deposits (FA-2) at all localities. There is an intraformational flooding surface present at almost all the localities (Figs. 18 & 19). Interfingering floodplain deposits (FA-3), crevasse splay deposits (FA-4) and fluvial distributary channel deposits (FA-5) are observed.

The distal part of the transect includes the Myklegardhfjellet locality and the Agardhfjellet locality. At these localities, the Glitrefjellet Member, consists of fine grained deposits with isolated coarser grained sandbars (Midtkandal & Nystuen, 2009). A regional intraformational flooding surface (Figs. 18 & 19) caps the fluvial deposits (FA-5) and marks a basinwards jump in facies associations towards shallow marine facies (FA-6, FA-7 and FA-8).

The thickness of Helvetiafjellet Formation varies significantly throughout the transect. The Festningen Member is between 10-17 m thick, while the Glitrefjellet Member varies between 40-76 m in thickness. The sediments are generally thickening towards the west.

5.5.1.2 Interpretation

Transect 1 shows mostly minor variations in facies associations between the logged sections, with a general increase in marine facies associations upwards in the vertical succession and towards the south. This is supported by the epicontinental sea located in the south (Steel & Worsley, 1984) and evidence of rise in relative sea-level during deposition of the Helvetiafjellet Formation. The underlying Rurikfjellet and overlying Carolinefjellet formations are interpreted to represent offshore deposits (FA-1 and FA-9). This is in accordance with previous published work from the same formations (Gjelberg & Steel, 1995; Midtkandal & Nystuen, 2009). The Barremian subaerial unconformity (Parker, 1967; Steel & Worsly, 1984;

Midtkandal & Nystuen, 2009) and the lower Aptian flooding surface are present (Grundvåg et al., 2017) and act as boundaries between the three formations (Fig. 19).

A regional intraformational flooding surface is observed at the top of the Festningen Member, suggesting a minor flooding of the area. Most of the Glitrefjellet Member consists of alternating fluvial deposits (FA-5) and coastal plain deposits (FA-3 and FA-4). However, a regional intraformational flooding surface caps the sediments in the uppermost part of the Glitrefjellet Member. Based on the presence of shell-fragments, wave-ripple lamination and heterolithic bedding, these deposits have been interpreted as shallow marine deposits (Midtkandal & Nystuen, 2009).

An important observation is the significant variations in thickness within the transect. Previous work has observed an overall thinning towards the northwestern part of Svalbard. However, an overall increase in thickness has been observed towards the west. Possible reasons for the variations in thickness will be discussed in Chp. 6.2.

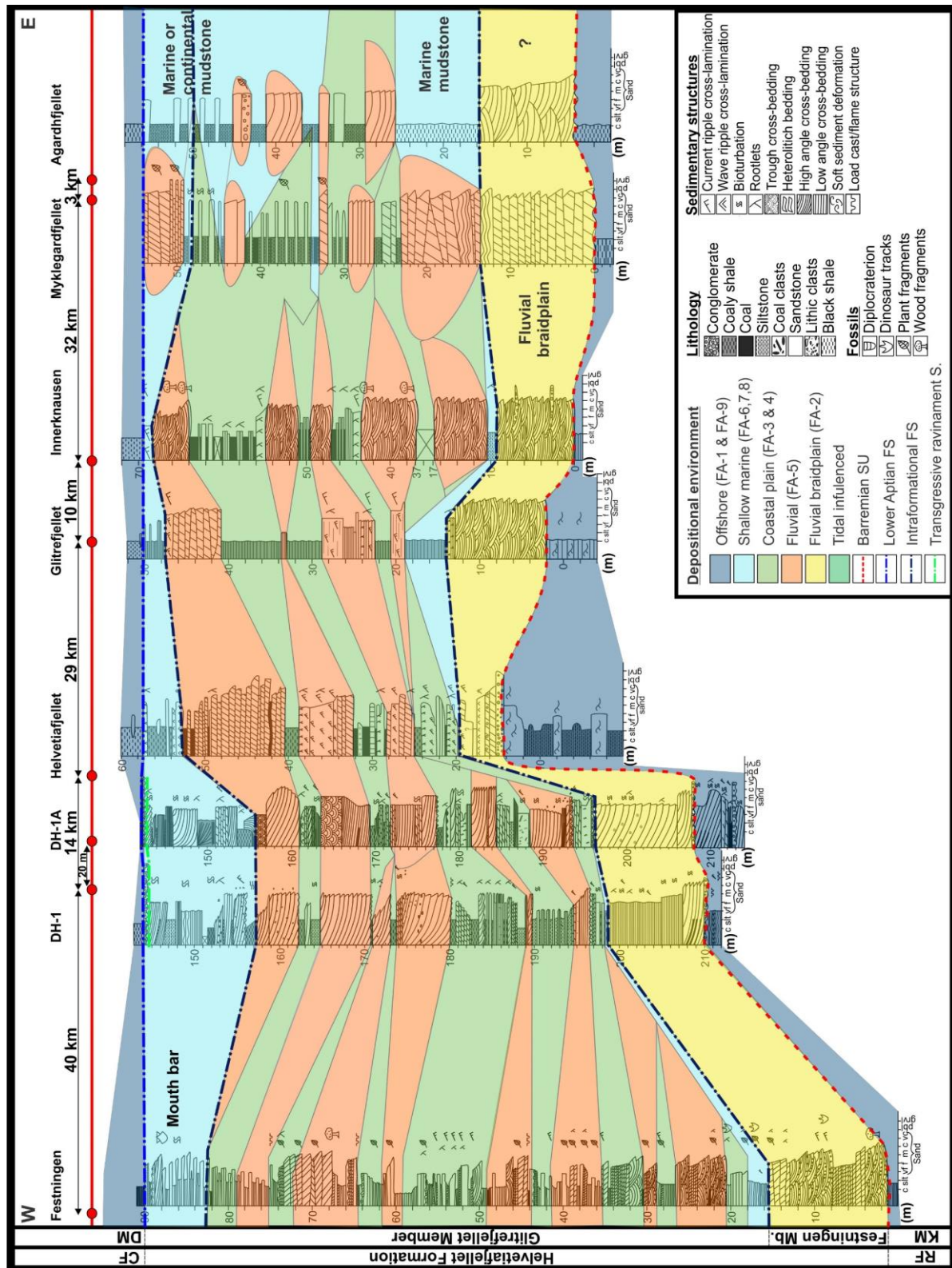


Figure 19: Vertical representative profiles (1:200 cm) through transect 1 showing the lithological variability and interpreted facies associations of the Helvetiafjellet Formation. The Helvetiafjellet Formation shows a general trend of thinning towards the east (see Fig. 20 for location). Red circles illustrate the distance between the localities and are not to scale. Logs modified from the Festningen (Grundvåg, 2017, unpublished), Helvetiafjellet (Gjelberg & Steel, 1995), Giltrefjellet (Midtkandal et al., 2008; Dypvik et al, 1991), Innerknausen (Nemec, 1992), Myklegardfjellet (Birkenmajer, 1984) and Agardhfjellet (Midtkandal & Nysten, 2009) localities.

5.5.2 Transect 2 - Festningen to Kvalvågen (NW-SE)

5.5.2.1 Description

Transect 2 (northwest-southeast) is 120 km long and includes the Festningen, Ullaberget and Kvalvågen localities. The thickness of the Helvetiafjellet Formation varies within transect 2 (Fig. 20), with a significant thickening towards the Festningen locality (Fig. 20). The Festningen Member is generally 8-16 m thick. At Ullaberget locality, the thickness of Louiseberget bed is 20 m. The Glitrefjellet Member varies between 74 meters in the proximal part (the Festningen locality) and 66 meters in the distal part (the Kvalvågen locality). There is an increase in marine influenced facies associations at the Kvalvågen locality, consisting of deposits of delta front, mouth bars and shoreface/shallow marine environments (Onderdonk & Midtkandal, 2010).

Offshore deposits are restricted to the Rurikfjellet Formation and are observed at all locations. The lowermost part of the unit can be seen as a change in facies association from mudstone (FA-1, Table 2) to coarse-grained sandstone (FA-2, Table 2), marked by the Barremian SU (Fig. 18). The Festningen Member consists of fluvial braidplain deposits (FA-2), while the Glitrefjellet Member consists of coastal plain deposits (FA-3 and FA-4) and fluvial deposits (FA-5), and the Ullaberget locality consists of tidal-influenced deposits (Gjelberg & Steel, 1995; Midtkandal & Nystuen, 2009). The lowermost unit is restricted to the Louiseberget bed and consists of very different facies associations than the rest of the Helvetiafjellet Formation.

The Kvalvågen locality has been described by Onderdonk & Midtkandal (2010). The succession consists of fluvial braidplain deposits (FA-2) in the lowermost part and is restricted to Festningen Member. The Glitrefjellet Member is mainly dominated by fine grained sediments in the lowermost part. Upwards-coarsening packages are observed towards the middle of the formation. A package of 16 m consists of coarse-grained sandstone interfingering with thin intervals of mudstone. Plant fragments, together with current ripple-lamination and soft sediment deformation, are observed. A regional extending intraformational surface can be traced across transect 2. The uppermost part of the Glitrefjellet Member consists of a semi-regional surface at the base of two sandstone packages. The trace fossil *Skolithos* has been observed at the base of the first package.

5.5.2.2 Interpretation

Significant variations in the lateral distribution of different facies associations can be seen within transect 2 (Fig. 20). The underlying Rurikfjellet and overlying Carolinefjellet formations are interpreted to represent offshore deposits and are separated by the Barremian subaerial unconformity at the base and the lower Aptian flooding surface at the top (Parker, 1967; Midtkandal & Nystuen, 2009).

The Festningen locality is interpreted to represent proximal facies associations. Fluvial braidplain deposits (FA-2) are interpreted to belong to the Festningen Member. Most of the Glitrefjellet Member consists of fluvial deposits (FA-5) and coastal plain deposits (FA-3 and FA-4). Based on the shell-fragments, the uppermost package has been interpreted to represent mouth bar deposits.

The Ullaberget locality shows different characteristics than the other investigated localities due to the presence of tidal-influenced deposits (Gjelberg & Steel, 1995; Midtkandal & Nystuen, 2009). The lowermost unit is restricted to the Louiseberget Bed and consists of very different facies associations than the rest of the Helvetiafjellet Formation. Midtkandal & Nystuen (2009) have interpreted this unit to include a bayhead- delta overlain by lagoonal deposits. Fluvial braidplain deposits (FA-2) stratigraphically belonging to the Festningen Member overlays the Louiseberget Bed. The lowermost part of Glitrefjellet Member has been interpreted to include a tidal channel in an estuary, a tidal flat and a tidal channel (Grundvåg, 2017, unpublished). This is in accordance with previous published work from the same locality (Gjelberg & Steel, 1995; Midtkandal & Nystuen, 2009). The middle part of the Glitrefjellet Member is mainly dominated by coastal plain deposits (FA-3 and FA-4). However, two intervals containing *Diplocraterion* suggest shallow marine facies associations. The uppermost part of the Glitrefjellet Member consists of shallow marine facies associations. The boundary has been interpreted as a regional intraformational flooding surface (IFS; Figs. 18 & 20). A thin bed containing *Diplocraterion* supports the interpretation of a shallow marine environment. Lagoonal deposits are underlying barrier bar deposits. The boundary is represented by a semi-regional transgressive ravinement surface (TRS; Figs. 18 & 20).

The Kvalvågen locality is mainly influenced by shallow marine deposits, which are described in detail by Onderdonk & Midtkandal (2010). Fluvial braidplain deposits (FA-2) are interpreted to belong to the Festningen Member. Based on the very fine-grained and thick succession, the lowermost part of the Glitrefjellet Member is interpreted to represent prodelta deposits. Three upwards coarsening packages containing current ripple cross-lamination on the top are interpreted to represent mouth bar deposits. The middle part of the Glitrefjellet Member consists of a thick unit of sandstone interpreted to be delta top deposits, including current ripple cross-lamination, load cast structures and plant fragments. The unit is capped by a regional intraformational flooding surface (IFS; Figs. 18 & 20). The uppermost part of the Glitrefjellet Member is interpreted to represent barrier bars (Nemec et al., 1988; Onderdonk & Midtkandal, 2010). The base of the barrier bar is represented by a semi-regional transgressive ravinement surface, which will be discussed in Chp. 6.4.

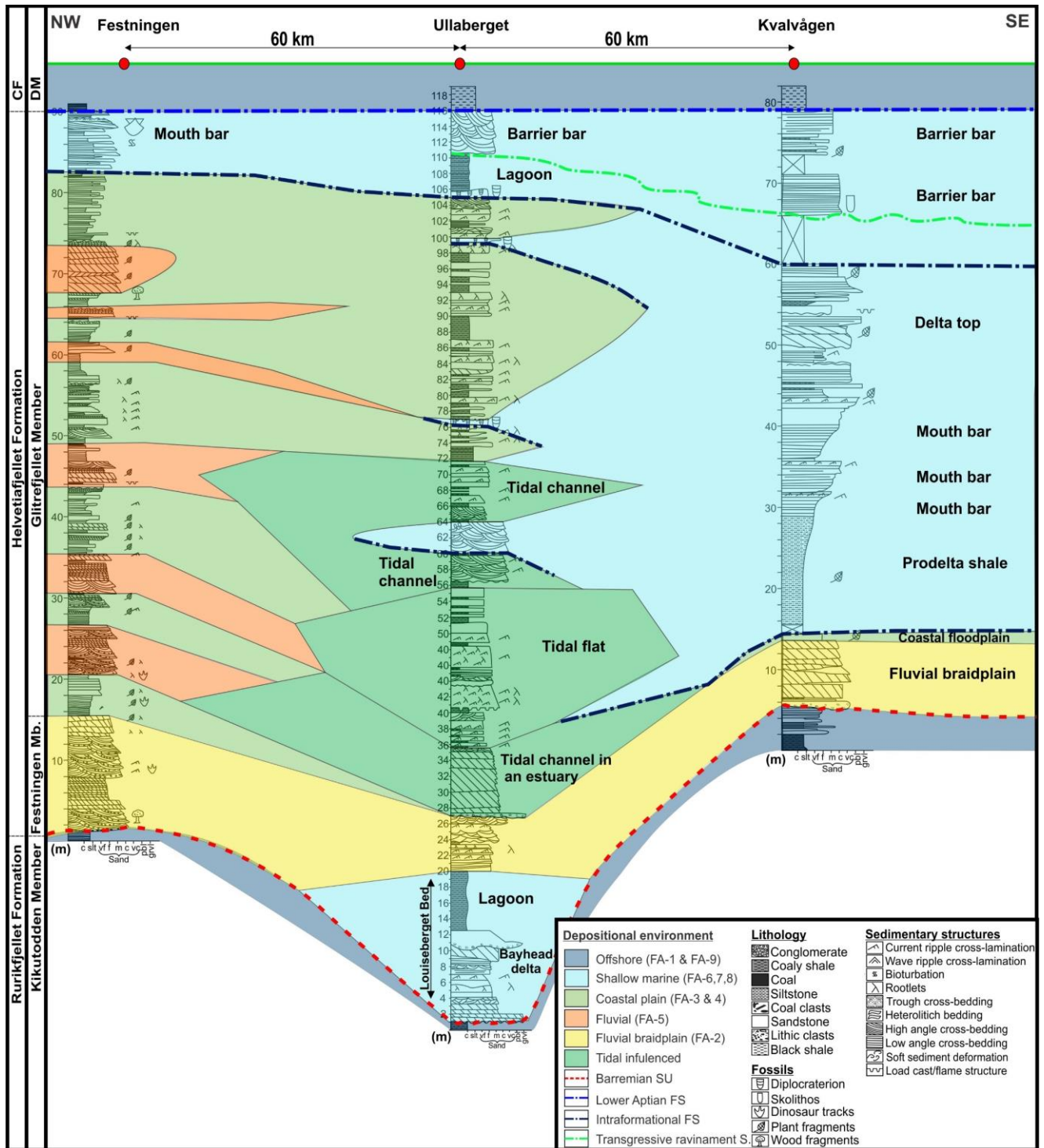


Figure 20: Vertical transect (1: 200 cm) from northwest to southeast showing the vertical and lateral sediment distribution. The Festningen locality is mainly influenced by fluvial and coastal plain FAs. The Ullaberget locality is mainly dominated by tidal influenced deposits which previously have been described by Nemeč (1992) and Midtkandal & Nystuen (2009). The Kvalvågen locality is mainly comprised of wave-dominated deposits and is based on the interpretations presented by Onderdonk & Midtkandal, 2010. Note that the delta top has been characterized as shallow marine in the figure. It may, however, be fluvial as well, depending on the local sea-level. The correlation panel is based on logs from the Festningen (Grundvåg, 2017, unpublished), Ullaberget (Grundvåg, 2017, unpublished) and Kvalvågen (Onderdonk & Midtkandal, 2010) localities.

6 Discussion

Although the Helvetiafjellet Formation has been given a lot of attention in previous published papers (e.g. Parker, 1967; Edwards, 1976; Nemeč et al., 1988; Nemeč, 1992; Gjelberg & Steel, 1995; Steel et al., 2000; Midtkandal et al., 2007, Midtkandal & Nystuen, 2009, Grundvåg & Olaussen, 2017), the Glitrefjellet Member remains poorly understood. Due to the outcrops being only partially exposed, it has been difficult to study in great detail. In this section, the results of the present study is compared to previous published work and some potential modern analogues in order to explain the depositional architecture of the Helvetiafjellet Formation.

6.1 Revised depositional model of the Helvetiafjellet Formation

In previous studies, the Helvetiafjellet Formation has been subdivided into two stratigraphic members; the Festningen Member and the Glitrefjellet Member (Parker, 1967; Edwards, 1976; Midtkandal & Nystuen, 2009). Most previous published work agrees in this division. However, the acknowledgment of the Glitrefjellet Member was for example rejected by Mørk et al (1999) as a result of the model presented by Gjelberg & Steel (1995). There have been disagreements among different researchers about the depositional evolution, and various attempts have been made to try to reconstruct its depositional history, thus resulting in several suggestions of depositional models (Nagy, 1970; Nemeč 1992; Gjelberg & Steel, 1995; Steel et al., 2000; Midtkandal & Nystuen, 2009; Fig. 7). Of these, the models that received the most attention will be discussed below.

Gjelberg & Steel (1995) suggested a transgressive depositional model, with diachronous development of the formation. This model received a lot of attention and is based on the regressive-transgressive model of Nemeč (1992; Fig. 7). It shows a clear back-stepping trend with a shoreline located just south of the present-day shoreline. The transition from the uppermost part of the Helvetiafjellet Formation into the open marine Carolinefjellet Formation is a result of the ratio between the rise in relative sea-level and the rate of sediment supply. Midtkandal & Nystuen (2009) argued for an aggradational setting with low-angle facies belts. A combination of autogenic and allogenic processes were controlling the

stacking patterns in the uppermost part of the unit. Notably, no upward increase in marine influenced sediments were observed within their study area.

Findings in this thesis, on the other hand, suggest a model somewhere between the transgressive model presented by Gjelberg & Steel (1995) and the aggradational setting presented by Midtkandal & Nystuen (2009). Based on the facies analysis and the correlation panels (Figs. 19 & 20), it can be argued that Helvetiafjellet Formation was deposited in a deltaic setting, which is in accordance with previous studies (Nemec et al., 1988; Nemec, 1992; Steel et al., 2000; Midtkandal & Nystuen, 2009). Regional paleocurrent direction measurements show that the source area was located north-west in Svalbard (Gjelberg & Steel, 1995; Midtkandal et al., 2007). The architectural pattern of the formation indicates that the formation was deposited as an overall long-term rise in relative sea-level (Nemec, 1992). This is in accordance with the basinal subsidence related to major fault systems prominently caused by a decrease in HALIP activity and overall worldwide eustatic sea-level in Early Cretaceous (Worsely, 1986). However, both sediment supply and relative sea-level has also influenced the depositional evolution of the Helvetiafjellet Formation. In addition, autogenic factors, such as delta lobe switching and river channel avulsion have played an important role in controlling facies distribution at a local scale (e.g. Midtkandal et al., 2007; Midtkandal & Nystuen, 2009)

6.2 Regional depositional trends and controls

The vertical relationship of the facies associations as documented in the cores also shows a lateral depositional trend within the two regional transects (Figs. 19 & 20). Seven depositional units were defined based on the vertical stacking pattern of DH-1, suggesting that the Helvetiafjellet Formation was deposited in a deltaic shoreline setting, which is in accordance with previous studies (Steel & Worsley, 1984; Nemeč, 1992; Gjelberg & Steel, 1995).

The Rurikfjellet Formation has been interpreted as prodelta deposits (FA-1; Steel & Worsley, 1984; Nemeč et al., 1988; Dypvik et al., 1991; Midtkandal et al., 2008; Gjelberg & Steel, 2012), suggesting deposition in a distal position (depositional unit 1; Fig. 18) and delta front progradation prior to the formation of the subaerial unconformity at the base of the Helvetiafjellet Formation. The unconformity formed as a result of uplift and erosion in the Barremian (Parker, 1967; Steel & Worsley, 1984; Midtkandal & Nystuen, 2009). Due to high sedimentary input from the source area in the northwest, a fluvial braidplain (FA-2) was deposited at all locations in transect 1 and 2 (Depositional unit 2; Fig. 18). A regional relative sea-level rise and fluvial aggradation have to be invoked in order to provide accommodation space for such a regionally extensive braidplain. FA-2 stratigraphically belongs to the Festningen Member (Parker, 1967; Midtkandal et al., 2008). The Glitrefjellet Member consists of multiple facies associations ranging from coastal plain facies to delta facies to transgressive delta facies (Table 2; Fig. 21), and represents depositional unit 3, 4, 5 and 6 (Fig. 18). The facies associations include floodplain deposits (FA-3), crevasse splay deposits (FA-4) and fluvial distributary channel deposits (FA-5), delta front (FA-7), delta plain (FA-6), and wave-reworked deposits (FA-8). Tidal influenced facies have also been described by Gjelberg & Steel (1995) and Midtkandal & Nystuen (2009) at e.g. the Ullaberget Locality. These deposits indicate deposition in a distal part of the depositional environment when the sediment supply has been outpaced by the rise in relative sea-level, thus resulting in shoreline retreat towards the northwest of Svalbard (Figs. 19 & 20). The boundary between the Helvetiafjellet Formation and the overlying Carlinefjellet Formation is shown by an abrupt change in facies associations, reflecting a dramatic and regional increase in water depth. This suggests that the boundary represents a flooding surface, referred to as a lower Aptian Flooding surface (Midtkandal et al., 2016; Grundvåg et al., 2017; Figs. 18, 19 & 20).

Previous studies have interpreted the lower part of the Carolinefjellet Formation as open marine shelf (Gjelberg & Steel, 1995) to barrier bar (Mutrux et al., 2008) deposits. However, they have been interpreted to represent offshore transition deposits (FA-9) based on observations in this thesis (Figs. 10, 11 & 17). There is a general increase in shallow marine deposits (FA-6, FA-7 and FA-8) towards the south eastern part of the two transects (Figs. 19 & 20). This is in accordance with previous observations of localities in the same area (e.g. the Agardhfjellet locality; Midtkandal & Nystuen, 2009 and the Kvalvågen locality; Nemec et al., 1988). The abovementioned factors are summarized in the depositional model of the facies associations of the Rurikfjellet, Helvetiafjellet and Carolinefjellet formations (Fig. 21).

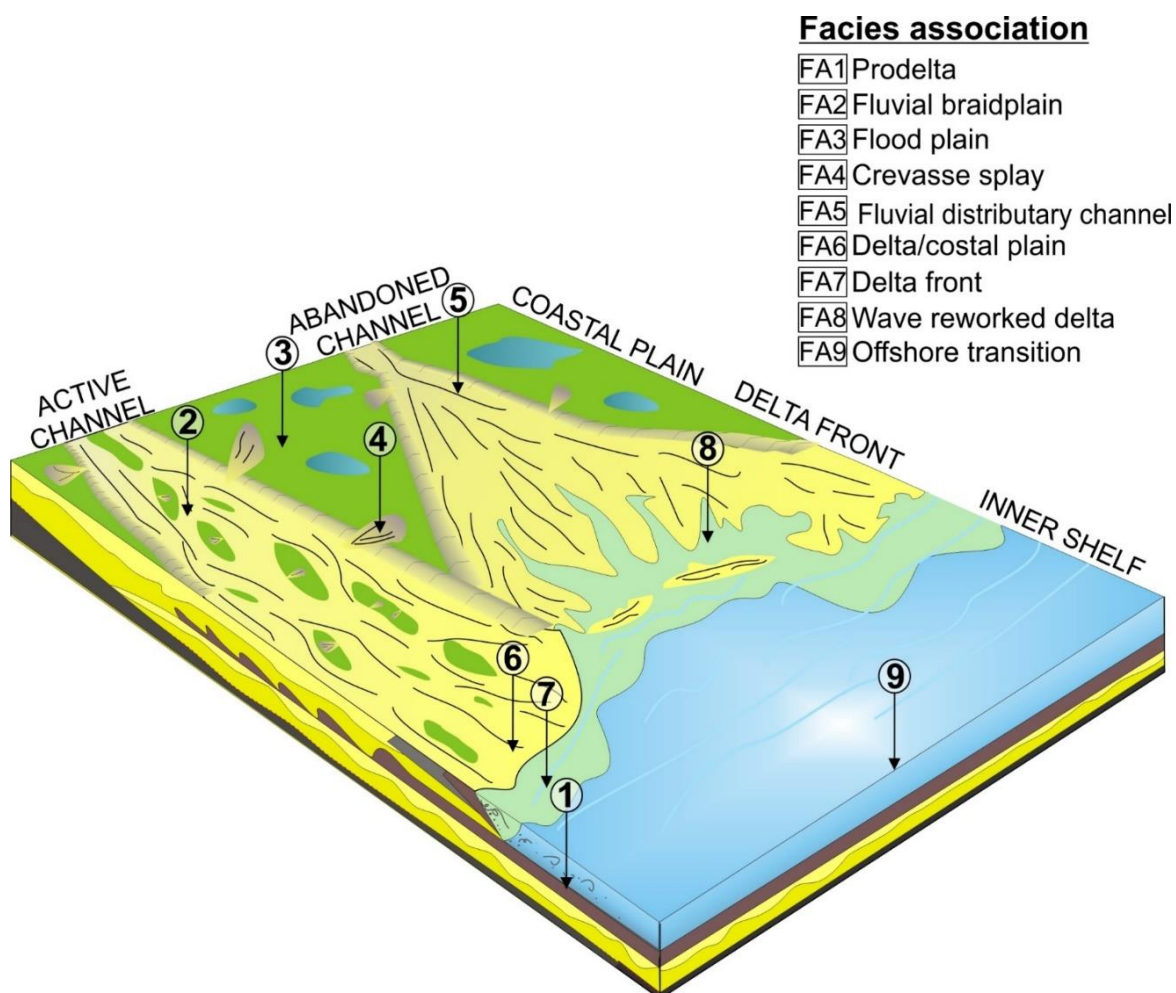


Figure 21: Depositional model of the recognized FAs in the Helvetiafjellet Formation based on interpretations of DH-1 and DH-1A. The study area ranges from the proximal part (coastal plain) to the distal part (inner shelf). The upper part of Rurikfjellet Formation is represented by FA-1. Helvetiafjellet Formation is represented by FA-2 to FA-8. FA-2 is the only FA in the Festningen Member. Glitrefjellet Member consists of FA-3 to FA-8. The upper boundary is represented by the Lower Aptian Flooding Surface and separated the Helvetiafjellet Formation and the Carolinefjellet Formation. The Carolinefjellet Formation is represented by offshore transition deposits (FA-9). The FA are numbered based on when they first are observed within the logged section. The names are given based on the interpreted depositional environment. Note that the model is not to scale and is used as a visualization of the depositional environment. Based on model presented by Grundvåg (2015).

Transect 1 (Fig. 19) and Transect 2 (Fig. 20) illustrate that the sediments prograded from the proximal part in the northwest towards the distal part in the southeast during Early Cretaceous. This is in accordance with paleocurrent measurements observed at different localities at Spitsbergen (Gjelberg & Steel, 1995; Midtkandal et al., 2007), and an overall thickening towards the south (Birkenmajer, 1975). These observations have been linked to the emplacement of the HALIP in the north, and uplift and southwards tilting in the north western parts of Spitsbergen during the Early Cretaceous (Steel & Worsley, 1984; Maher, 2001; Dörr et al., 2011). The HALIP led to crustal updoming and development of a subaerial unconformity (Gjelberg & Steel, 1995; Grundvåg & Olausen, 2017). In combination with a general high sediment input and the long-term relative rise in sea-level, accommodation space was created and resulting in deposition of the Helvetiafjellet Formation above the subaerial unconformity (Corfu et al., 2013). In contrast to all previous published work, transect 1 (Fig. 19) and transect 2 (Fig. 20) indicate that the thickness of Helvetiafjellet Formation varies significantly throughout the two transects. Both in transect 1 and 2 (Figs. 19 & 20), an overall increase in thickness towards the proximal area, located in the northwest, is observed. In transect 2, though, the Ullaberget locality is observed as significantly thicker. The latter is indicative of deposition in a semi-regional incised valley (Midtkandal & Nystuen, 2009).

There has been great uncertainties around the driving force of basin subsidence. Bott (1976) points out three main factors that appear to be involved. The factors include gravity loading by either sediments or water, thermal events with subsequent cooling, and response of the continental crust to tensional stress. Gravity-based subsidence is mostly restricted to the outer shelf, however, and will therefore not be taken into account in this paper.

The deposits of the Helvetiafjellet Formation are considered to have accumulated in a slowly subsidising basin that was covered by a shallow, low-angle epicontinental sea (Steel & Worsley, 1984). This, together with the low-gradient shelf and coastal plain, made the accumulation of the deposits very sensitive to fluctuations in relative sea-level and sediment input (Midtkandal et al., 2008). The terrigenous input during deposition of the Festningen Member and the lower part of the Glitrefjellet Member was significant, but eventually the sediment input was outpaced by basinal subsidence and relative rise in sea-level in the

upper part of the Glitrefjellet Member. This resulted in the distal facies progressively overlapping the older strata northwards (Steel & Worsley, 1984). The cause of these variations may be a result of movements along regional faults (e.g. the Billefjorden and Lomfjorden fault zones), possibly governed by HALIP activity. Unfortunately, it is not well established what caused the basin subsidence and lateral variations in thickness.

6.2.1 Movements along regional faults, possibly governed by HALIP activity

Thermal activity contributes to basin subsidence as the lithosphere is exposed to uplift by thermal expansion, followed by subsequent cooling causing subsidence (Bott, 1976; Lutgens et al., 2012). This has been closely studied at mid-ocean ridges where the warm magma rises towards the Earth's surface and solidifies. As the magma becomes cooler and denser it sinks into the asthenosphere (Lutgens et al., 2012)

High Arctic Large Igneous Province (HALIP) became evident from the Late Triassic (Steel & Worsley, 1984; Mørk et al., 1999) and continued into the Early Cretaceous. Emplacement of sills and dykes related to magmatic activity in the (HALIP), caused crustal updoming during the early Barremian in the north-eastern parts of Svalbard (Maher, 2001; Midtkandal & Nystuen, 2009) and applied tectonic stress on the major fault zones (e.g. Billefjorden and Lomfjorden fault zones). Volcanic rocks in the shape of lava flows have been reported from Kong Karls Land and Frantz Josef Land (500 km east of Svalbard; Worsley, 1986; Fig. 1). As the HALIP activity decreased during deposition of the Helvetiafjellet Formation in the Barremian to Aptian, it can therefore be assumed that the basin subsidence may be linked to the solidification and sinking of magma. As the magmatic rocks cooled down and sank, new tectonic stress was applied on the major fault zones, thus resulting in basin subsidence and thicker successions in the western part in Svalbard (Fig. 22).

There are several major north-south trending fault zones located in Svalbard (Dörr et al., 2011), but for this study the Billefjorden Fault Zone and the Lomfjorden Fault Zone are of particular interest (Fig. 21). During the Mesozoic, Svalbard as a whole was considered relatively stable (Worsley, 1986). However, the regional fault zones were repeatedly reactivated at later stages (Nemec, 1992; Dörr et al., 2011), and it has been discussed

whether they were active during Cretaceous or not (Nemec et al., 1988; Onderdonk & Midtkandal, 2010).

The thickness changes within the present study area in Svalbard provide indirect evidence for movement along the Billefjorden and Lomfjorden fault zones. The thickness variations indicates that the area west of the Billefjorden Fault Zone subsided most rapidly during the deposition of Helvetiafjellet Formation (Fig. 24) and the thickness of the Festningen locality is approximately 80 m. The area between Billefjorden Fault Zone and Lomfjorden Fault Zone has also been subsidising, but at a lower rate. The areas towards the north-eastern part of Svalbard, e.g. the Agardhfjellet locality (Fig. 19) consist of very thin deposits (Birkenmajer K. , 1984) and is approximately 50 m thick.

These variations in thickness of the deposits indicate a lower rate of subsidence at the platform in the east compared to areas located in the west. During the Early Cretaceous, Svalbard was a part of a larger platform that was relatively tectonically stable (Nemec, 1988; Torsvik et al., 2002). The area was probably connected to the Lomonosov High, as well as north-east Greenland (Grantz et al, 2011; Grundvåg & Olaussen, 2017). In general, sediments deposited on stable platforms are less disturbed and follow the topography of the platform. Therefore, it can be argued that the sediments in the north western part are exposed to a higher rate of subsidence and thus thicker than the sediments on the eastern part of Svalbard.

Although representing a system that formed in a highly rifted paleo-landscape, the depositional architecture of the Jurassic Ness Formation in the North Sea may represent a partly valid ancient analogue to the observed trends of the Helvetiafjellet Formation. In previous studies of the Ness Formation in the northern North Sea, thickness variations observed within the formation were interpreted to be associated with syndepositional differential subsidence (Ryseth, 2000). During the Jurassic in the North Sea, subsidence caused basins to form along the rift-axes, and sediments were deposited within the rift basins. Areas of high subsidence typically have a higher preservation potential of floodplain deposits (Ryseth, 2000).

6.2.2 A secondary source area

There is a distinct difference in the composition of the sediments in Svalbard, which suggests that a secondary source area must have been present during deposition of the Helvetiafjellet Formation (Fig. 22). The eastern parts of Svalbard (e.g. Kvalhovden north of the Kvalvågen locality) are represented by a notable volcanic signature in the deltaic deposits (Edwards, 1978; Worsley, 1986). This suggests the presence of a volcanic source terrain in the north and east of Svalbard, which is also reflected in the mineral composition of the sediments deposited on the east coast. In contrast, the western parts of Svalbard have clastic basement components (Edwards, 1978 A; Maher et al., 2004). The HALIP activity has been placed in the north-eastern part of Svalbard, most commonly as sills, but dykes are also present (Maher, 2001). If the HALIP was the only source area, the sediments in the proximal part should also contain more volcanic material. The clastic material has therefore been supplied from a source situated along the western and north-western margin of Svalbard (Birkenmajer, 1984).

Numerous works have therefore pointed out another source area north-west of Svalbard (Steel & Worsley, 1984; Worsley, 1986; Gjelberg & Steel, 1995; Mørk et al., 1999; Gjelberg & Steel, 2012). Dating of sediments from the Wandel Sea Basin of North Greenland shows a similar range of U- Pb ages as the deposits in Svalbard. Based on these similarities, it has been discussed that they may have shared a common source (Røhr et al., 2008). The sedimentary provenance area was probably located in north-east Greenland (Røhr et al., 2008) or somewhere between Greenland and Svalbard and was present during most of the Mesozoic (Mørk et al., 1999). This is in accordance with paleocurrent measurements observed at different localities at Spitsbergen and north-east Greenland, indicating a sediment transport towards south- southeast (Birkenmajer, 1984; Gjelberg & Steel, 1995; Dypvik et al., 2002; Midtkandal et al., 2007).

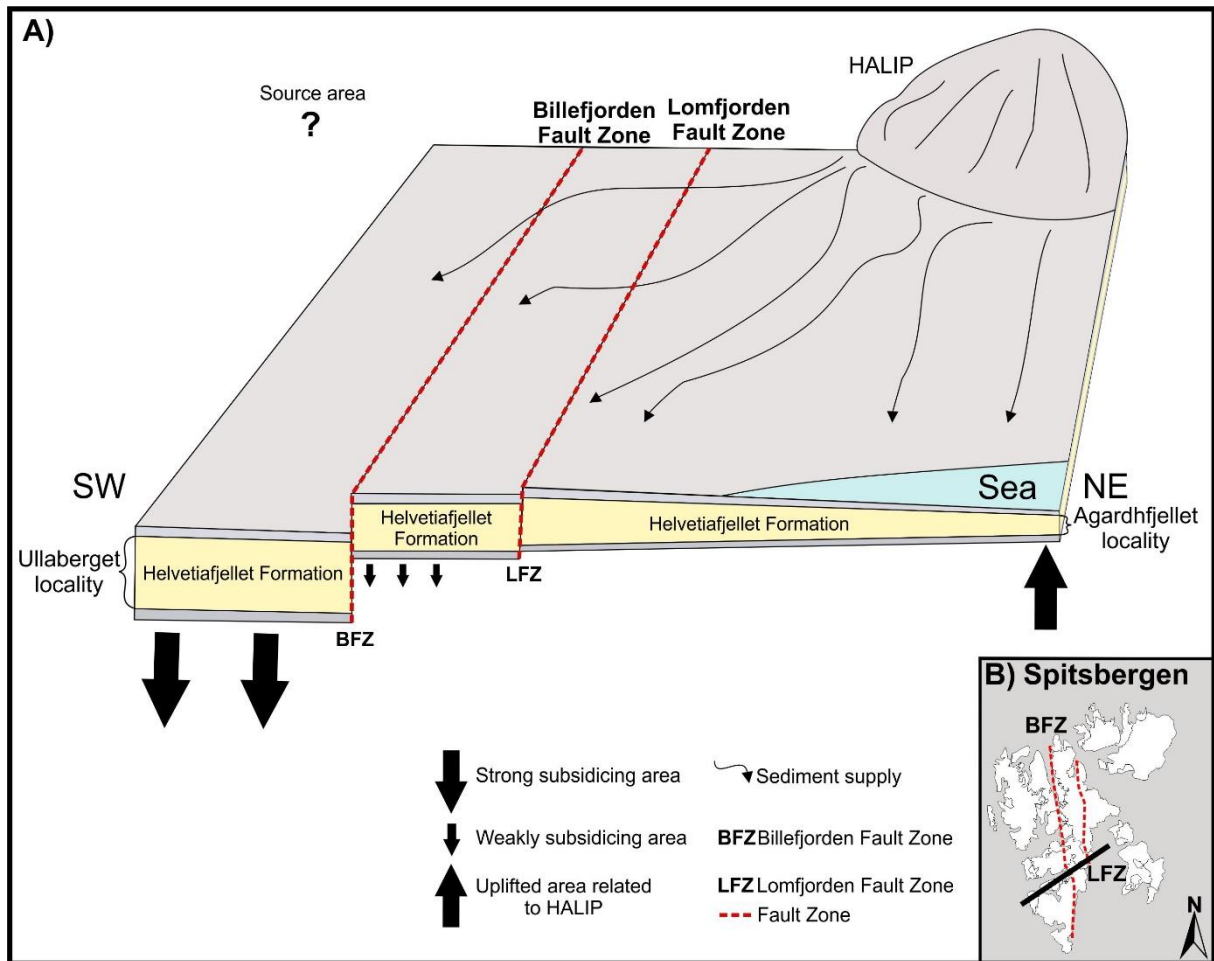


Figure 22: A) Conceptual model based on the observations in transect 1 and transect 2. The cause of the significant variations in thickness may be a result of movements along regional faults (Billefjorden and Lomfjorden fault zones), possibly governed by HALIP activity. The eastern part of Svalbard was linked to a larger platform, and is probably less affected, thus reflected in the thickness variations. The Ullaberget locality is approximately 80 m thick and the Agardhfjellet locality is approximately 50 m thick. A clastic source area in the north-western part has been inferred by numerous papers (e.g. Steel & Worsley, 1984; Worsley, 1986; Gjelberg & Steel, 1995. **B)** Location map showing the position of the model (black line) and the two faults, Billefjorden Fault Zone (BFZ) and Lomfjorden Fault Zone (LFZ). The figure is not to scale, and is based on previous published work by Birkenmajer (1984), Nemeč et al. (1988), Dypvik et al. (1991), Nemeč (1992), Maher (2001), Midtkandal et al. (2008), Midtkandal & Nystuen (2009), Onderdonk & Midtkandal (2010), Grundvåg (2017, unpublished).

The factors causing the observed variations in thickness within transect 1 (Fig. 19) and transect 2 (Fig. 20) are difficult to interpret due to the lack of available data. This creates further difficulties when evaluating primary controlling factors and their interactions. The present study suggests that activity along regional fault zones and magma cooling related to decreasing activity of the HALIP could be possible factors that may have been crucial due to the regional depositional trends observed in Spitsbergen. A different source area consisting of clastic material have been influencing the deposits on the western part of Svalbard.

6.3 Modern analogues for the Glitrefjellet Member

Modern analogues to the Helvetiafjellet Formation have received less attention in previous published works (noble exception by Gjelberg & Steel, 2012), but can contribute with understanding of the aerial distribution of the facies associations, interpreting paleoclimate and hydrocarbon reservoirs predictions. A modern analogue that shows similar characteristics as the Festningen Member (fluvial braidplain with very low gradient) has not been found, as modern braidplain generally tends to have higher gradients and coarser grain-size than what is inferred for the Festningen Member (Gjelberg & Steel, 2012). As a result, the Glitrefjellet Member is given more attention in the following discussion. Multiple considerations should be kept in mind when comparing modern deposits to ancient deposits. Factors such as human impacts, climate changes and the shoreline position will affect the deposits (most large modern delta systems are located on the inner shelf following the eustatic highstand). Since the deltas form between the land and ocean, their morphology will be influenced by the interplay of fluvial and marine forces (tidal- and wave energy). For this reason, depositional features can be used to determine if the coastline is mainly tidal- or wave influenced.

Important features for a modern analogue for the lower part of the Glitrefjellet Member should include deposits typical of a delta plain. This includes floodplain deposits (FA-3), crevasse splay deposits (FA-4), fluvial distributary channels (FA-5) and tide-influenced deposits (e.g. the Ullaberget location in transect 2 described by Midtkandal & Nystuen, 2009).

Important features for a modern analogue for the upper part of the Glitrefjellet Member should include delta plain deposits (FA-6), delta front deposits (FA-7) and wave-reworked delta deposits (FA-8). These deposits have been observed in the distal part of transect 2 (Fig. 20). Gjelberg & Steel (2012) discussed different modern analogues with braidplain deposits that could be comparable to the Helvetiafjellet Formation. They mentioned the Palana river system, the Ebro River and Tagliamento River as potential analogues. However, these modern analogues did not display the features documented in this thesis and other analogues were chosen.

Potential analogues for the Glitrefjellet Member include the Mahakam delta (Fig. 23) and the Pamlico Sound (Fig. 24).

6.3.1 The Mahakam delta

Mahakam delta is located on the east coast of Indonesia (Fig. 23 B) and shows similar characteristics with the lower part of the Glitrefjellet Member (Storms et al., 2005; Gastaldo et al., 2009). The delta plain (e.g. the Festningen locality; transect 2) includes floodplain deposits (FA-3), crevasse splay deposits (FA-4), and fluvial distributary channel deposits (FA-5). Whereas the intertidal zone (e.g. the Ullaberget locality; transect 2) includes tidal flats and tidal channels in estuary, which has been described in Midtkandal & Nystuen (2009). There is no record of how extensive the tidal-influenced deposits within the Glitrefjellet Member is, and it is therefore hard to determine if Mahakam delta can be used as a valid modern analog with regards to the lateral extent. However, it does show many of the same characteristics described by previous works where the coastal plain has been flooded during sea-level rise. This has resulted in strong tidal reworking. The Ullaberget locality, which is described by Midtkandal et al (2008), shows many of the same characteristics.

Meandering channels show a high sinuosity in the upper part of the delta plain in Mahakam delta. The trunk channel is split into a few major distributaries (Fig. 23) as they get further down towards the sea. Frequent abandonment of channels is observed within the delta. Sandy delta lobes can be observed where the channel mouth meets the ocean (Fig. 23 C). Based on these observations, the delta is interpreted to be tidal-dominated. Elongated mid-channel bars are seen with the longest axis perpendicular to the ocean (Fig.23 C). Within the same area, the trunk channels divide into many smaller meandering channels. The observations are also in accordance with tide-dominated estuary depositional models presented by numerous works (Allen, 1991; Nichols, 2009; Dalrymple et al., 2012).

The Mahakam delta shows many similar characteristics to the Ullaberget locality, which shows characteristics of tidal flats and tidal sand bars described by Midtkandal & Nystuen (2009). Due to the absence of barrier bars and lagoons, the Mahakam delta is therefore suggested to represent an analogue only to the lower part of the Glitrefjellet Member.

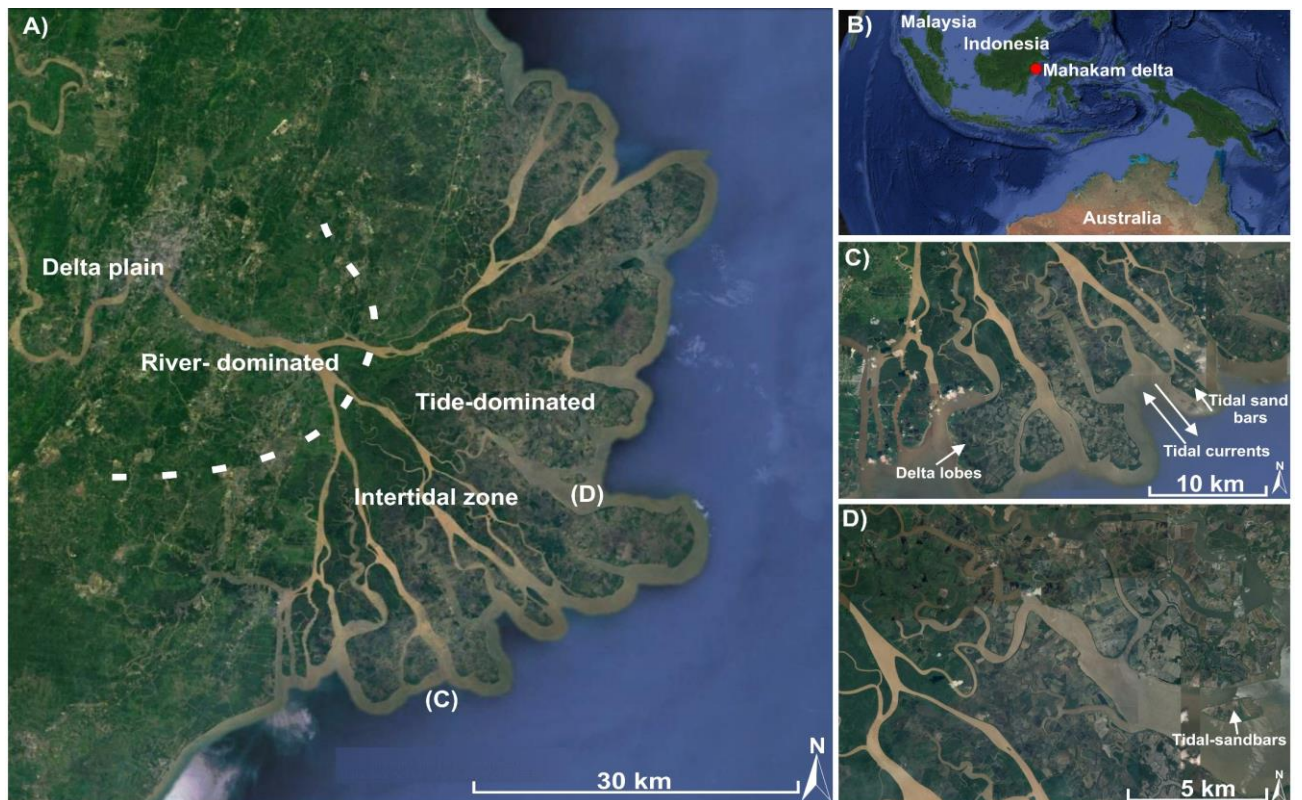


Figure 23: Mahakam delta is a tide-dominated delta. **A)** Overview of the delta interpreted with a river-dominated part at the delta plain and a tide-dominated part in the intertidal zone. This line represents the facies boundary between fluvial sediments and marine (tidally influenced) sediments. Note the increasing number of distributary channels towards the ocean. **(C)** and **(D)** represents the locations of the detailed pictures **C)** and **D)**. **B)** Geographic location of the delta **C)** Extensive reworking of the delta is done by tidal processes. The direction of the elongated tidal channels show the tidal flow. **D)** Meandering channels and overbank deposits. The inactive parts consists of a green colour due to vegetation, while the active and/or reworked parts are brown. Avulsion of channels can be seen within the intertidal zone. All the pictures are retrieved from Google Earth (<https://earth.google.com/web/>).

6.3.2 The Pamlico Sound

A modern example of an erosional transgressive coastline is represented by the second largest estuarine system Pamlico Sound on the east coast of U.S.A. (Grand et al., 2011; Zaremba et al., 2016; Fig. 23). The distributary rivers come from the northwest and end up in an estuary (90 m long; Fig. 23 C), which leads out to a protected area, suggested to be influenced by both fluvial and marine water. This area is interpreted to represent lagoonal conditions. The coastal plain is protected by barrier bars (15-30 m from the shore) located perpendicular to the coastline (Fig. 23 D). Based on the presence of a coastal plain, estuaries, lagoon and barriers Pamlico Sound has been interpreted to represent wave-reworked delta deposits. This is in accordance with previous observations of wave-dominated coastlines (e.g. Davis & Hayes, 1984).

In general, transgressive deposits can be recognized as a landward shift of facies or an upward deepening of facies capped by a maximum flooding surface. Transgression is closely associated with a rise in relative sea-level and commonly results in shoreface retreat and drowning of barrier bars or barrier bar migration (Cattaneo & Steel, 2003). Simple transgressive lags are often overlain by more distal facies and tend to erosively overlie shallower or more proximal facies (Cattaneo & Steel, 2003). In contrast to river deltas that are supplied by both fluvial and marine processes, barrier and lagoon systems are mostly supplied by marine processes (McCubbin, 1982).

The deposition of the uppermost part of the Glitrefjellet Member is characterized by relative rise in sea-level, which is supported by the eustatic sea-level rise during Early Cretaceous (Ramkumar, 2016; Fig. 8). In general, the Helvetiafjellet Formation represents deposits in a wide range of spectrums from deltaic deposits (e.g. the Adventdalen locality; Nemec, 1992; Fig. 20) in the proximal part to bay/lagoonal (e.g. the Ullaberget locality; Steel et al., 1978; Fig. 20) and barrier bars (e.g. the Kvalvågen locality; Edwards, 1976; Fig. 20) in the distal part.

Pamlico Sound displays several characteristics in common with transect 2 (Fig. 20) and is therefore considered to be a modern analogue. Pamlico Sound is approximately 75 km from the upper part of the estuary to the barrier system. In transect 2 (Fig. 20), the estuary (the

Ullaberget locality) and barrier bars (the Kvalvågen locality) are located 60 km apart from each other. The lateral extent is therefore very similar and the Pamlico Sound can be considered to be a modern analogue, showing the characteristics of the upper marine-influenced part of the Glitrefjellet Member. The barrier bars have protected the estuary deposits at the Ullaberget locality from wave-erosion. However, at one point the barrier complex started to migrate landwards as a response to the sea-level rise. This is seen as a barrier bar located stratigraphically at the top of the Glitrefjellet Member, at the Ullaberget locality (Fig. 20). As the barrier-bars migrated further towards the north-west (towards DH-1 and DH-1A), it drowned the coastal plain on its way. The wave energy reworked the deposits and finer material was brought basinwards. This resulted in a transgressive lag deposited in the proximal part (e.g. DH-1 and DH-1A; Figs. 17 & 18).

There is a general decrease in marine influence towards the proximal part of transect 2 (Fig. 20). This may be related to the fact that it took longer time before the transgression flooded the coastal plain.

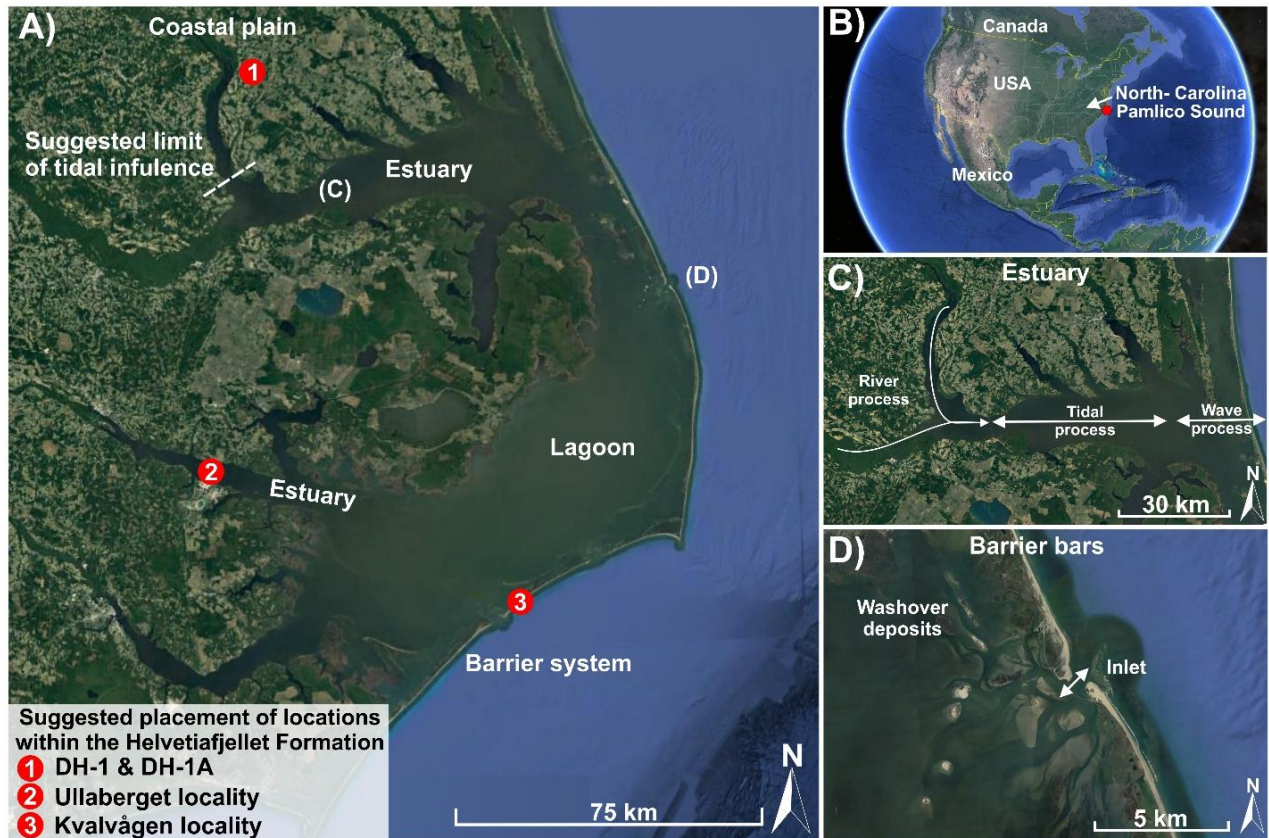


Figure 24: A) Pamlico Sound showing features of a wave-dominated estuary. The area between the coastal plain and barriers is represented by lagoonal conditions. The outer part of the wave-dominated estuary is represented by barrier bars consisting of clastic material which is reworked by longshore drift. Red circles indicate the suggested placement of locations within the Helvetiafjellet Formation. (C) and (D) indicates the position of the detailed images C) and D). B) Geographic location of the modern analogue. Pamlico Sound is located on the east coast of North-Carolina, U.S.A. C) An estuary is typically classified according to the dominating processes. These are river-process, tidal-process, and wave-process (Dalrymple et al., 1992). D) The inlet will exchange water from the open sea and the lagoon. Barrier bars and washover deposits are present. All the pictures are retrieved from Google Earth (<https://earth.google.com/web/>)

Given the above, the Glitrefjellet Member represents a deltaic coastline where a long-term relative rise in sea-level has remarkable impact on the deposition especially in the upper part of the strata. The barrier and estuary facies particularly represent the retreat of the entire delta system.

6.4 Depositional evolution and sequence stratigraphic development

The development of the Helvetiafjellet Formation has been reported in numerous studies (e.g. Parker, 1967; Birkenmajer, 1984; Steel & Worsley, 1984; Nemec et al., 1988; Nemec, 1992; Gjelberg & Steel, 1995; Midtkandal & Nystuen, 2009). The overlying and underlying units will not be discussed in great detail here as they are not a part of the main study. As the correlation panels (Figs. 19 & 20) show, similar development is seen across the outcrop window in Svalbard. The marine influence, however, is decreasing towards the northwest, suggesting that the shoreline was retreating stepwise and at a variable rate. This is supported by the paleoflow direction, which has been established going from north-west to south-east (Gjelberg & Steel, 1995; Midtkandal, 2007). Throughout the outcrop window (Fig. 25), the depositional evolution and regionally developed sequence boundaries are put into a regional context, going from north to south.

By combining the results from the facies analysis and evaluating it with regards to the modern analogues and previous published work, paleographic maps were constructed (Fig. 28). The maps aim to reconstruct the depositional evolution of Helvetiafjellet Formation into a regional paleogeographic setting, with special attention given to the Glitrefjellet Member. The five maps (Fig. 28) show how changes in the relative sea-level closely followed by changes in the position of the shoreline, thus reflected in the depositional environment.

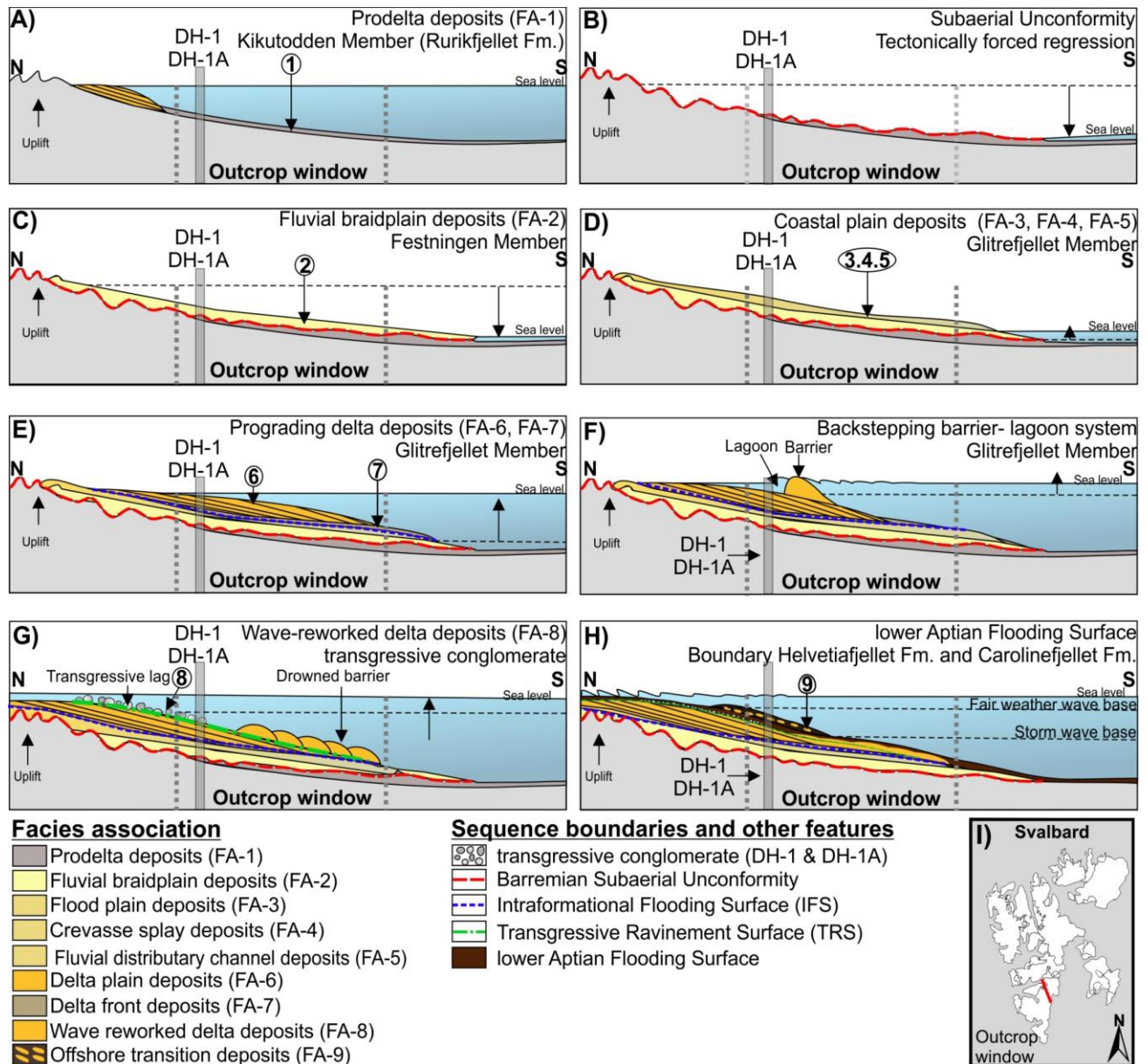


Figure 25: Depositional evolution of the Helvetiafjellet Formation showing Svalbard with the source area in the north and the basin south of Spitsbergen. The outcrop window (approximately 200 km long) is based on observations in this thesis, including the transect 1 and 2. **A)** Prodelta deposits (FA-1) stratigraphically belonging to the Rurikfjellet Formation **B)** Tectonically forced regression and formation of the Barremian Subaerial Unconformity **C)** Relative sea-level rise in combination with high sediment input results in deposition of the fluvial braidplain deposits (FA-2) belonging to Festningen Member. **D)** The sea-level continues to rise and the sediment influx is still high. Deposition of floodplain deposits (FA-3), crevasse splay deposits (FA-4) and fluvial distributary channels (FA-5) at the coastal plain. **E)** An intraformational flooding surface (IFS) is deposited under the prograding delta deposits. It marks the first significant proof of a long-term relative rise in sea-level during deposition of the Helvetiafjellet Formation. Delta plain deposits (FA-6) and delta front deposits (FA-7) are deposited above the IFS. **F)** Barriers are deposited in the south-east with lagoons and estuaries in the west. **G)** Drowned barrier bars observed in the east due to a significant rise in relative sea-level. As the coastal plain is flooded, wave processes erode the surface and leaves behind a transgressive lag, which can be observed in the proximal part of the study area. The Transgressive ravinement surface (TRS) marks the base of the barrier bars as they are eroded and represents the paleo-shoreline. **H)** The lower Aptian flooding surface is deposited with a regional extent and marks the boundary between the Helvetiafjellet Formation and the Glitrefjellet Member. **I)** Map of Svalbard showing the location of the outcrop window. The source area is located in the north and the receiving basin is located in the south. The conceptual model is based on previous work by Parker (1967), Gjelberg & Steel (1995), Midtkandal & Nystuen (2009), Grundvåg & Olausen (2017) and is not to scale.

6.4.1 Relative high-sea level: the Rurikfjellet Formation

In the Early Cretaceous, Svalbard was a part of an extensive low-angle platform that was covered by a shallow epicontinental sea (Fig. 1). The uppermost succession of the Rurikfjellet Formation in the proximal part (e.g. DH-1) has been interpreted to represent prodelta deposits (FA-1; Figs. 12; 25 A). These deposits have a regional extent over Svalbard (e.g. the Kvalvågen locality described by Onderdonk & Midtkandal (2010), and consists of open marine deposits (Parker, 1967; Edwards, 1976; Midtkandal et al, 2007). The Rurikfjellet Formation shows an overall regressive development towards the southeast (Dypvik et al., 1991) as a response to uplift in the north. This suggests deposition during a high relative sea-level, which is in accordance with the eustatic sea-level during this period (Haq et al., 1988; Ramkumar, 2016; Fig. 8). The uplifted area produced a significant new source area of volcanic detritus in the north-northeastern parts of Svalbard (Maher, 2001; Figs. 25 B; 28 B). A west- northwestern source area contributes with clastic materials in the proximal part of the outcrop window (north-west).

6.4.2 Fall in relative sea-level: Barremian SU

In the early Barremian, the Spitsbergen platform was exposed to tectonic uplift as a consequence of a multiple stages of sea-floor spreading and magmatism, often referred to as HALIP (Maher, 2001; Corfu et al., 2013; Fig. 28 B). The crustal updoming is interpreted as the cause for the tectonically forced regression which led to the formation of the Barremian subaerial unconformity (Corfu et al., 2013). The uplift continued through the late Cretaceous (Worsley, 2008). The depositional evolution of the Helvetiafjellet Formation was largely affected by the tectonic activity, which is reflected by the clastic character of the sediments in the west, and the volcanic character of the sediments in the east (Worsley, 1968; Maher, 2001).

The extent of the regional subaerial unconformity has previously been discussed by several authors (e.g. Gjelberg & Steel, 1995; Midtkandal et al., 2008). They suggested that the subaerial unconformity is easily recognized in the northwesterly locations, but grades conformably upwards into Helvetiafjellet Formation in the southeast of Svalbard where it appears as less erosive (Edwards, 1976; Steel & Worsley, 1984; Gjelberg & Steel, 1995). However, later work suggest that the regional subaerial unconformity is more extensive and

complex than first suggested, and that some sediments periodically may even bypassed the southern parts of Spitsbergen and deposited further out on the Barents Shelf (Grundvåg & Olausen, 2017). The crustal updoming led to forced regression and subaerial exposure, resulting in formation of the Barremian subaerial unconformity (Fig.25 B). Accommodation space was generated as the relative sea-level started to rise, and, together with the significant sediment input, resulted in deposition of fluvial braidplain deposits (FA-2; Figs.12 & 25 C).

6.4.3 Rise in relative sea-level and high sediment input: IFS

A coaly shale unit has been interpreted to represent an intraformational flooding surface (Fig. 18) with semi-regional extent (Fig. 19) and has been interpreted to represent the boundary between the Festningen Member and the Glitrefjellet Member. Deposition of the lower Glitrefjellet Member is deposited on the coastal plain (Fig.25 D). Autogenic processes control the channel position and thickness variations (Midtkandal & Nystuen, 2009), and play an important part in the lateral distribution of the coastal deposits. A distinct surface marks the boundary between the coastal deposits and the delta deposits (Fig. 25 E). The intraformational flooding surface (IFS; Figs. 18 & 25 E) reflects a period with very rapid rise in sea-level which outpaces the sedimentary influx.

A combination of a rise in relative sea-level and high-sediment supply from the uplifted area in the north, lead to formation of a braidplain. In the present study, an intraflooding surface (Figs. 18 & 19) suggests that the area was flooded after deposition of the Festningen Member. The surface is recognized as a coaly shale bed in DH-1 and DH-1A and has a semi-regional extent in transect 1 (Fig. 19) capping the underlying Festningen Member. This has not recently been mentioned by Grundvåg & Olausen (2017). The intraformational flooding surface has been interpreted to be formed by transgression and supports the relative rise in sea-level during deposition of the Helvetiafjellet Formation.

6.4.4 Continued rise in relative sea-level and high sediment input: IU

Deposition of the middle Glitrefjellet Member (Fig. 28 D) is dominated by a coastal plain environment with meandering channel deposits and associated overbank deposits (Edwards, 1976) in the proximal area. Autogenic factors are most important as the channels migrate laterally over the coastal plain. Intraformational unconformities are formed at the base of the channels. As the channels reach the ocean, the carry capacity decreases and the sediments are deposited as mouth bars in deltas (Gjelberg & Steel, 1995). Due to the high sediment influx, the deltas are prograde out into the ocean and form delta lobes (Midtkandal et al., 2007).

Tidal influence in estuaries dominate the deposits at the Ullaberget locality (Fig. 20), followed by prodelta and mouthbar deposits at the Kvalvågen locality in the distal part of the outcrop window (described by Onderdonk & Midtkandal, 2010).

A delta is prograding as long as the sediment supply is higher than the erosive factors.

Channel avulsion will cut the sediment supply and lead to abandonment.

However, this is the first significant sign that the Helvetiafjellet Formation was deposited in an overall long-term rise in relative sea-level. This is supported by an overall rise in eustatic sea-level during Early Cretaceous (Haq et al, 1988; Haq, 2014; Ramkumar, 2016; Fig. 8).

The surface suggests that the delta either was flooded due to autogenic forcing (e.g. delta lobe switch) or due to allogenic forcing (e.g. eustatic sea-level rise or tectonic forcing on sediment supply). There is an alternating change between delta plain deposits (FA-6) and delta front deposits (FA-7) in the uppermost part of the Glitrefjellet Member. This may be a result of delta lobe switching forced by avulsion of the fluvial distributary river (FA-5) as the water surface decreased during the transgression.

6.4.5 Increased rate in relative sea-level and low sediment input: TRS

Shorelines of epicontinental seas are mainly affected by wave energy and tidal energy (Swift & Thorne, 1991). However, they have also been observed in unusual situations where significant erosion or subsidence has occurred at the same time as a slowly falling sea level (Cattaneo & Steel, 2003). These situations are very rare and will not be taken into consideration here. Cattaneo & Steel (2003) argue for two main criteria that can be used to identify transgressive deposits. The first criteria takes account for a systematic landward

shift of facies with a regional extent, often seen as a retrogradational pattern. Short regressions may, however, be visible in the overall transgression due to higher sediment supply. The second criteria is to look for an abrupt upward-deepening of facies. In many cases, a prominent transgressive ravinement surface is present at the base of the succession. The transgressive ravinement surface reflects when the relative sea-level rise exceeds the rate of sediment supply (Nichols, 2009).

Barriers are prominent depositional features in many coastlines. The progradational trend of barriers are well understood, but the landward migration formed by transgression is more controversial. Nonetheless, since barriers are observed as sensitive to changes in the sea-level, they can be used as supporting evidence of either transgression or regression. Two contrasting scenarios of how barriers respond to a marine transgression have been proposed. The first scenario is considered to be the most established, and states that transgressive deposits accumulate during landward moving of a coastline and require a relative rise in sea-level in order to accumulate (Swift, 1968; Sanders & Kumar, 1975; Cattaneo & Steel, 2003). The second scenario suggests drowning of the barrier bar where it is located, while the lagoon and the landward side of the barrier widens. At one point a new barrier is formed above the old lagoonal deposits in a landward position (Sanders & Kumar, 1975). This is most common when the rate of subsidence or sea-level rise is very high and the gradient of the slope is low (McCubbin, 1982). Similar ancient deposits that are deposited under these two scenarios have been described from the Upper Cretaceous Almond Formation in Wyoming, U.S.A. (McCubbin, 1982).

According to Fisher (1961), best evidence of shoreface retreat is the exposure of lagoonal deposits on the seaward side of the barriers. As the barrier migrates landward with the rise of the sea level, they will overlay the lagoonal deposits until the lagoonal deposits are on the seaward side of the barrier (Sanders & Kumar, 1975). The deposits will then be influenced by open-ocean fauna.

The Barremian period in Svalbard is mainly dominated by a long-term rise in relative sea-level (Gjelberg & Steel, 1995; Midtkandal & Nystuen, 2009). This is supported by the general warm climate in the Early Cretaceous, which gave rise to greenhouse conditions and high

eustatic sea-levels (Hallam, 1985; Haq et al., 1987; Harland & Kelly, 1997; Ramkumar, 2016; Fig. 8).

The study area, including the correlation panels, indicates that the Helvetiafjellet Formation has been a large backstepping barrier-lagoon system. Barriers (up to 20 m thick) have been recognized in conjunction with shallow marine lagoon and bay deposits in the upper part of the Helvetiafjellet Formation, located in the southern and eastern parts of Svalbard (Nemec et al., 1988; Nemec, 1992; Gjelberg & Steel, 1995). Estuaries have been reported at the Ullaberget locality (Midtkandal et al., 2008). This indicates that the deltaic environment was reworked by tidal- and wave currents as the sea-level continued to rise during deposition of the Glitrefjellet Member. Delta deposits are dominating the uppermost part of the Glitrefjellet Member at the Adventdalen locality (DH-1 and DH-1A; Fig. 18). As the relative sea-level continued to rise the barriers in the east were drowned and left behind (Fig. 26). The delta deposits in the more proximal areas (e.g. DH-1) were flooded and wave-reworking marks the deposits with the transgressive ravinement surface (TRS; Figs. 18, 19, 20, 26 & 27) and the overlying conglomerate (Fig. 25 G). It has a semi-regional extent, but is assumed to be present as a transgressive lag towards the proximal part in the Adventdalen locality (DH-1 and DH-1A). A regional extensive flooding surface (Figs. 18, 19 & 20) suggests allogenic controlling factors related to basin subsidence and eustatic sea-level rise. Deposition of a mud blanket is commonly referred to as the lower Aptian shale. The mud blanket is overlaying the reworked delta deposits and coastal plain in the northwestern part (e.g. Festningen, DH-1, DH-1A and Helvetiafjellet localities) and on top of barrier deposits in the southeast (e.g. Kvalvågen locality).

Based on the present study, it is reasonable to assume that the evidence presented in this thesis suggests that a backstepping barrier complex developed during deposition of the uppermost Glitrefjellet Member. However, the depositional evolution of the uppermost part of the Glitrefjellet Member has formed differently depending on the distance from the ocean and the force of the influencing factors. As so, two different potential models (Figs. 26 & 27) have been developed as a result of observations from the facies analysis and correlation panels (Figs. 10, 11 & 20). The first model explains the transgressive character of a tidal dominated environment, represented by the observations from the Ullaberget and

the Kvalvågen localities. The second model explains the character of a backstepping barrier complex reaching the coastal plain, represented by the Adventdalen (DH-1 and DH-1A) and Kvalvågen localities. Pamlico Sound, a potential modern analogue presented in this thesis, will be used as a reference in the discussion of the depositional evolution of the backstepping barrier complex.

6.4.5.1 Ullaberget locality – Kvalvågen locality (NW-SE)

The distance between the Ullaberget locality and the Kvalvågen locality is approximately 60 km. Midtkandal et al (2008) has suggested estuarine conditions at the Ullaberget locality (Fig. 26 D). This is in accordance with the logged section presented in transect 2, modified from Grundvåg (2017), unpublished. While wave energy has an effect on sediments within a short reach, tides can influence lagoons, estuaries and the intertidal zones for hundreds of kilometers landward from the shore (Daidu, 2013). The estuarine deposits are therefore considered to be more sensitive to changes in relative sea-level. The potential modern analogue Pamlico Sound (Fig. 26 C) illustrates the distance that the barriers would have to retreat in order to reach the suggested location of the Ullaberget locality. As the estuary is open towards the barrier system, it is more sensitive to even minor changes in relative sea-level.

The suggestion of a backstepping barrier complex is sufficiently supported by the following evidence: the presence of a landward shift in facies from the Kvalvågen locality to the Ullaberget locality, lagoonal deposits underlying the barrier bar at the Ullaberget locality (Fig. 20) and the transgressive ravinement surface at the base of the barriers (Fig. 26 & 27). The deposits at the Ullaberget locality include tidal influenced deposits in the lower part, fluvial and coastal plain deposits in the middle part and lagoonal- and barrier deposits in the uppermost part of the Glitrefjellet Member (Midtkandal et al., 2008; Grundvåg, 2017, unpublished). The Glitrefjellet Member is deposited in an overall rise in relative sea-level (Gjelberg & Steel, 1995; Midtkandal & Nystuen, 2009). This is supported by an intraformational flooding surface marking an abrupt change in water depth to shallow marine lagoonal conditions in the uppermost part of the Glitrefjellet Member. A semi-regional transgressive ravinement surface is marking the boundary between the lagoonal deposits and the overlaying barrier.

In general, barriers will respond by migrating landwards as the sea-level is rising. According to the two scenarios presented by Sanders & Kumar (1975), barrier bar deposits that overlay the lagoonal deposits at the Ullaberget locality (Fig. 20) suggest in-place drowning. This is further supported by the transgressive ravinement surface, reflecting higher rise in relative sea-level than sediment supply, thus resulting in drowning of the barrier. The depositional evolution of the Ullaberget locality is illustrated in Fig. 26 D-H, where the estuary is exposed to a rise in sea-level, resulting in landward migration and drowning of barrier bars. As the sea-level continued to rise, the drowned barriers were finally capped by the lower Aptian flooding surface.

Ullaberget - Kvalvågen

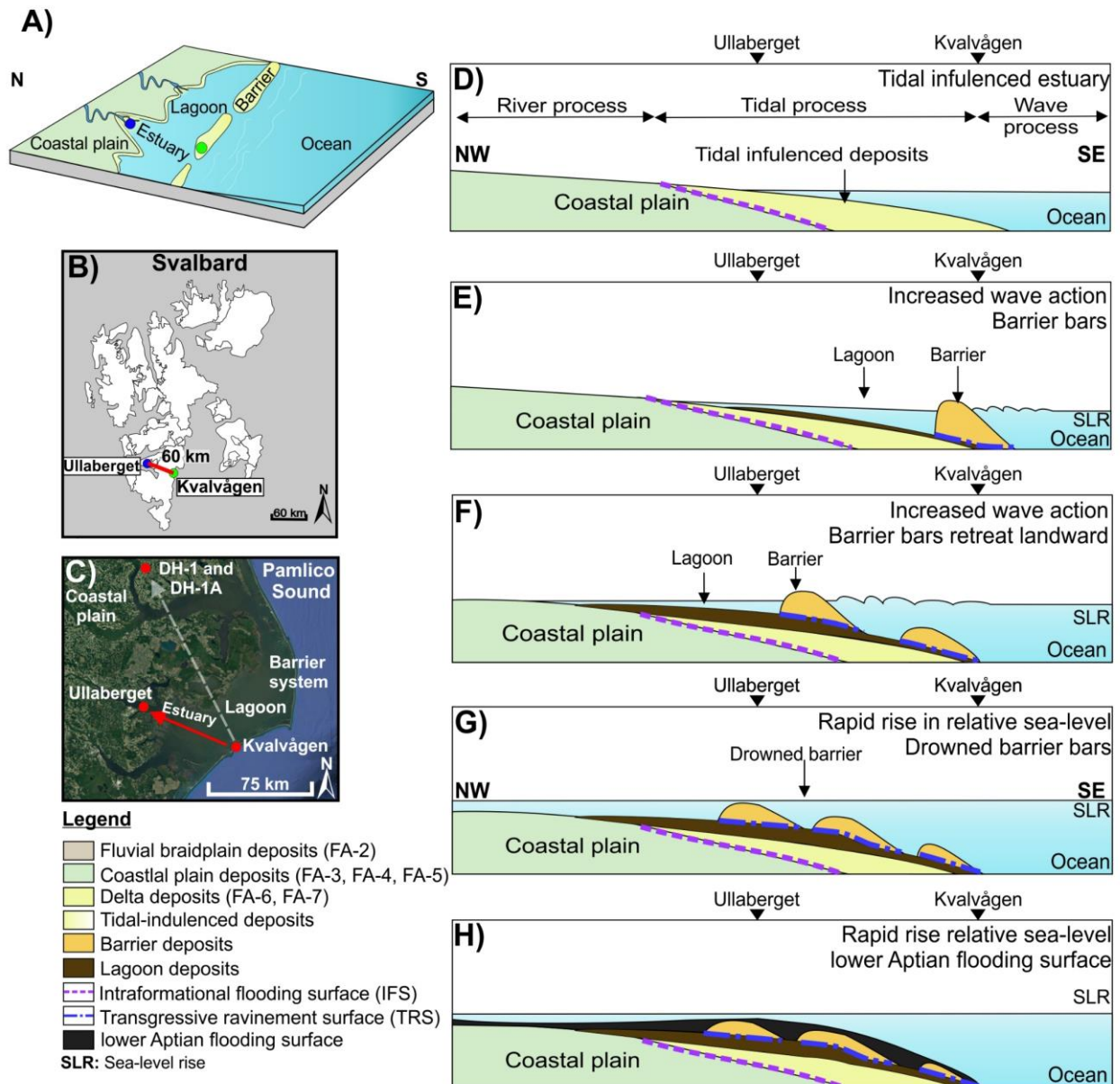


Figure 26: Conceptual model of the evolution of the backstepping barrier bar-complex at the Ullaberget locality. There are no observed delta deposits at the Ullaberget locality. However, tidal deposits including bay-head delta, lagoonal deposits, tidal flat deposits and tidal channel deposits have been observed as presented in transect 2 (Fig. 20). An intraformational flooding surface is overlaying fluvial and coastal plain deposits. **A)** Geological model showing the location of the Ullaberget and Kvalvågen localities. **B)** Geographic placement of Ullaberget and Kvalvågen localities with approximately 60 km between the localities. **C)** Pamlico Sound is considered a modern analogue to the barrier complex. Red arrow indicates the outcrop window of the depositional evolution in D)-H). White arrow indicates the conceptual model presented in Fig. 27, showing the depositional evolution from Kvalvågen to DH-1 and DH-1A. **D)** The estuary at the Ullaberget locality is tidal-influenced and is divided in three zones described by Dalrymple (1992). **E)** Barrier bars are developing as a result of increased wave action. **F)** The barrier bars start to migrate landward. As the sea-level rise exceeds the sediment supply they drown. When the sediment supply increases, a new barrier will be deposited further landward. **G)** At one point the sea-level drastically increases and the last barrier is drowned. **H)** A thick layer of mudstone and shale is overlaying the barrier deposits and has been interpreted to represent the regional extending lower Aptian flooding surface.

6.4.5.2 *Adventdalen locality (DH-1 and DH-1A) and Kvalvågen locality (N-S)*

The Adventdalen locality and the Kvalvågen locality show significant variations in facies associations compared with Ullaberget and Kvalvågen localities. The distance is significantly longer (approximately 100 km in total). It is therefore suggested that it is more slowly affected by sea-level changes, thus resulting in continuous landward migration of the barriers during deposition of the uppermost part of Glitrefjellet Member.

The facies transition seen from the fluvial distributary channel deposits (FA-5) to the delta front deposits (FA-6) in the uppermost part of the Glitrefjellet Member at the Adventdalen locality indicates a significant rise in relative sea-level and the formations of a local intraformational flooding surface (IFS; Fig. 18). A polymictic conglomerate is bounded by the underlying transgressive ravinement surface and the overlying lower Aptian flooding surface (Fig. 18).

The barrier system located at the Kvalvågen locality (described by e.g. Nemec, 1992; Nemec et al., 1988; Gjelberg & Steel, 1995) started to migrate at the same time as the rise in sea-level. The barriers continuously migrated landward together with the sea-level, reflected by the stepwise change in facies associations. This is supported by eustatic sea-levels, which was generally high during this period (Ramkumar, 2016; Fig. 8). However, a rapid rise in the sea-level drowned the barriers further out on the shelf. The sea-level continued to rise and flooded the shallow coastal plain. Most of the barriers are completely eroded, while a transgressive lag is observed at the Adventdalen locality (DH-1 and DH-1A; Figs. 10, 11 & 18).

The transgressive lag is evidence of the backstepping barrier-bar complex (Fig. 27), and provides new information about how far north the shoreline retreated during the long-term transgressive trend observed in this thesis.

Adventdalen - Kvalvågen

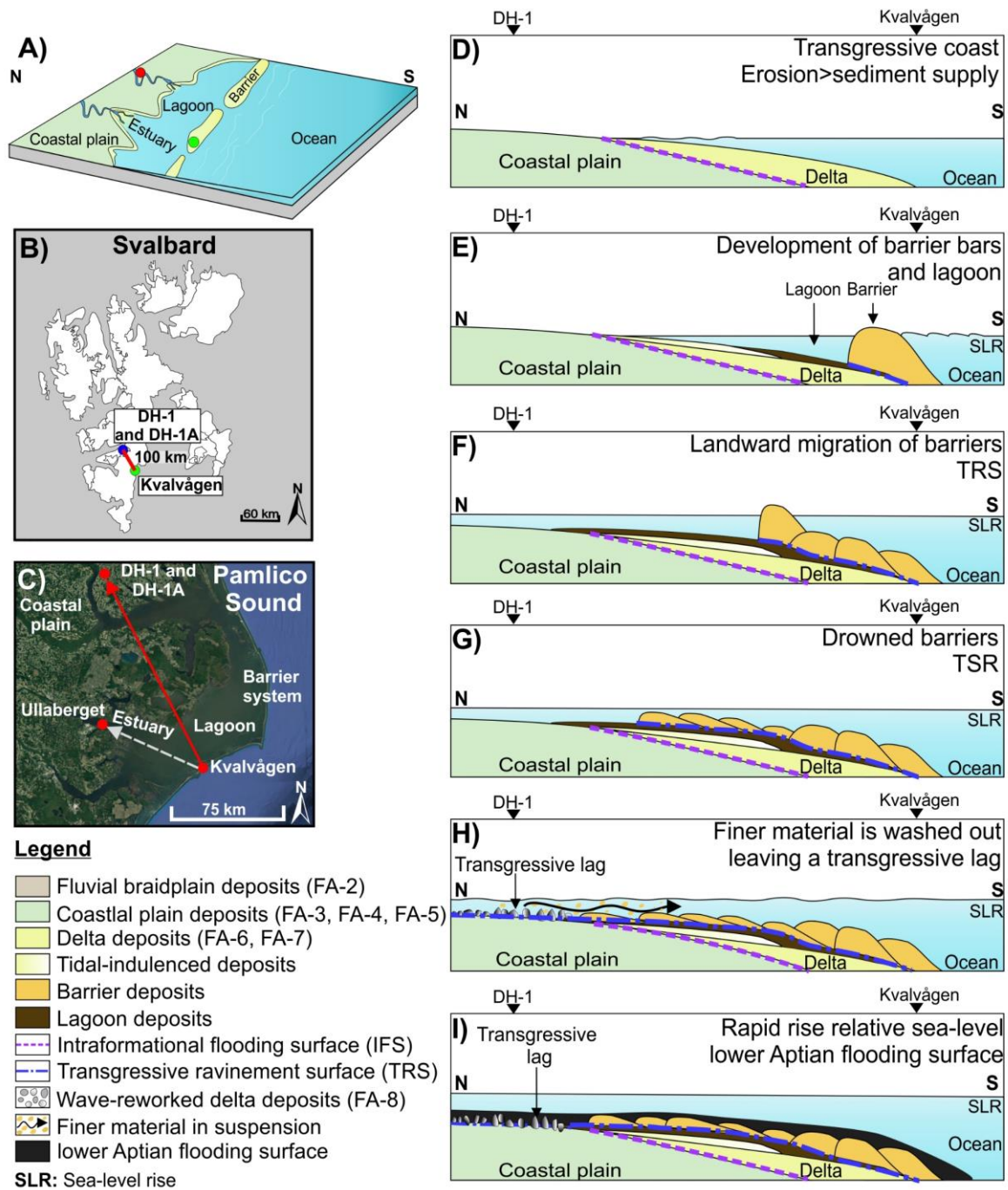


Figure 27: Conceptual, schematic representation of the transgressive development in the uppermost part of Glitrefjellet Member. **A)** Model of the coastal plain (DH-1 and DH-1A locality) and the wave-dominated delta (the Kvalvågen locality). **B)** Map of Spitsbergen showing the geographic position of the localities located approximately 100 km apart from each other, which represents the outcrop window of the figures D) - I). **C)** The potential modern analogue Pamlico Sound illustrates the potential position of the Adventdalen locality (DH-1 and DH-1A) and the Kvalvågen locality. **D)** A transgressive coast is formed when the erosion is greater than the sediment supply. **E)** Development of lagoon and barriers as the wave influence increases. **F)** Landward migration of the barriers as the sea-level continues to rise. The sediment supply is greater than the sediments eroded, thus the barrier can follow the sea-level rise. **H)** Transgressive lag formed by wave erosion caused by very rapid rise in sea-level. The barrier drowned further out on the shelf as the water flooded the coastal plain. **I)** Transgressive lag observed at the Adventdalen locality (DH-1 and DH-1A) is overlaid by black shale representing the lower Aptian flooding surface.

6.4.6 Flooding of the Helvetiafjellet Formation: lower Aptian FS

The boundary between the Helvetiafjellet Formation and the Carolinefjellet Formation has been discussed during the last decades by several authors (Parker, 1967; Nemec, 1992; Gjelberg & Steel, 1995; Midtkandal & Nystuen, 2009). The boundary can be seen as a regional extensive interval of shale in transect 1 (Fig. 19) and 2 (Fig. 20).

Previous published work has placed the boundary based on the evidence of marine influence (e.g. Steel et al., 1978). However, the upper Glitrefjellet Member shows several evidences of marine influence at different locations (e.g. the Kvalvågen locality and the Ullaberget locality in transect 2). The marine influence can be seen as wave reworked sediments (e.g. as the regional extensive transgressive ravinement surface and Diplocraterion at the Ullaberget locality). The flooding surface is therefore suggested to be further up in the stratigraphic succession and is characterized by a mudstone deposits capping the Helvetiafjellet Formation. The overlying Carolinefjellet formation consists of offshore transition deposits (FA-9; Fig. 17) and shows characteristics typical of an open marine shelf setting.

Due to the limited occurrence of biostratigraphically useful fossils within the Helvetiafjellet and Carolinefjellet formation, there has been a rise in efforts over the last decade to reduce the uncertainties in dating the boundary (Vickers et al., 2017). Other dating methods such as carbon-isotope stratigraphy have been used in order to date the boundary more precisely. Based on the new dating methods, the age of the boundary has been suggested to be of Barremian-Aptian age. This is further supported by the fact that the lithostratigraphic boundary between the Helvetiafjellet and the Carolinefjellet formations fits with the OAE1a, which is related to a global anoxic event (Midtkandal et al., 2016).

6.4.7 High sea-level: The Carolinefjellet Formation

The Carolinefjellet formation is interpreted to be deposited in a more marine-influenced environment than the underlying Helvetiafjellet Formation (Nagy, 1970; Gjelberg & Steel, 1995, Hurum et al., 2016) and has a regional extent. This is in accordance with the results in this thesis, suggesting offshore transition deposits (FA-9; Fig. 25 H). The interpretation is further supported by the high eustatic sea-level at the time (Fig. 8).

However, there has been some debate with regards to the depositional models of the Helvetiafjellet Formation (Nagy, 1970; Nemec, 1992; Gjelberg & Steel, 1995; Midtkandal & Nystuen, 2009; Fig. 6). This thesis agrees with the general interpretation of deposition during a long-term relative sea-level rise, which is reflected in the deposition of coarse grained fluvial deposits (the Festningen Member) which grade upward into coastal plain deposits and shallow marine facies (the Glitrefjellet Member). However, new discoveries have led to a new interpretation of the uppermost part of the Glitrefjellet Member. The barrier sandstones on the east coast of Svalbard (e.g. the Kvalvågen locality) is suggested to be linked to the transgressive lag observed in the northwestern part (e.g. the Adventdalen locality). This suggests that the uppermost part of the Glitrefjellet Member was a part of a large backstepping barrier-lagoon system. (Figs. 26 & 27).

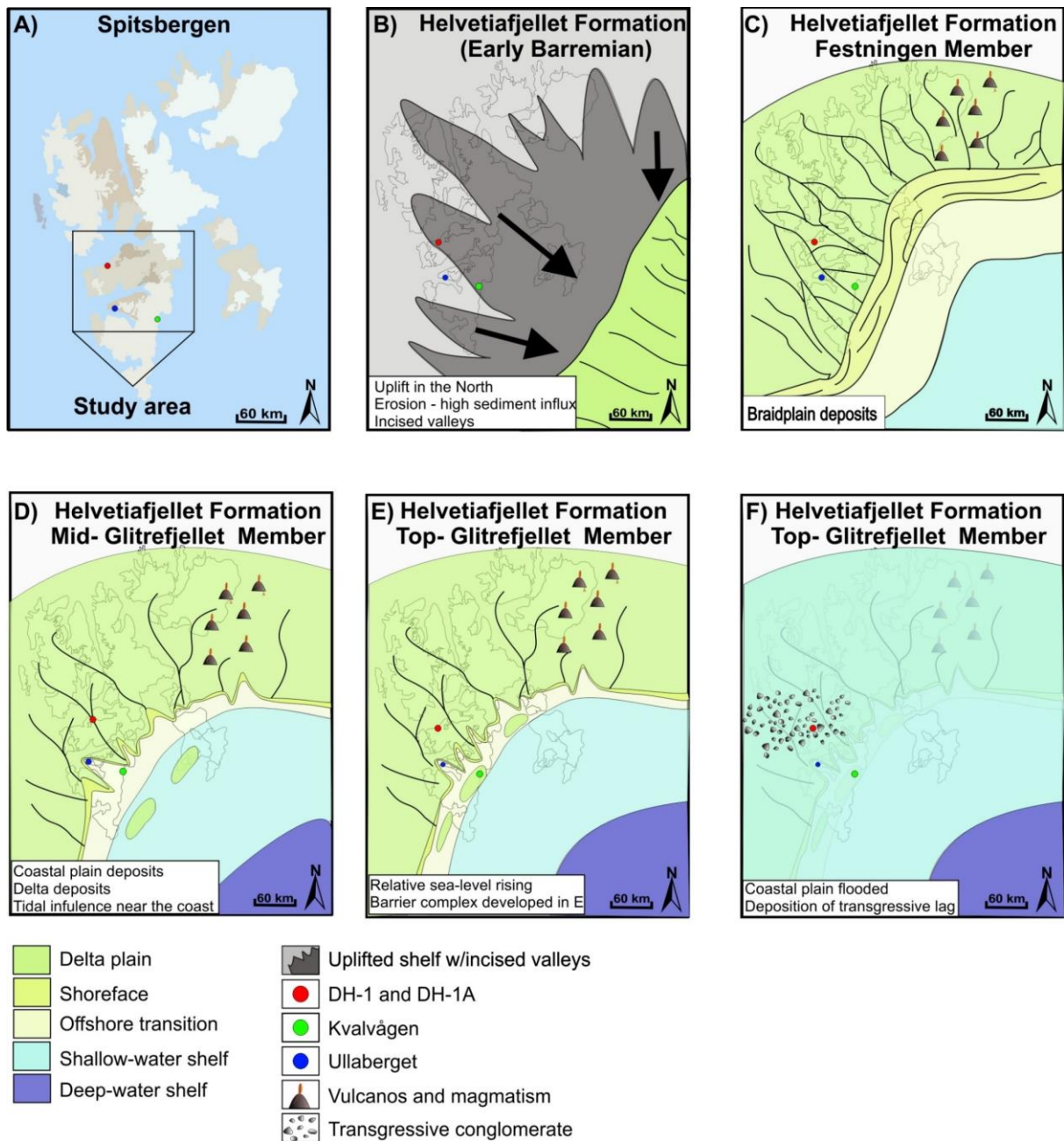


Figure 28: Generalized palaeogeographic reconstruction of Spitsbergen and the depositional evolution of the study area. **A)** Study area showing the geographic location of DH-1, DH-1A and Kvalvågen which has been used as reference areas. **B)** Tectonic uplift in Early Barremian (ca. 130 Mya) resulted in higher sediment influx from NW towards SE and deposition in incised valleys. **C)** Festningen Member is dominated by braidplain deposits. **D)** The middle of the Glitréfjellet Member is dominated by coastal plain and prograding delta deposits. The deposits are tidal influenced near the coast. **E)** The top of Glitréfjellet Member is dominated by estuaries accompanied by tidal channels and tidal flats at Ullaberget. A barrier complex in the E and can be seen at Kvalvågen. **F)** The coastal plain is flooded as well as the barrier bars. The erosion of the barrier bars results in deposition of a transgressive lag. This marks the top of the Helvetiafjellet Formation. Reconstructions are based on Grundvåg & Olaussen (2017).

7 Conclusions

This thesis presents a detailed facies analysis of the Helvetiafjellet Formation, based on core descriptions. For stratigraphic context, the uppermost part of the underlying Rurikfjellet Formation and the lowermost part of the overlying Carolinefjellet Formation have been included. For understanding the regional facies distribution, the facies analyses are combined with regional correlation panels constructed from previously published sections. In addition, comparisons to modern analogues provide a powerful tool in understanding the depositional evolution of the Helvetiafjellet Formation.

The main conclusions of this study are summarized below:

1. Fourteen lithofacies were recognized within Helvetiafjellet Formation based on core descriptions. These include conglomerate (F-1), massive sandstone (F-2), high angle tabular cross-bedded sandstone (F-3), trough cross-bedding (F-4), low angle tabular cross-bedded sandstone (F-5), interbedded sandstone and mudstone (F-6), lenticular/wavy/flaser bedded heterolithic sandstone (F-7), interlaminated sandstone and mudstone (F-8), ripple cross laminated sandstone (F-9), heterolithic lamination (F-10), siltstone/mudstone (F-11), black shale (F-12), coaly shale (F-13) and coal (F-14).
2. Facies analysis based on the pattern of lithofacies revealed nine facies associations reflecting different depositional environments, being prodelta deposits (FA-1, only in the Rurikfjellet Formation), fluvial braidplain deposits (FA-2), floodplain deposits (FA-3), crevasse splay deposits (FA-4), fluvial distributary channel deposits (FA-5), delta/delta plain deposits (FA-6), delta front deposits (FA-7), wave reworked delta deposits (FA-8) and finally offshore transition deposits (FA-9, lowermost Carolinefjellet Formation). Together, these mark deposition during an overall long-term rise in sea level. The first sign of a long-term rise in relative sea-level and marine influence in the Glitrefjellet Member is presented by the development of an intraformational marine flooding surface where delta deposits occur on top of flood plain deposits.

3. Two major sequence stratigraphic surfaces have been recognized in this study, together with several smaller surfaces. The underlying Rurikfjellet Formation is separated from Helvetiafjellet Formation by the Barremian Subaerial Unconformity, whereas the overlying Carolinefjellet Formation is separated by the lower Aptian Flooding Surface. Three types of minor surfaces have been recognized within the unit: intraformational unconformities (IU), intra flooding surface (IFS) and a transgressive ravinement surface (TRS).
4. By comparing and correlating the logged cores with previously published sections, the regional architecture and lateral changes in facies were documented. The succession shows significant variations in thickness and shows an overall thickening towards the NW from approximately 50 m in the Agardhbukta area to approximately 80 m at the Festningen locality. The cause of these variations may be a result of movements along regional faults (e.g. the Billefjorden and Lomfjorden fault zones), possibly governed by HALIP activity. This is very interesting as previous published work generally reports an overall thickening towards the south.
5. Two potential modern analogues show some of the same characteristics as the Glitrefjellet Member. The Mahakam delta is interpreted to be tide-dominated and shows similar characteristics to the lower part of the Glitrefjellet Member. Pamlico Sound is interpreted to be wave-dominated and is suggested to be similar to the upper part of the Glitrefjellet Member.
6. Important Sequence stratigraphic surfaces in the Helvetiafjellet Formation included a Barremian Subaerial Unconformity formed during regional uplift, a semi-regional intraformational flooding surface possibly reflecting subsidence related to decreasing HALIP activity, intraformational unconformities related to fluvial channel incision, a transgressive ravinement surface formed during wave erosion and reworking of the flooded coastal plain, and a regionally-extensive lower Aptian Flooding Surface.
7. The depositional evolution observed in this thesis of the Helvetiafjellet Formation is consistent with the general understanding of the Helvetiafjellet Formation. However,

the regional facies distribution documented in this study suggests that there is a link between the barrier sandstones described on the east coast of Spitsbergen to the conglomerate in more proximal areas (e.g. occurring in the described cores in the Adventdalen area). Together, this suggests that the uppermost part of the Glitrefjellet Member is a part of a large backstepping barrier-lagoon system. This also reveals new information about how far north the shoreline retreated as the transgressive ravinement surface and its associated transgressive lag has been observed in the proximal part of the study area (e.g. the Adventdalen locality).

8 References

- Ahokas, J., Nystuen, J., & Martinius, A. (2014). Depositional dynamics and sequence development in a tidally influenced marginal marine basin: Early Jurassic Neill Klintner Group, Jameson Land Basin, East Greenland. In A. Martinius, R. Ravnås, J. Howell, R. Steel, & J. Wonham (Eds.), *From Depositional Systems to Sedimentary Successions on the Norwegian Continental Margin* (Vol. 46, pp. 291- 338). Chichester, UK: Wiley- Blackwell.
- Allaby, M. (2013). *Oxford Dictionary of Geology & Earth Sciences*. Oxford: Oxford University Press.
- Allen, G. (1991). Sedimentary processes and facies in the Gironde estuary: a recent model for macrotidal estuarine systems. (D. Smith, G. Reinson, B. Zaitlin, & R. Rahmani, Eds.) *Clastic Tidal Sedimentology*, 16, pp. 29-40.
- Allen, G. (1998). *Sedimentation in the modern and Miocene Mahakam delta*. Indonesian Petroleum Association.
- Bache, F., Sutherland, R., & King, P. (2014). Use of ancient wave-ravinement surfaces to determine palaeogeography and vertical crustal movements areound New Zealand. *New Zealand Journal of Geology and Geophysics*, 57(4), 459-467.
- Bhattacharya, J. (2011). Practical problems in the application of the sequence stratigraphic method and key surfaces: integrating observations from ancient fluvial–deltaic wedges with Quaternary and modelling studies. *Sedimentology*, 58, 120-169.
- Birkenmajer, K. (1975). Jurassic and Lower Cretaceous sedimentary formations of SW Torell Land, Spitsbergen. *Studia Geologica Polonica*, 44, 7-43.
- Birkenmajer, K. (1984). Sedimentary features of the Helvetiafjellet Formation (Barremian) at Agarhdbukta, East Spitsbergen. *Studia Geologica Polonica*, 59-90.
- Bott, M. (1976). Mechanisms of basin subsidence - an introductory review. *Tectonophysics*, 36, 1-4.
- Bown, T., & Kraus, M. (1981). Lower Eocene alluvial paleosols (Willwood formation, northwest Wyoming, U.S.A.) and their significance for paleoecology, paleoclimatology, and basin analysis. *Palaeogeography, paleoclimatology, palaeoecology*, 34, 1-30.
- Braathen, A., Bælum, K., Christensen, H., Dahl, T., Eiken, O., Elvebakk, H., . . . Vagle, K. (2012). The Longyearbyen CO2 Lab of Svalbard, Norway - initial assessment of the geological conditions for CO2 sequestration. *Norwegian Journal of Geology*, 92, 353-376.
- Brekke, H., & Olaussen, S. (2013). Høyt hav og lave horisonter. Kritt, jordas drivhustid; 146-66 millioner år. In I. B. Ramberg, I. Bryhni, A. Nøttvedt, & K. Rangnes, *Landet blir til - Norges geologi* (pp. 422-447). Trondheim: Norsk Geologisk Forening.
- Brierly, G., Ferguson, R., & Woolfe, K. (1997). What is a fluvial levee? *Sedimentary Geology*, 114, 1-9.
- Buchan, S. H., Challinor, A., Harland, W. B., & Parker, J. R. (1965). The Triassic Stratigraphy of Svalbard. *Norsk Polarinstitutt Skrifter* 135, 5-93.
- Burns, C., Mountney, N., Hodgson, D., & Colombera, L. (2017). Anatomy and dimensions of fluvial crevasse-splay deposits from the Cretaceous Castlegate Sandstone and Neslen Formation, Utah, U.S.A. *Sedimentary Geology*, 351, 21-35.
- Cattaneo, A., & Steel, R. (2003). Transgressive deposits: a review of their variability. *Eart-Science Reviews*, 62, 187-228.

- Catuneanu, O. (2006). Stratigraphic Surfaces . In O. Catuneanu, *Principles of sequence stratigraphy* (Vol. 1, pp. 105-159). Boston: Elsevier.
- Cohen, K. M., Finney, S. C., Gibbard, P. L., & Fan, J.-X. (2013). The ICS International Chronostratigraphic Chart. 199-204. Retrieved from <http://www.stratigraphy.org/ICSchart/ChronostratChart2017-02.pdf>
- Collignon, M., & Hammer, Ø. (2002). Petrography and sedimentology of the Slottsmøya Member at Janusfjellet, central Spitsbergen. *Norwegian Journal of Geology*, 92, 89-101.
- Corfu, F., Polteau, S., Planke, S., Faleide, J., Svensen, H., Zayoncheck, A., & Stolbov, N. (2013). U-Pb geochronology of Cretaceous magmatism on Svalbard and Franz Josef Land, Barents Sea Large Igneous Province. *Geological Magazine*, 125, 1-9.
- Daidu, F. (2013). Classifications, sedimentary features and facies association of tidal flats. *Journal of Palaeogeography*, 2(1), 66-80.
- Dallmann, W. K. (2015). Physical geography. In W. K. Dallmann, *Geoscience Atlas of Svalbard* (pp. 20-23). Tromsø: Norsk Polarinstitutt.
- Dalrymple, R., Nackay, D., Ichaso, A., & Choi, K. (2012). Processes, Morphodynamics, and Facies of Tide-Dominated Estuaries. In R. Davis, & J. Dalrymple, *Principles of Tidal Sedimentology* (pp. 79-107). London: Springer Dordrecht Heidelberg.
- Dalrymple, R., Zaitlin, B., & Boyd, R. (1992). Estuarine Facies Models: Conceptual basis and stratigraphic implications. *Journal of Sedimentary Petrology*, 62, 1130-1146.
- Davis, J., & Hayes, M. (1984). What is a wave-dominated coast? (B. Greenwood, & R. Davis, Eds.) *Hydrodynamics and Sedimentation in Wave-Dominated Coastal Environments*, pp. 313-329.
- Donovan, D., & Jones, E. (1979). Causes of world-wide changes in sea level. *Journal of the Geological Society*, 136(2), 187-192.
- Dypvik, H., Håkansson, E., & Heinberg, C. (2002). Jurassic and Cretaceous palaeogeography and stratigraphic comparisons in the North Greenland-Svalbard region. *Polar Research*, 91-108.
- Dypvik, H., Nagy, J., Backer-Owe, K., Andressen, A., Haremo, P., Bjærke, T., . . . Elverhøi, A. (1991). The Janusfjellet Subgroup (Bathonian to Hauterivian) on central Spitsbergen: a revised lithostratigraphy. *Polar Research*, 9(1), pp. 21-43.
- Dörr, N., Clift, P., Lisker, F., & Spiegel, C. (2013). Why is Svalbard an island? Evidence for two-stage uplift, magmatic underplating, and mantle thermal anomalies. *Tectonics*, 32, 473-486.
- Dörr, N., Lisker, F., Clift, P., Carter, A., Gee, D., Tebenkov, A., & Spiegel, C. (2011). Late Mesozoic-Cenozoic exhumation history of northern Svalbard and its regional significance: Constraints from apatite fission track analysis. *Tectonophysics*, 514-517, 81-92.
- Edwards, M. (1976). Depositional environments in Lower Cretaceous regressive sediments, Kikutodden, Sørkapp Land, Svalbard. *Norsk Polarinstitutt Årbok 1974*, 35-50.
- Edwards, M. (1978 A). A regional survey of composition, provenance and diagenesis of sandstones in the Lower Cretaceous Helvetiafjellet Formation, Svalbard. *Norsk Polarinstitutt Årbok 1977*, 343-345.
- Edwards, M. (1978). Depositional environments in Lower Cretaceous regressive sediments, Kikutodden, Sørkapp Land, Svalbard. *Norsk Polarinstitutt Årbok 1977*, 343-345.

- Edwards, M. (1979). Sandstone in Lower Cretaceous Helvetiafjellet Formation, Svalbard: Bearing on Reservoir Potential of Barents Shelf. *The American Association of Petroleum Geology*, 63(12), 2193-2203.
- Elvevold, S., Dallmann, W., & Blomeier, D. (2007). *Geology of Svalbard*. Tromsø: Norwegian Polar Institute.
- Faleide, J. I., Gudlaudsson, S. T., & Jacquart, G. (1984). Evolution of the western Barents Sea. *Marine and Petroleum Geology*, 1(2), 123-128.
- Faleide, J., Tsikalas, F., Breivik, A., Mjelde, R., Ritzmann, O., Engen, Ø., . . . Eldholm, O. (2008). Structure and evolution of the continental margins off Norway and the Barents Sea. *Episodes*, 31, 82-91.
- Fielding, C. (2010). Planform and facies variability in asymmetric deltas: facies analysis and depositional architecture of the turonian ferron sandstone in the Western Henry Mountains, South-Central Utah, U.S.A. *Journal of Sedimentary Research*, 80, 455-479.
- Fisher, A. (1961). Stratigraphic record of transgressing seas in light of sedimentation on Atlantic coast of New Jersey. *Bulletin of the American Association of Petroleum Geologists*, 45(10), 1656-1666.
- Gastaldo, R., Allen, G., & Huc, A.-Y. (2009). The tidal character of fluvial sediments of the modern Mahakam River delta, Kalimantan, Indonesia. In B. Flemming, & A. Bartholomä, *Tidal Signatures in Modern and Ancient Sediments* (pp. 171-181).
- Gjelberg, J., & Steel, R. (1995). Helvetiafjellet formation (Barremian-Aptian), Spitsbergen: characteristics of a transgressive succession. In R. J. Steel (Ed.), *Sequence stratigraphy on the northwest European Margin* (pp. 571-593). Amsterdam: Elsevier.
- Gjelberg, J., & Steel, R. (2012). Depositional model for the Lower Cretaceous Helvetiafjellet Formation on Svalbard - diachronous vs. layer-cake models. *Norwegian Journal of Geology*, 92, 41-54.
- Glørstad-Clark, E., Faleide, J., Lundschieen, B., & Nysten, J. (2010). Triassic seismic sequence stratigraphy and paleogeography of the western Barents Sea area. *Marine and Petroleum Geology*, 27, 1448-1475.
- Grand, P., Culver, S., Mallinson, D., Farrell, K., Corbett, D., Horton, B., . . . Buzas, M. (2011). Rapid Holocene coastal change revealed by high-resolution micropaleontological analysis, Pamlico Sound, North Carolina, USA. *Quaternary Research*, 76, 319-334.
- Grantz, A., Hart, P., & Childers, V. (2011). Geology and tectonic development of the Amerasia and Canada basins, Arctic Ocean. In A. Spencer, D. Gautier, A. Stopupakova, K. Sørensen, A. Spencer, D. Gautier, A. Stoupakova, A. Embry, & K. Sørensen (Eds.), *Arctic petroleum geology* (pp. 771-799). London: Geological Society.
- Grogran, P., Østvedt-Ghazi, A., Larssen, G., Fotland, B., Nyberg, K., Dahlgren, S., & Eidvin, T. (1999). Structural elements and petroleum geology of the Norwegian sector of the northern Barents Sea. *Petroleum Geology of Northwest Europe; Proceedings of the 5th Conference*, 5, 247-259.
- Grundvåg, S.-A. (2015). Cretaceous. In W. K. Dallmann, *Geoscience Atlas of Svalbard* (pp. 122-125). Tromsø: Norsk Polarinstitutt.
- Grundvåg, S.-A. (2017). Lower Cretaceous basin studies in the Arctic (Sedimentary logs from field notebook) unpublished raw data.
- Grundvåg, S.-A., & Olaussen, S. (2017). Sedimentology of the Lower Cretaceous at Kikutodden and Keilhaufjellet, southern Spitsbergen: implications for an onshore-offshore link. *Polar Research*, 36(1), 1-20.

- Grundvåg, S.-A., Marin Restropo, D. L., Kairanov, B., Sliwinska, K., Nøhr-Hansen, H., Jelbye, M., . . . Olausson, S. (2017). The Lower Cretaceous succession of the northwestern Barents Shelf: Onshore and offshore correlations. *Marine and Petroleum Geology*, *86*, 834-857.
- Grøsfjeld, K. (1992). Palynological age constraints on the base of the Helvetiafjellet Formation (Barremian) on Spitsbergen. *Polar Research*, *11*(1), 11-19.
- Hallam, A. (1985). A review of Mesozoic climates. *Journal of the Geological Society*, *142*(3), 433-445.
- Haq, B. (2014). Cretaceous eustasy revisited. *Global and Planetary Change*, *113*, 44-58.
- Haq, B., Hardenbol, J., & Vail, P. (1987). Chronology of fluctuating sea levels since the Triassic. *American Association for the Advancement of Science*, *235*(4793), 2266-1167.
- Haq, B., Hardenbol, J., & Vail, P. (1988). Mesozoic and Cenozoic chronostratigraphy and cycles of sea-level change. *The Society of Economic Paleontologists and Mineralogists*, *42*, 71-108.
- Harland, M., Francis, J., Brentnall, S., & Beerling, D. (2007). Cretaceous (Albian- Aptian) conifer wood from Northern Hemisphere high latitudes: Forest composition and palaeoclimate. *Review of Palaeobotany and Palynology*, *143*, 167-196.
- Harland, W. B. (1969). Contribution of Spitsbergen to Understanding of Tectonic Evolution of North Atlantic Region. In M. Kay, *North Atlantic: Geology and Continental Drift* (pp. 817-851). American Association of Petroleum Geologists Memoir 12.
- Harland, W. B., & Kelly, S. R. (1997). Jurassic - Cretaceous history. In W. Harland, *The Geology of Svalbard, Memoirs* (Vol. 17, pp. 363-387). London: Geological Society.
- Harland, W. B., Pickton, C. A., & Wright, N. J. (1976). Some coal-bearing strata in Svalbard. *Norsk Polarinstitutt Skrifter* *164*, 7-28.
- Heintz, N. (1962). Dinosaur-footprints and polar wandering. *Norsk Polarinstitutt Årbok* *1963*, 35-43.
- Henriksen, E., Ryseth, A., Larssen, G., Heide, T., Rønning, K., Sollid, K., & Stoupakova, A. (2011). Tectonostratigraphy of the greater Barents Sea: implications for petroleum systems. In A. Spencer, A. Embry, D. Gautier, A. Stoupakova, & K. Sørensen (Eds.), *Arctic Petroleum Geology* (pp. 163-195). London: Geological Society, Memoir 35.
- Hurum, J. H., Druckenmiller, P. S., Hammer, Ø., Nakrem, H. A., & Olausson, S. (2016). The theropod that wasn't there: an ornithomimid tracksite from the Helvetiafjellet Formation (Lower Cretaceous) of Boltodden, Svalbard. In B. P. Kear (Ed.), *Mesozoic biotas of Scandinavia and its Arctic territories* (pp. 189-206). London: Geological Society.
- Hurum, J. H., Roberts, A. J., Dyke, G. J., Grundvåg, S.-A., Nakrem, H. A., Midtkandal, I., . . . Olausson, S. (2016 A). Bird or maniraptoran dinosaur? A femur from the Albian strata of Spitsbergen. *Palaeontologia Polonica*, *67*, 137-147.
- Hutsky, A., Fielding, C., Hurd, T., & Clark, C. (2012). Sedimentology and Stratigraphy of the Upper Cretaceous (Cenomanian) Frontier Formation, Northeast Bighorn Basin, Wyoming, U.S.A. *Geological Society of America*, *49*(3), 77-98.
- Hwang, I.-G., & Heller, P. (2002). Anatomy of a transgressive lag: Panther Tongue Sandstone, Star Point Formation, central Utah. *Sedimentology*, *49*(5), 977-999.
- Jung, M., Burt, T., & Bates, P. (2004). Toward a conceptual model of floodplain water table response. *Water Resources Research*, *40*, 1-13.

- Koevoets, M. J., Abay, T. B., Hammer, Ø., & Olausson, S. (2016). High-resolution organic carbon-isotope stratigraphy of the Middle Jurassic-Lower Cretaceous Agardhfjellet Formation of central Spitsbergen, Svalbard. *Palaeogeography, Palaeoclimatology, Palaeoecology*, 449, 266-274.
- Koevoets, M., Hammer, Ø., Olausson, S., Senger, K., & Smelror, M. (2018). Integrating subsurface and outcrop data of the Middle Jurassic to Lower Cretaceous Agardhfjellet Formation in central Spitsbergen. *Norwegian Journal of Geology*, 98(4), 1-34.
- Lane, L. S. (1997). Canada Basin, Arctic Ocean: Evidence against a rotational origin. *Tectonics*, 16(3), 363-387.
- Lutgens, F., Tarbuck, E., & Tasa, D. (2012). Origin and Evolution of the Ocean Floor. In F. Lutgens, E. Tarbuck, & D. Tasa, *Essentials of Geology* (11th ed., pp. 392-435). New Jersey: Pearson Education.
- Maher, H. (2001). Manifestations of the Cretaceous High Arctic Large Igneous Province in Svalbard. *The Journal of Geology*, 109, 91-104.
- Maher, H. D., Hays, T., Shuster, R., & Mutrux, J. (2004). Petrography of Lower Cretaceous sandstones on Spitsbergen. *Polar Research*, 23, 147-165.
- Markwick, P., & Rowley, D. (1998). The geological evidence for Triassic to Pleistocene glaciations: implications for eustasy. In J. Pindell, & C. Drake (Eds.), *Paleogeographic evolution and non-glacial eustasy, northern South America. SEPM Special Publication 58* (pp. 17-43). Tulsa: Society for Sedimentary Geology.
- Marshall, J. (2000). Sedimentology of a Devonian fault-bounded braidplain and lacustrine fill in the lower part of the Skrinkle Sandstones, Dyfed, Wales. *Sedimentology*, 47, 325-342.
- McCubbin, D. (1982). Barrier-Island and Strand-Plain Facies. (P. Scholle, & D. Spearing, Eds.) *Sandstone Depositional Environments*, pp. 247-279.
- Midtkandal, I., & Nystuen, J. (2009). Depositional Architecture of a Low-gradient Ramp Shelf in an Epicontinental Sea: the Lower Cretaceous on Svalbard. *Basin Research*, 21, 655-675.
- Midtkandal, I., Nystuen, J. P., & Nagy, J. (2007). Paralic sedimentation on an epicontinental ramp shelf during a full cycle of relative sea-level fluctuation; the Helvetiafjellet Formation in Nordenskiöld Land, Spitsbergen. *Norwegian Journal of Geology*, 87, 343-359.
- Midtkandal, I., Nystuen, J., Nagy, J., & Mørk, A. (2008). Lower Cretaceous lithostratigraphy across a regional subaerial unconformity in Spitsbergen: the Rurikfjellet and Helvetiafjellet formations. *Norwegian Journal of Geology*, 88, 287-304.
- Midtkandal, I., Svensen, H., Planke, S., Corfu, F., Polteau, S., Torsvik, T., . . . Olausson, S. (2016). The Aptian (Early Cretaceous) oceanic anoxic event (OAE1a) in Svalbard, Barents Sea, and the absolute age of the Barremian-Aptian boundary. *Elsevier: Palaeogeography, Palaeoclimatology, Palaeoecology*(463), 126-135.
- Mutrux, J., Maher, H., Shuster, R., & Hays, T. (2008). Iron ooid beds of the Carolinefjellet Formation, Spitsbergen, Norway. *Polar Research*, 27, 28-43.
- Müller, R. D., & Spielhagen, R. F. (1990). Evolution of the Central Tertiary Basin of Spitsbergen: towards a synthesis of sediment and plate tectonic history. *Palaeogeography, Palaeoclimatology, Palaeoecology*, 80(2), 153-172.
- Mørk, A. (1978). Observations on the stratigraphy and structure of the inner Hornsund area. *Norsk Polarinstitutt Årbok 1977*, 61-70.

- Mørk, A., Dallmann, W., Dypvik, H., Johannessen, E., Larssen, G., Nagy, J., . . . Worsley, D. (1999). Mesozoic lithostratigraphy. In W. Dallmann, *Lithostratigraphic lexicon of Svalbard, Review and recommendations for nomenclature use. Upper Palaeozoic to Quaternary bedrock* (pp. 127-214). Tromsø: Norwegian Polar Institute.
- Mørk, A., Knarud, R., & Worsley, D. (1982). Depositional and diagenetic environments of the Triassic and Lower Jurassic succession of Svalbard. (A. Embry, & H. Balckwill, Eds.) *Arctic Geology and Geophysics*, pp. 371-398.
- Nagy, J. (1970). Ammonite faunas and stratigraphy of Lower Cretaceous (Albian) rocks in southern Spitsbergen. *Norsk Polarinstitutt Skrifter* 152, 1-58.
- Nakrem, H. A., Orchard, M. J., Weitschat, W., Hounslow, M. W., Beatty, T. W., & Mørk, A. (2008). Triassic conodonts from Svalbard and their Boreal correlations. *Polar Research*, 27, 523-539.
- Nemec, W. (1992). Depositional controls on plant growth and peat accumulation in a braidplain delta environment: Helvetiafjellet Formation (Barremian-Aptian), Svalbard. *Geological Society of America*, 209-226.
- Nemec, W., Steel, R. J., Gjelberg, J., Collinson, J. D., Prestholm, E., & Øxnevad, I. E. (1988). Anatomy of Collapsed and Re-established Delta Front in Lower Cretaceous of Eastern Spitsbergen: Gravitational Sliding and Sedimentation Processes. *The American Association of Petroleum Geologists Bulletin* 72, 454-476.
- Nichols, G. (2009). *Sedimentology and Stratigraphy* (Vol. 2nd Ed.). UK: Wiley-Blackwell.
- Nøttvedt, A., & Johannessen, E. (2013). Grunnlaget for Norges oljerikdom, seinjura, et øyhav vokser frem; 164-145 millioner år. In I. B. Ramberg, I. Bryhni, A. Nøttvedt, & K. Rangnes, *Landet blir til* (pp. 386-421). Trondheim: Norsk geologisk forening.
- Nøttvedt, A., Cecchi, M., Gjelberg, J. G., Kristensen, S. E., Lønøy, A., Rasmussen, A., . . . Van Veen, P. M. (1992). Svalbard-Barents Sea correlation: A short review. In T. O. Vorren, E. Bergsager, Ø. A. Dahl-Stamnes, E. Holter, B. Bohansen, E. Lie, & T. B. Lund, *Arctic Geology and Petroleum Potential* (pp. 363-375). Amsterdam: Elsevier.
- Olaussen, S. (2015). Jurassic. In W. K. Dallmann, *Geoscience Atlas of Svalbard* (pp. 118-121). Tromsø: Norsk Polarinstitutt.
- Onderdonk, N., & Midtkandal, I. (2010). Mechanisms of collapse of the cretaceous helvetiafjellet formation at Kvalvågen, eastern Spitsbergen. *Marine and Petroleum Geology*, 27, 2118-2140.
- Parker, J. (1967). The Jurassic and Cretaceous sequence in Spitsbergen. *Geological Magazine*, 104(5), 487-505.
- Polteau, S., Hendriks, B., Planke, S., Ganerød, M., Corfu, F., Faleide, J., . . . Myklebust, R. (2016). The Early Cretaceous Barents Sea Sill Complex: Distribution, ⁴⁰Ar/³⁹Ar geochronology, and implications for carbon gas formation. *Palaeogeography, Palaeoclimatology, Palaeoecology*, 441, 83-95.
- Price, G., & Nunn, E. (2010). Valanginian isotope variations in glendonites and belemnites from Arctic Svalbard: Transient glacial temperatures during the Cretaceous greenhouse. *Geological Society of America*, 38(3), 251-254.
- Ramkumar, M. (2016). *Cretaceous Sea Level Rise: Down Memory Lane and the Road Ahead*. Amsterdam: Elsevier.
- Rider, M., & Kennedy, M. (2011). *The geological interpretation of well logs* (Vol. 3). Scotland: Rider-French consulting Ltd.
- Riis, F., Lundschiën, B., Høy, T., Mørk, A., & Mørk, M. (2008). Evolution of the Triassic shelf in the northern Barents Sea region. *Polar Research*, 27, 318-338.

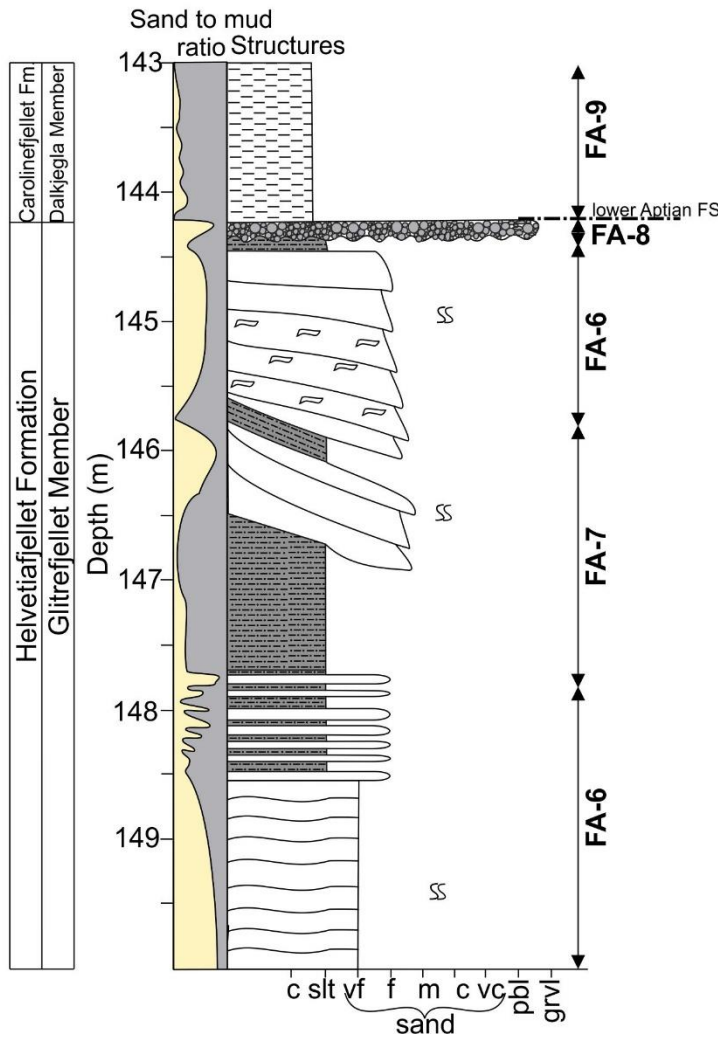
- Rygel, M., Fielding, C., Bann, K., Frank, T., Birgenheier, L., & Tye, S. (2008). The Lower Permian Wasp Head Formation, Sydney Basin: high-latitude, shallow marine sedimentation following the late Asselian to early Sakmarian glacial event in eastern Australia. *Sedimentology*, *55*, 1517-1540.
- Ryseth, A. (2000). Differential subsidence in the Ness Formation (Bajocian), Oseberg area, northern North Sea: facies variation, accommodation space development and sequence stratigraphy in a deltaic distributary system. *Norsk Geologisk Tidsskrift*, *80*, 9-26.
- Røhr, T., Andersen, T., & Dypvik, H. (2008). Provenance of Lower Cretaceous sediments from Svalbard and NE Greenland: A detrital zircon study. *The Geological Society of London*, *165*(3), 755-767.
- Sanders, J., & Kumar, N. (1975). Evidence of Shoreface Retreat and In-Place "Drowning" During Holocene Submergence of Barriers, Shelf off Fire Island, New York. *Geological Society of America Bulletin*, *86*, 65-76.
- Senger, K., Tveranger, J., Ogata, K., Braathen, A., & Planke, S. (2014). Late Mesozoic magmatism in Svalbard: a review. *Earth-Science Reviews*, *139*, 123-144.
- Smelror, M., & Dypvik, H. (2006). The Sweet Aftermath: Environmental Changes and Biotic Restoration Following the Marine Mjølnir Impact (Volgian-Ryazanian Boundary, Barents Shelf). In C. Cockell, I. Gilmour, & C. Koeberl (Eds.), *Biological Processes Associated with Impact Events. Impact Studies*. (pp. 143-178). Springer, Berlin, Heidelberg.
- Smelror, M., & Larssen, G. B. (2016). Are there Upper Cretaceous sedimentary rocks preserved on Sørkapp Land, Svalbard? *Norwegian Journal of Geology*, 1-12.
- Smith, D., & Pickton, C. (1976). The Helvetiafjellet Formation (Cretaceous) of North-East Nordenskiöld Land, Spitsbergen. 47-55.
- Steel, R. (1977). Observations on some Cretaceous and Tertiary sandstone bodies in Nordenskiöld Land, Svalbard. *Norsk Polarinstitutt Årbok 1976*, 43-66.
- Steel, R., & Worsley, D. (1984). Svalbard's post-Caledonian strata - an atlas of sedimentational patterns and palaeographic evolution. In A. Spencer (Ed.), *Petroleum geology of the North European Margin* (pp. 109-135). London: Norwegian Petroleum Society/ Graham & Trotman.
- Steel, R., Crabaugh, J., Schellpeper, J., Mellere, D., Plink-Bjorklund, P., Deibert, J., & Loeseth, T. (2000). Deltas vs. Rivers on the Shelf Edge: Their Relative Contributions to the Growth of Shelf-Margins and Basin Floor Fans (Barremian and Eocene, Spitsbergen). In P. Weimer (Ed.), *Deep-water reservoirs of the world. Gulf Coast Section Society of Economic Paleontologists and Mineralogists Foundation 20th Annual Bob F. Perkins Research Conference* (Vol. 20, pp. 981-1009). Houston: Gulf Coast Section Society of Economic Palaeontologists and Mineralogists Foundation.
- Steel, R., Gjelberg, J., & Haarr, G. (1978). Helvetiafjellet Formation (Barremian) at Festningen, Spitsbergen - a field guide. *Norsk Polarinstitutt Årbok 1978*, 111-128.
- Steel, R., Gjelberg, J., Helland-Hansen, W., Kleinspehn, K., Nøttvedt, A., & Rye-Larsen, M. (1985). The Tertiary strike-slip basins and orogenic belt of Spitsbergen. (K. Biddle, & Christi-Blick, Eds.) *37*, pp. 339-359.
- Storms, J., Hoogendoorn, R., Dam, R., Hoitink, A., & Kroonenberg, S. (2005). Late- Holocene evolution of the Mahakam delta, East Kalimantan, Indonesia. *Sedimentary Geology*, *180*, 149-166.

- Suess, E., Hesse, Hesse, K., Müller, P., Ungerer, C., & Wefer, G. (1982). Calcium carbonate hexahydrate from organic-rich sediments of the Antarctic shelf: precursors of glendonites. *Science*, *216*, 1128-1130.
- Swift, D. (1968). Coastal erosion and transgressive stratigraphy. *Journal of Geology*, *76*, 444-456.
- Swift, D., & Thorne, J. (1991). Sedimentation on continental margins, I: a general model for shelf sedimentation. In D. Swift, G. Oertel, R. Tillman, & J. Thorne, *Shelf Sand and Sand Bodies: Geometry, Facies and Sequence Stratigraphy* (pp. 3-31). Blackwell, Oxford: The International Association of Sedimentologists, Special Publication 14.
- Torsvik, T., Carlos, D., Mosar, J., Cocks, L., & Malme, T. (2002). Global reconstructions and North Atlantic paleogeography 440 Ma to Recent. In E. Eide, *Batlas. Mid Norway plate reconstruction atlas with global and Atlantic perspective* (pp. 18-39). Trondheim: Geological Survey of Norway.
- Torsvik, T., Van der Voo, R., Preeden, U., Mac Niocaill, C., Steinberger, B., Doubrovine, P., . . . Cocks, L. (2012). Phanerozoic polar wander, palaeogeography and dynamics. *Earth-Science Reviews*, *114*, 325-368.
- Ulicny, D. (1999). Sequence stratigraphy of the Dakota Formation (Cenomanian) southern Utah: interplay of eustasy and tectonics in a foreland basin. *Sedimentology*, *46*, 807-836.
- Vail, P., Mitchum, R., & Thompson, S. (1977). Seismic stratigraphy and global changes of sea level. Part 4. Global cycles of relative changes of sea level. In C. Payton (Ed.), *Seismic Stratigraphy- Applications of Hydrocarbon Exploration* (Vol. 26, pp. 83-97). Memoirs of American Association of Petroleum Geologists.
- van Gelder, A., van den Berg, J., Cheng, G., & Xue, C. (1994). Overbank and channelfill deposits of the modern Yellow River delta. *Sedimentary Geology*, *90*, 293-305.
- Vickers, M. L., Price, G. D., Jerrett, R. M., & Watkinson, M. (2017). Stratigraphic and geochemical expression of Barremian–Aptian global climate change in Arctic Svalbard. *Geosphere*, *12*(5), 1-12.
- Worsley, D. (1986). *The geological history of Svalbard: evolution of an Arctic archipelago*. Stavanger: Norwegian State Oil Company.
- Worsley, D. (2008). The post-Caledonian development of Svalbard and the western Barents Sea. *Polar Research*, *27*, 298-317.
- Xue, C. (1993). Historical changes in the Yellow River delta, China. *Marine Geology*, *113*, 321-329.
- Yang, W. (2007). Transgressive wave ravinement on an epicontinental shelf as recorded by an Upper Pennsylvanian soil-nodule conglomerate-sandstone unit, Kansas and Oklahoma, U.S.A. *Sedimentary Geology*, *197*, 189-205.
- Zaremba, N., Mallinson, D., Leorri, E., Culver, S., Riggs, S., Mulligan, R., . . . Mitra, S. (2016). Controls on the stratigraphic framework and paleoenvironmental change within a Holocene estuarine system: Pamlico Sound, North Carolina, USA. *Marine Geology*, *379*, 109-123.
- Århus, N. (1992). Some dinoflagellate cysts from the Lower Cretaceous of Spitsbergen. *Grana*, *31*(4), 305-314.

9 Appendix

9.1 Appendix A: DH-1 in scale 1:50 cm

DH-1 Scale 1:50 cm



Facies association

- FA1 Prodelta
- FA2 Fluvial braidplain
- FA3 Flood plain
- FA4 Crevasse splay
- FA5 Fluvial distributary channel
- FA6 Delta/costal plain
- FA7 Delta front
- FA8 Wave reworked delta
- FA9 Offshore transition

Lithology

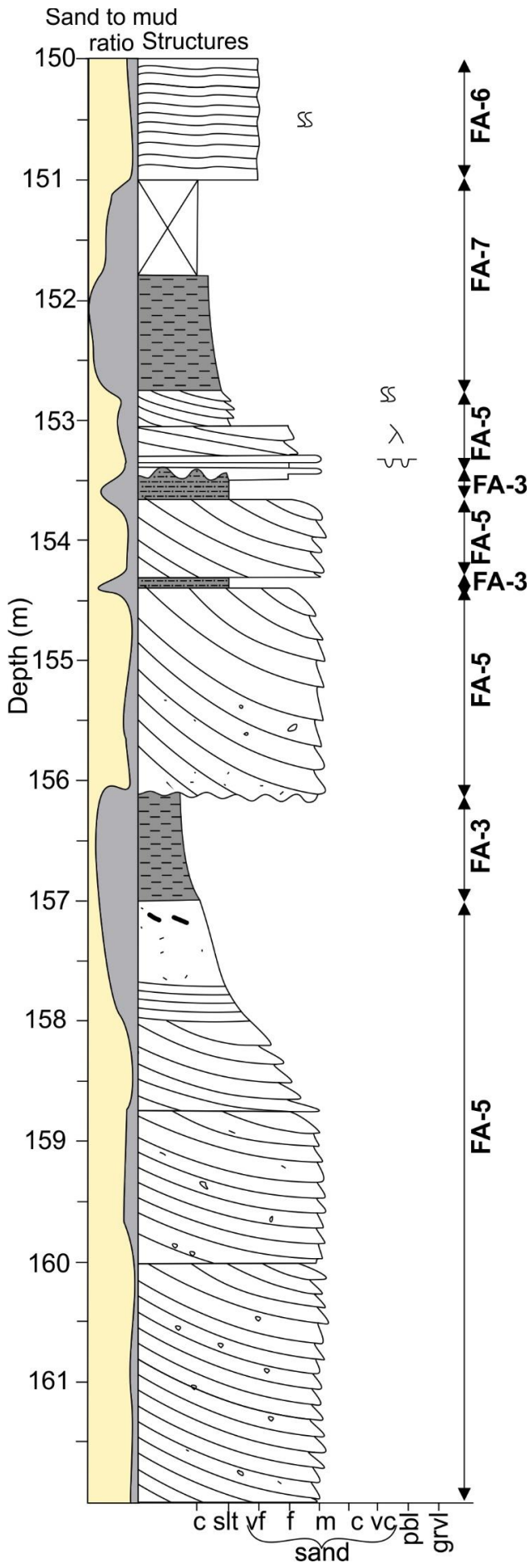
- Conglomerate
- Coaly shale
- Coal
- Siltstone
- Coal clasts
- Sandstone
- Lithic clasts
- Black shale

Sedimentary structures

- Ripple cross-lamination
- Bioturbation
- Rootlets
- Trough cross-bedding
- Horizontal bedding
- Heterolithic bedding
- High angle tabular cross-bedding
- Low angle tabular cross-bedding
- Soft sediment deformation
- Load cast/flame structure

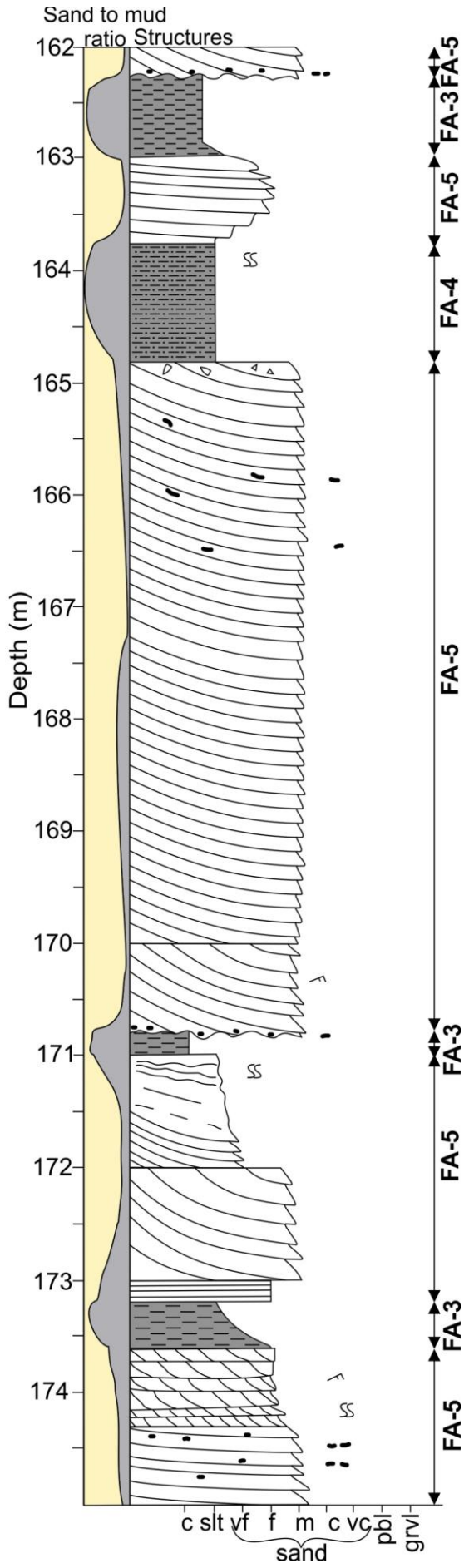
CF: Carolinefjellet Formation
 DM: Dalkjegla Member
 RF: Rurikfjellet Formation
 KM: Kikutodden Member

Helvetiafjellet Formation
Glitrefjellet Member

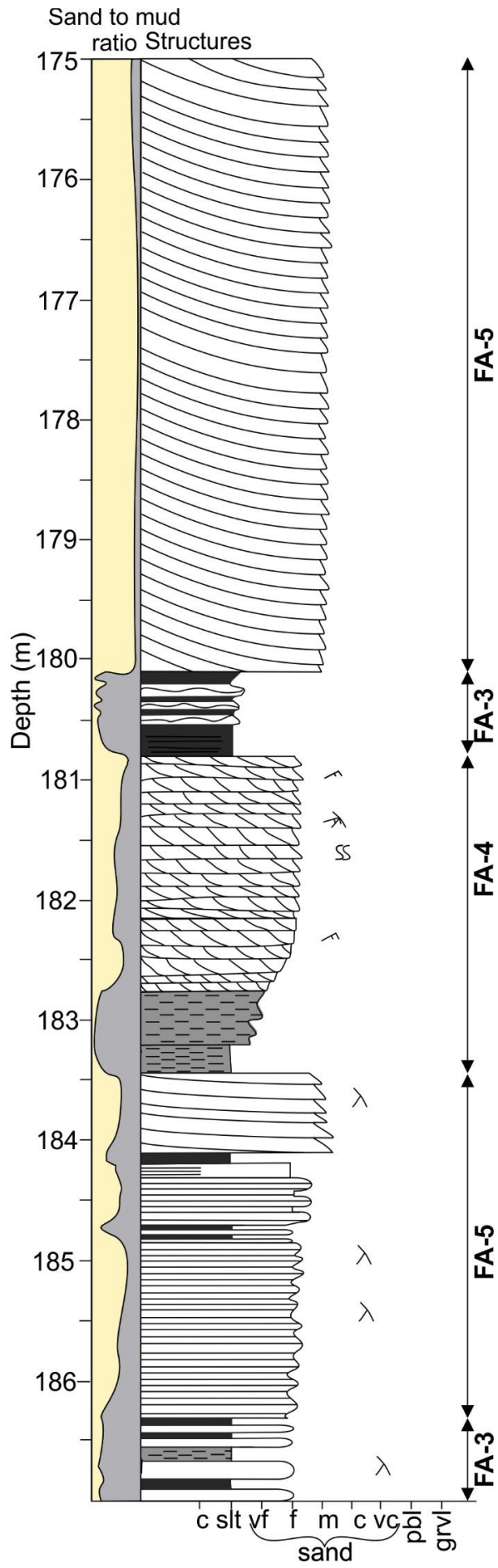


==

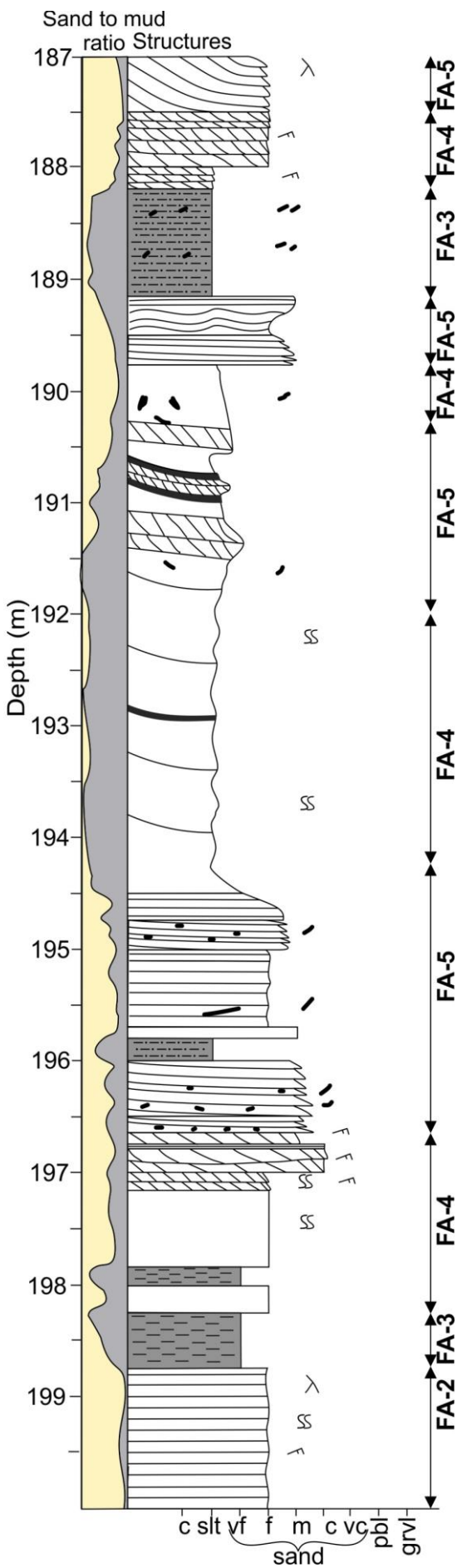
Helvetiafjellet Formation
Glitrefjellet Member

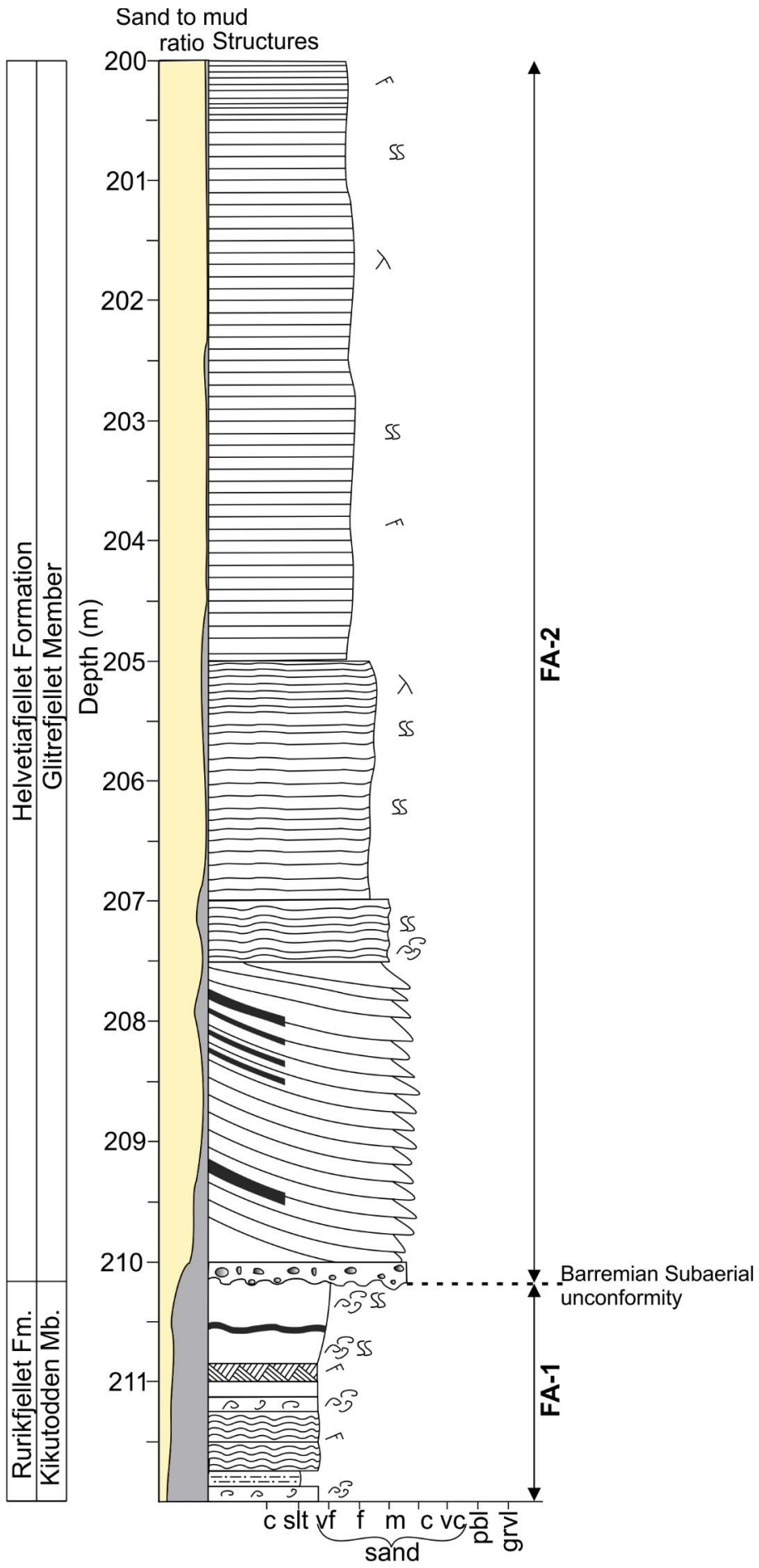


Helvetiafjellet Formation
Glitrefjellet Member

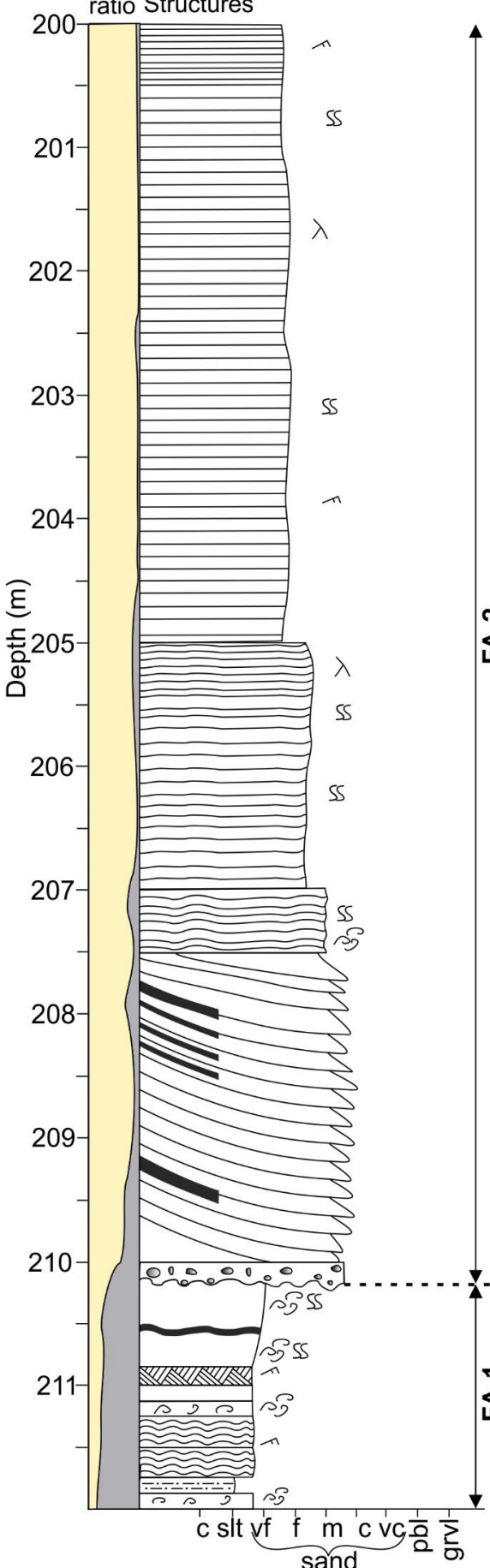


Helvetiafjellet Formation
 Giltrefjellet Member





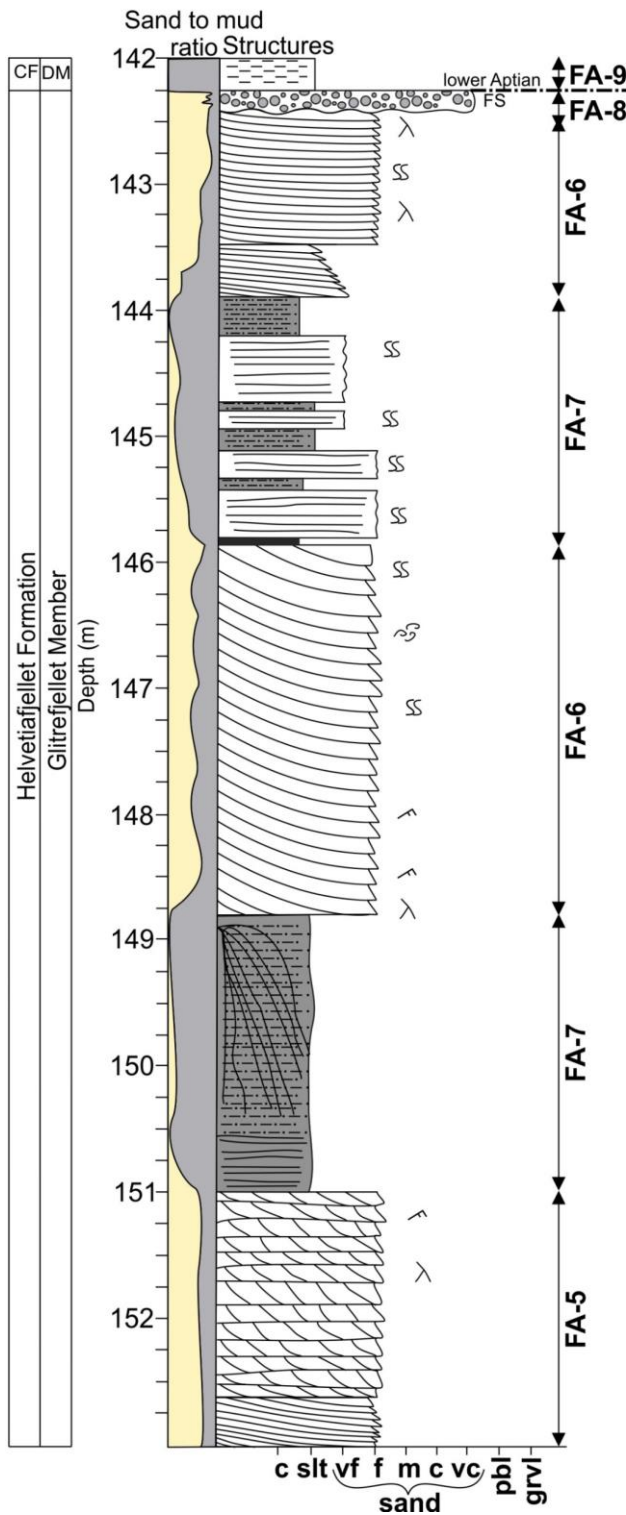
Rurikfjellet Fm.
 Kikutodden Mb.



c slt vf f m c vc pbl grvl
 sand

9.2 Appendix B: DH-1A in scale 1:50 cm

DH-1A Scale 1:50 cm



Facies association

- FA1 Prodelta
- FA2 Fluvial braidplain
- FA3 Flood plain
- FA4 Crevasse splay
- FA5 Fluvial distributary channel
- FA6 Delta/costal plain
- FA7 Delta front
- FA8 Wave reworked delta
- FA9 Offshore transition

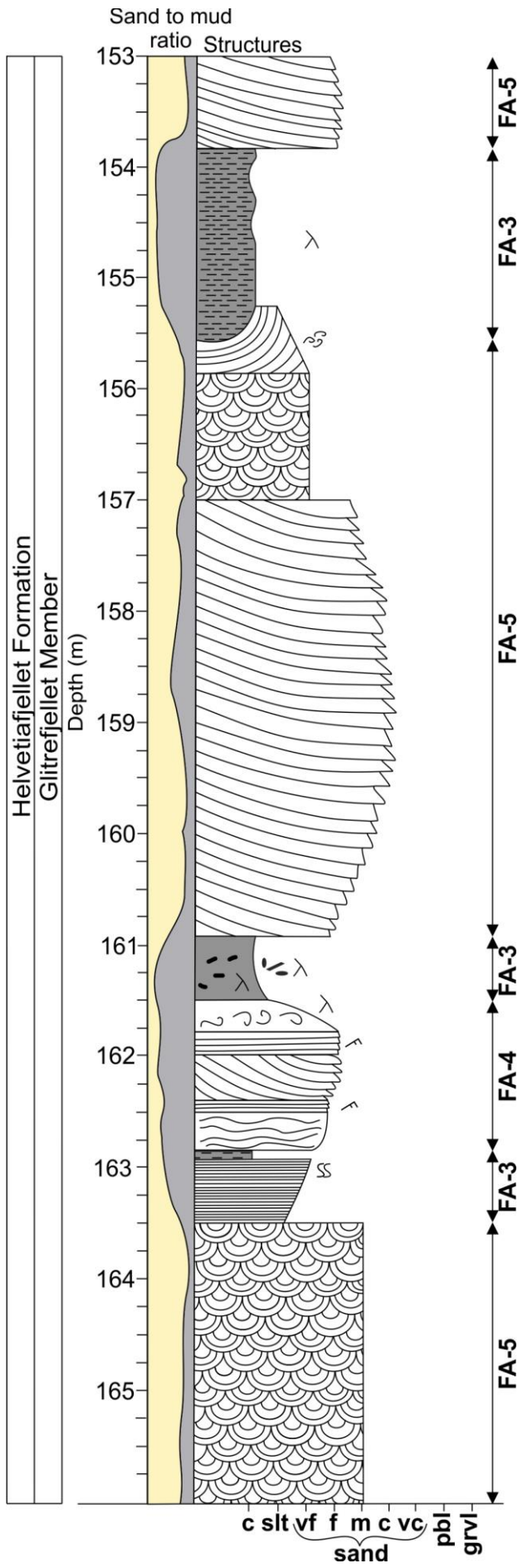
Lithology

- Conglomerate
- Coaly shale
- Coal
- Siltstone
- Coal clasts
- Sandstone
- Lithic clasts
- Black shale

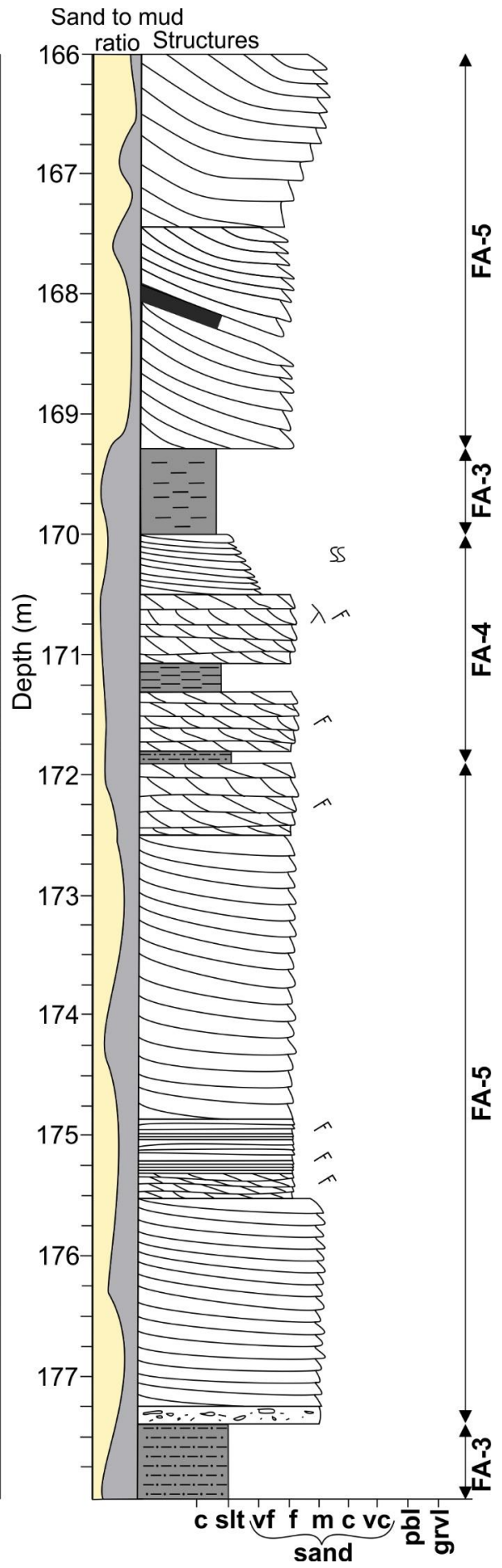
Sedimentary structures

- Ripple cross-lamination
- Bioturbation
- Rootlets
- Trough cross-bedding
- Horizontal bedding
- Heterolithic bedding
- High angle tabular cross-bedding
- Low angle tabular cross-bedding
- Soft sediment deformation
- Load cast/flame structure

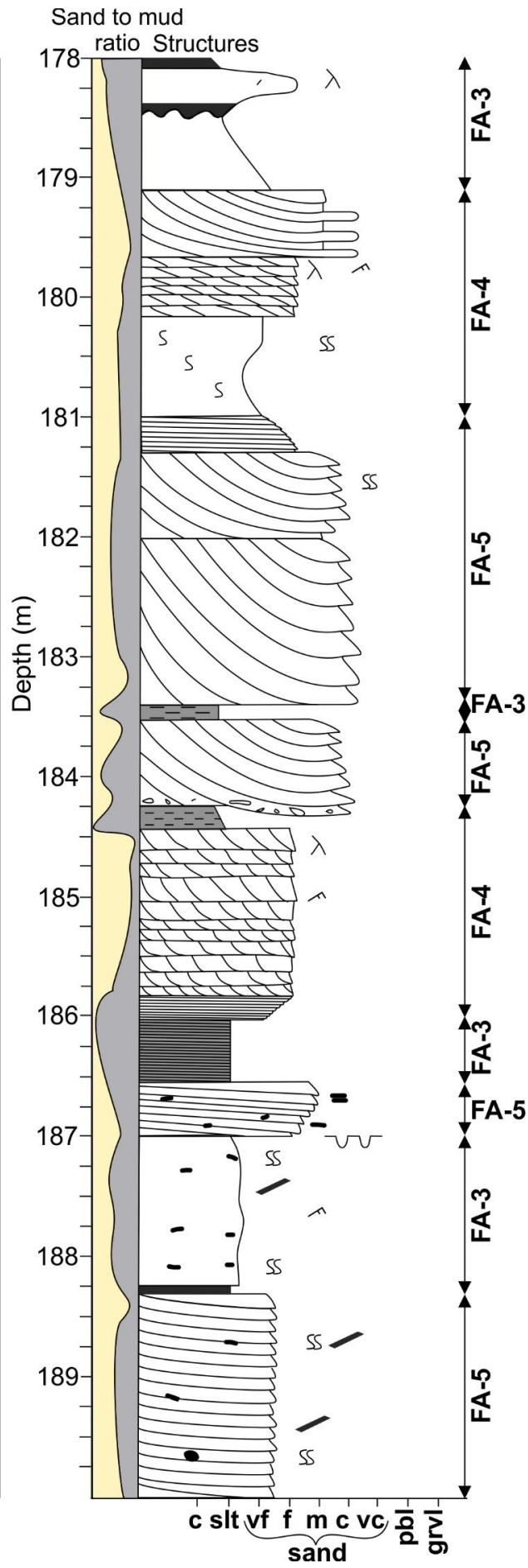
CF:Carolinefjellet Formation
DM:Dalkjegla Member
RF: Rurikfjellet Formation
KM: Kikutodden Member



Helvetiafjellet Formation
Glitrefjellet Member



Helvetiafjellet Formation
Glitrefjellet Member



x

